Exposure of neuronal networks to GSM mobile phone signals

Daniela Moretti

N° d'ordre: 4864

THÈSE

présentée à l'

Université Bordeaux 1

ÉCOLE DOCTORALE DES SCIENCES PHYSIQUES ET DE L'INGENIEUR

par **Daniela MORETTI**

pour obtenir le grade de DOCTEUR

Spécialité Électronique

EXPOSURE OF NEURONAL NETWORKS TO GSM MOBILE PHONE SIGNALS

Soutenue le 1 octobre 2013

Après avis des rapporteurs

Mme	Michela CHIAPPALONE	Chercheur (HDR),	IIT Genova (Italie)
M.	Rodney O'CONNOR	Chercheur (HDR),	Université de Limoges

Devant la commission d'examen formée de :

M. Ferdinando BERSANI	Professeur des universités	Università di Bologna (Italie)	Examinateur
Mme Michela CHIAPPALONE	Chercheur (HDR)	IIT Genova (Italie)	Rapporteur
M. Jean Marc EDELINE	Directeur de recherche	Université Paris-Sud	Président du jury
M. André GARENNE	Maitre de conférence	Université Bordeaux 2	Directeur de thèse
M. Philippe LEVEQUE	Directeur de recherche	Université de Limoges	Examinateur
Mme Noëlle LEWIS	Professeur des universités	Université Bordeaux 1	Directeur de thèse
M. Rodney O'CONNOR	Chercheur (HDR)	Université de Limoges	Rapporteur
M. Bernard VEYRET	Directeur de recherche	Université Bordeaux 1	Examinateur

Remerciements

Les travaux présentés dans ce mémoire se sont déroulés au laboratoire de l'Intégration des Matériaux aux Systèmes (IMS) à Bordeaux. Je tiens tout d'abord à remercier mon directeur de thèse Mme Noëlle Lewis et mon co-directeur de thèse M. André Garenne pour avoir dirigé mon travail de recherche.

Je voudrais remercier le président du jury M. Jean Marc Edeline, M. Philippe Lévêque, M. Ferdinando Bersani pour l'intérêt qu'ils ont porté à mon travail en acceptant de participer au jury de thèse.

Je remercie également Mme Michela Chiappalone et M. Rodnney O'Connor pour avoir accepté avec enthousiasme (malgré les vacances d'été) leur rôle de rapporteurs, mais aussi pour leurs lectures attentives et leurs suggestions.

Je tiens particulièrement à remercier Michela et ses collaborateurs pour leur accueil chaleureux au sein du laboratoire IIT de Gênes, ainsi que pour leur disponibilité (même après le stage!) et leur convivialité.

Je remercie M. A. Curutchet (ADV-TECH, Mérignac, France) pour son travail dans la conception du système expérimental; M. Giovannelli Jean François et M. Ferré Guillame pour leurs précieux conseils en traitement du signal, M. Stéphane Azzopardi et M. Raphaël Roder pour leur collaboration pendant les mesures avec la camera IR.

Je remercie tous les membres du groupe Bioélectronique, en particulier Yannick pour ses observations qui m'ont toujours apportée de bonnes idées ainsi que Florian, le guru de MatLab.

Pendant mes 3 ans de thèse, j'ai eu la chance d'avoir été intégrée au sein de l'équipe Bioelectromagnetisme, dirigée par Isabelle Lagroye. Le cadre enrichissant, autant sur le plan scientifique que sur le plan humain, associé au dynamisme et à la rigueur (mais aussi à la rigolade) ont permis l'aboutissement de ce travail.

Je remercie Florence et Emmanuelle pour leur minutieux travail, toujours accompagné de leur bonne humeur (même à 8 h le vendredi matin !), Yann, mon collègue officiel de bureau (même si ce n'est plus vrai), Renaud, Murielle, Annabelle, Isabelle, Hiroshi, Alban, Saliha et Manon pour avoir contribué de différentes façons à la réalisation de cette thèse.

Enfin je remercie Bernard pour sa patience et sa confiance, pour les échanges scientifiques quotidiens et pour les nombreux post-it avec les articles déterminatifs pluriels français que je retrouve encore collés à droite et à gauche dans mes anciennes notes.

Ce fût un plaisir d'avoir travaillé avec vous tous !

P.S. un grand Merci pour Constanze et Laurent sans qui mon pot de thèse aurait été une catastrophe totale.

Résumé étendu en français

INTRODUCTION

L'utilisation des appareils et des systèmes émettant des champs électromagnétiques (CEM) radiofréquence (RF) est en augmentation rapide. Les effets possibles de ces CEM RF sur les systèmes biologiques ont donc été un sujet de préoccupation et de débat scientifique public pendant les vingt dernières années. Le présent travail de recherche concerne un aspect de l'interaction des CEM RF avec le système nerveux.

La proximité entre le téléphone mobile et le cerveau lors d'une communication téléphonique et le fait que les neurones soient des cellules excitables impliquent que le système nerveux central (SNC) est une cible potentielle de l'exposition aux RF. Les résultats des études expérimentales chez l'homme sur l'électroencéphalogramme (EEG) et le sommeil, sous exposition aux RF, supportent cette hypothèse mais, en raison de la variété des conditions expérimentales, aucun effet n'a été solidement établi. Toutefois, le consensus est que les effets sanitaires potentiels correspondants sont probablement négligeables. Néanmoins, il est important de comprendre comment des effets biologiques non thermiques pourraient être produits par l'exposition aux RF de faible niveau.

La recherche actuelle en laboratoire se concentre en grande partie sur les effets de l'exposition aux RF non-thermiques sur le système nerveux et il devient nécessaire d'utiliser des modèles cellulaires et animaux pour déterminer si des effets biologiques existent, pour les caractériser et confirmer les observations humaines. En effet, les effets observés l'ont été à l'échelle macroscopique (par exemple dans le cas de l'EEG) avec des observations « moyennées » sur le cortex et il est souhaitable de réduire l'échelle de complexité biologique.

Dans ce contexte, notre projet vise à une amélioration substantielle de la compréhension de la réponse en temps réel de l'activité électrique des réseaux de neurones à l'exposition aux RF, à des niveaux non thermiques. Dans notre protocole expérimental, un signal GSM de téléphonie mobile est appliqué à des neurones en culture et leur activité est enregistrée au moyen d'une technique d'électrophysiologie extracellulaire. L'objectif est d'observer si des effets existent et de définir leur mécanisme.

L'utilisation de réseaux neuronaux in vitro est basée sur l'hypothèse que les principes d'organisation opérant au niveau des populations neuronales in vivo sont intrinsèques aux neurones et donc manifestés dans les réseaux in vitro.

Nous avons développé un dispositif expérimental dédié à la gamme des GHz pour l'exposition simultanée des réseaux neuronaux et le suivi de leur activité électrique. Pour recueillir l'activité électrique, les neurones primaires sont cultivés sur des réseaux de microélectrodes (MEA). En raison de l'absence de tels dispositifs d'exposition basés sur des MEA, un système d'exposition a été développé sur la base d'une cellule électromagnétique transversale (TEM) ouverte, en collaboration avec le groupe de Philippe Lévêque du laboratoire XLIM à Limoges. Ce système d'exposition a été caractérisé, avec une dosimétrie détaillée, ainsi que le préconise l'Organisation mondiale de la Santé (OMS) dans ses recommandations de recherche de 2006 et 2010.

Synthèse des chapitres

Le manuscrit est organisé en cinq chapitres commençant par le chapitre 1 d'introduction.

La première partie du chapitre 2 est dédiée au bioélectromagnétisme : à la suite d'un rappel des bases, nous décrivons l'état de l'art sur les conclusions des rapports de recherche sur les effets biologiques des RF et en particulier sur le système nerveux. Les résultats obtenus à l'aide des approches complémentaires en termes de complexité biologique sont décrits : études sur les populations (épidémiologie), chez l'homme, l'animal et les cellules.

La deuxième partie du chapitre 2 contient la description des réseaux de neuronaux du point de vue des neurosciences. Les techniques d'électrophysiologie in vitro sont ensuite illustrées en détaillant les réseaux de microélectrodes (MEA) en particulier de type passif : fabrication, application et modélisation de l'interface cellule-électrolyte.

Dans le chapitre 3, nous présentons en détail les matériaux et les méthodes utilisées : 1) l'ensemble du protocole de culture de neurones primaires, 2) le système d'exposition de ces cellules aux RF et 3) son couplage avec une chaîne d'acquisition commerciale pour recueillir l'activité électrique des neurones.

Le système d'exposition est constitué d'une cellule TEM (transverse électromagnétique), qui a été caractérisée en termes de dosimétrie expérimentale et numérique. Pour l'exposition aux RF, le signal GSM a été choisi car il permet l'acquisition du signal électrophysiologique au cours des sept intervalles de temps vides correspondant à la modulation GSM. Le SAR utilisé est de 3,2 W/kg (GSM-1800).

Les enregistrements de l'activité électrique des neurones pendant l'exposition aux RF GSM présentent des interférences. Parmi les différentes méthodes conçues pour éliminer l'artefact dû aux RF, les meilleures performances ont été obtenues avec un filtre fréquentiel coupe-bande éliminant les harmoniques du signal GSM.

L'analyse des données a été réalisées à l'aide de SpyCode, un logiciel dédié, développé par l'Université de Gênes en Italie et adapté à nos besoins. Toutes les métriques considérées sont générées directement par SpyCode. Pour évaluer l'activité neuronale en termes de spikes et de bursts, deux métriques ont été considérées comme les plus représentatives : le Mean Firing Rate (MFR) and le Bursting Rate (BR). D'autres métriques relatives aux bursts ont été considérées.

Des expériences préliminaires sont rapportées au début du chapitre 4, qui démontrent la faisabilité du projet dans son ensemble. Une expérience complète a été ensuite effectuée pour augmenter la puissance statistique, améliorer les conditions expérimentales et observer des cultures d'âges différents. Les résultats sont présentés en détail dans la deuxième partie du chapitre 4. Une diminution de l'activité des cultures (en termes de MFR et BR) a été observée pendant l'exposition. Les effets de l'exposition sont phasiques et réversibles.

L'interprétation des résultats est donnée dans le chapitre 5, dans lequel on analyse les effets des RF en fonction de différents paramètres. Des hypothèses sur le mécanisme d'interaction des effets sont présentées. Les résultats analogues obtenus par exposition des neurones à d'autres agents et publiés sont discutés.

Dans le chapitre 6, nous décrivons les nouvelles perspectives que ce travail ouvre en ce qui concerne l'étude des effets de l'exposition aux signaux RF sur le fonctionnement du tissu neuronal. Des expériences pouvant être faites en utilisant le matériel déjà disponible sont décrites ainsi que des projets qui nécessiteront un important développement de l'équipement et des méthodes.

CONCLUSION

L'objectif principal de ce travail était d'évaluer la faisabilité de l'étude de l'activité électrique de réseaux neuronaux sous exposition aux signaux RF de téléphones portables à 1800 MHz. À cet effet, un système RF a été construit pour exposer les échantillons biologiques placés dans des MEA, et bien caractérisé en termes de dosimétrie. En dépit de la grande qualité de cette étude expérimentale et numérique, il reste une certaine incertitude sur le SAR et de la température au niveau des électrodes, en raison de leur très petite taille et les limites de la méthode FDTD. On peut estimer que le niveau SAR utilisé dans ce travail (3,2 W/kg), au niveau des neurones est connu avec une incertitude de 30%.

Il y a toujours la possibilité qu'un échauffement local des électrodes de quelques degrés Celsius puisse affecter l'activité des neurones adjacents.

Le signal GSM a été choisi car il permet l'acquisition du signal électrophysiologique au cours des sept intervalles de temps vides correspondant à la modulation GSM. L'interférence GSM présentent sur les signal acquis, causée par le champ RF durant l'intervalle de temps actif a été éliminée en utilisant un filtre spectral qui nous a permis d'utiliser les huit intervalles de temps. Nous avons démontré que l'artefact est principalement causé par une interférence directe de l'amplificateur avec les champs RF GSM.

Une analyse de sensibilité a montré une corrélation entre l'amplitude de l'effet et l'âge : la réduction de l'activité était plus marquée à deux semaines qu'à trois semaines.

Dans la littérature scientifique divers facteurs causent une action inhibitrice sur l'activité des réseaux neuronaux : des facteurs physiques (stimulation électrique principalement), des agents chimiques et pharmacologiques. Cependant, aucun n'agit de manière réversible et aussi rapidement que dans nos expérimentations.

La démonstration expérimentale de la faisabilité a donc été réalisée dans ce travail, ce qui ouvre de nouvelles perspectives concernant l'étude des effets de l'exposition aux signaux RF sur le fonctionnement du tissu neuronal.

1 INTRODUCTION

The everyday use of devices and systems emitting RF electromagnetic fields (EMF) is increasing rapidly. The possible effects of these RF EMF on biological systems have thus been a matter of public concern and scientific discussion for the last two decades. The present work belongs to the non-cancer research area and more specifically to RF interaction with the nervous system.

The close proximity between the mobile phone and the brain and the fact that neurons are excitable cells make the Central Nervous System (CNS) a most likely target of RF exposure. Experimental studies in humans on electroencephalogram (EEG) and sleep under RF exposure support this hypothesis but, due to the variety of experimental conditions, there are no well-established effects known. However, the consensus is that the corresponding potential health effects are probably negligible. Nonetheless, it is important to understand how these non-thermal biological effects can be produced by low-level RF exposure.

Current research is focused largely on the effects of non-thermal RF exposure on the nervous system and therefore it is becoming necessary to use cell and animal models to determine whether effects exist, can be characterized, and confirm human observations. The effects have been observed at the macroscopic scale (e.g., EEG) where observations are "averaged" over the cortex and it is desirable to decrease the scale of biological complexity.

In this context, our project should bring a substantial improvement in the understanding of the real-time response of electrical activity of neuronal networks to RF exposure, at non-thermal levels. In our experimental protocol, a mobile telephony GSM signal is applied to neurons in culture, and their activity is monitored using an extra-cellular electrophysiology technique. The aim is to observe whether effects exist and to determinate their mechanism.

Our main motivation for using *in-vitro* neuronal networks is the assumption that the organizing principles operating at the level of neuronal populations *in vivo* are intrinsic to neurons and therefore manifested in *in-vitro* cultured networks.

We have developed a dedicated experimental setup in the GHz range for the simultaneous exposure of neuronal networks and monitoring of their electrical activity. To collect the electrical activity, primary neurons are cultured on microelectrode arrays (MEA). Due to the lack of such MEA-based exposure setups and growing interest in neuronal investigations, a new MEA-based system for electrophysiological recordings was developed based on an open transverse electromagnetic (TEM), cell in collaboration with the group of Philippe Lévêque at the XLIM laboratory in Limoges. This exposure system is well defined, with detailed dosimetric characterization, as recommended by the World Health Organization (WHO) research agendas.

The present document is organized in five chapters starting with this introduction as the chapter 1.

In chapter 2, following a review of the basics of bioelectromagnetics we give a state-of-the-arts report of non-cancer research and, more specifically, on RF interaction with the nervous system, divided into several approaches in terms of biological integration, i.e., studies on populations (epidemiology), humans, animals, and cells. We then describe the neuronal networks from a neuroscience point of view and *in-vitro* electrophysiology techniques.

In chapter 3 we present in detail the materials and methods used: the whole process of culture of primary neurons, exposure system of these cells to RF, and its coupling with a commercial acquisition chain to collect the neuronal electrical activity, an *ad hoc* filter to remove the GSM interferences, and the analysis of the data carried out with a dedicated software.

Preliminary experiments are reported at the beginning of chapter 4, demonstrating the feasibility of the whole project. A large experiment was then performed to increase the statistical power, improve the experimental conditions, and include cultures with different ages. The results are presented in detail in the second part of chapter 4.

Interpretation of the results is given in Chapter 5, where we analyse the effects as a function of different parameters, speculate on the interaction mechanism behind the effects and present analogous published results obtained using exposures to other agents.

In Chapter 6, we describe the new perspectives that this work opens regarding the study of the effects of exposure to RF signals on neuronal tissue functioning. Further research that should be considered is outlined, starting with those experiments that can be done using the equipment already available and continuing with projects that will necessitate extensive development of the equipment and methods.

2 BIOELECTROMAGNETICS AND NEUROSCIENCE REVIEWS

2.1 RF and health

The term radiofrequency (RF) refers to the part of the electromagnetic spectrum (100 kHz to 300 GHz) used for radio communications purposes. Frequency bands within this range have been named formally by the International Telecommunications Union (ITU). Figure 2.1 shows these bands, together with the frequency ranges commonly used for various applications, such as telecommunications, medicine, and industry [AGNIR, 2012].

The everyday use of devices and systems emitting RF electromagnetic fields (EMF) has been increasing rapidly. The possible effects of RF EMF on biological systems have thus been a matter of public concern and scientific discussion. In the context of health risk assessment associated with wireless communications, mainly mobile telephony, research on biological effects has been very active since 1993: about 15 M €/year have been spent on research worldwide.

In the following paragraphs the mobile and wireless communication technologies are described as well as their interactions with the living and the biological effects in the specific case of the nervous system.

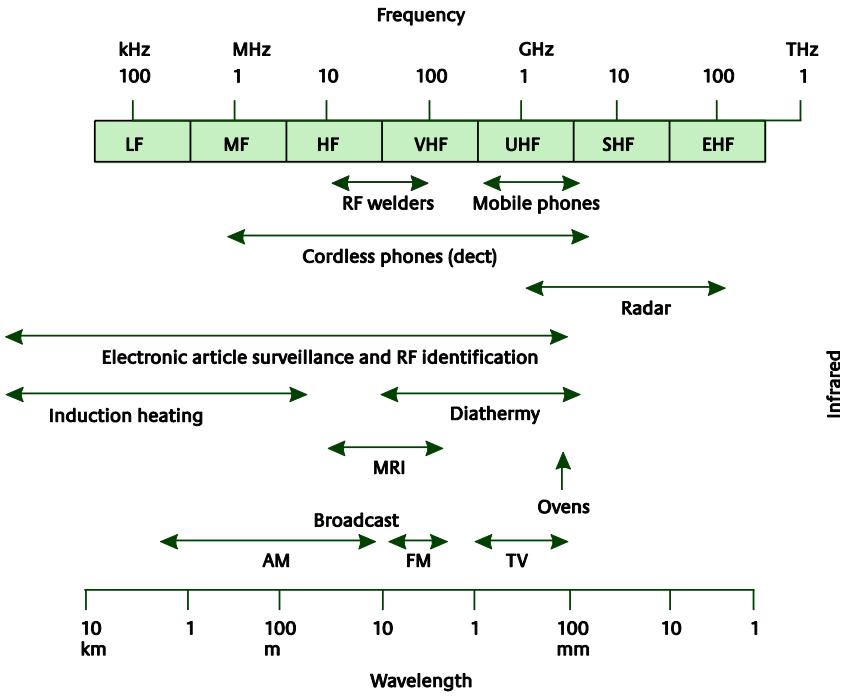

Figure 2-1: RF spectrum and sources. The International Telecommunications Union (ITU) band abbreviations are given as LF, low frequency; MF, medium frequency; HF, high frequency; VHF, very high frequency; UHF, ultra high frequency; SHF, super high frequency; and EHF, extremely high frequency [AGNIR, 2012]

2.1.1 Mobile telephony

The cellular mobile telephone network has undergone a very rapid growth since the early 1980s when analogue cellular radio systems were introduced in Europe. In many countries the penetration is approaching and sometimes exceeding 100%. The number of mobile phone users has reached 5 billions worldwide. This development has proceeded by steps based on the system generations described below which are all digital and based on phase modulation.

Second generation (2G) Systems

2G refers to the initial development of digital mobile communication systems. In Europe and parts of Asia and America, the GSM system has been dominating (GSM or Global Système Mobile). It features carrier frequencies at 900 and 1800 MHz (850 and 1900 MHz in the USA). The bandwidth of each frequency channel is around 200 kHz, and a 9.6 kbits/s data rate for encoded speech. It uses a "time division multiple access" (TDMA) protocol: each user is 'on' for 4.615/8 = 0.58 milliseconds and then on again periodically at a frequency of 217 Hz, (Fig. 2.2). The remaining 7/8 of the time is used for 7 other users. From the RF emission point of view it is a burst type of transmission from the handset. Apart from the access frequency of 217 Hz and its harmonics, there are various control and system signals giving rise to power variations at the frequency of 2 and 8 Hz. Japan has developed its own TDMA system operating in the 1.5 GHz band. North American developed a version of a code division multiple access (CDMA) standard. This version is a direct-sequence spread spectrum system where the users are 'on' simultaneously, but sorted by different codes.

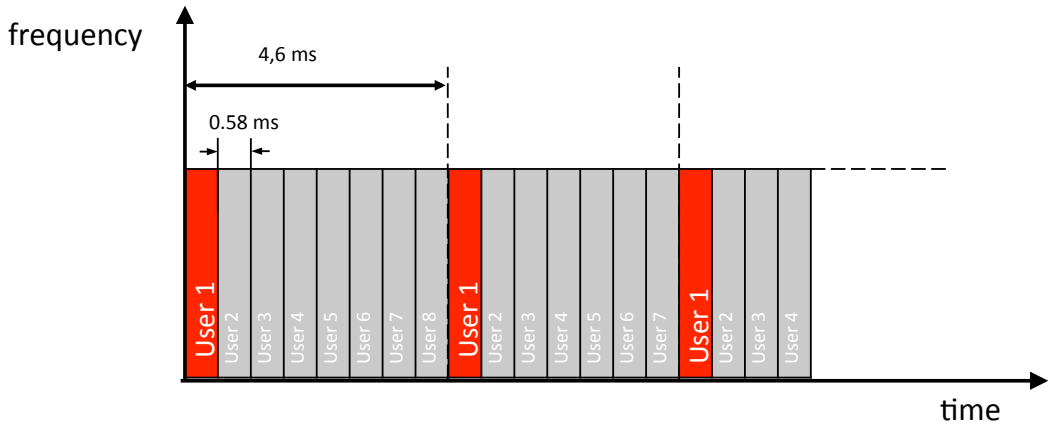

Figure 2-2: GSM TDMA protocol. Each user is 'on' for one out of 8 slots.

2.5G Systems

The popularity of the Internet and of personal computers has created a need for data rates higher than that available with 2G systems, which were designed mainly for voice applications. One of the systems that evolved was the "General Packet Radio Service" (GPRS) which supports a data rate of up

to 140.8 kbit/s and is packet based rather than connection oriented. It is deployed in many places where GSM is used. GPRS achieves the higher data rates by combining several timeslots. Another such system, "Enhanced Data rates for GSM Evolution" (EDGE) is an add-on enhancement for 2.5G GSM and GPRS networks and can carry data up to 236.8 kbit/s with 4 time slots.

3G Systems

3G has been deployed extensively in the last years and is known in Europe as "Universal Mobile Telecommunications System" (UMTS). It operates at frequencies between 1900 and 2200 MHz. Mobile phones are no longer used simply for voice communications, as users now ask for video games, email access, internet browsing, video telephony, high-speed data access and music downloads. Hence the requirement for 3G is for higher data rates, which can be as high as 2 Mbits/s. The global standard for 3G wireless communications, IMT-2000, is a family of 3G standards adopted by of the ITU. It includes the UMTS and wideband CDMA, or W-CDMA. The common feature is the use of spread spectrum as the dominant access scheme for multiple users.

CDMA-2000 is the North American version of the 3G protocol. It differs from UMTS mainly in the network architecture. CDMA-2000 uses one or more 1.25 MHz channels for each direction of transmissions. The specific frequency bands are 1885-2025 MHz and 2110-2200 MHz, for uplink (from user to base station) and downlink, respectively. W-CDMA (UMTS) uses a pair of 5-MHz channels, one in the 1900 MHz range for uplink and one in the 2100 MHz range for downlink. Thus, UMTS has wider bandwidth requirements. UMTS supports up to 2 Mbit/s data transfer rates, although rates can drop markedly in a heavily loaded site.

LTE/4G

LTE is a standard for wireless data communications technology and an evolution of the GSM/UMTS standards, which is paving the way for the coming 4G. It is being deployed in many countries worldwide. The goal of LTE is to increase the capacity and speed of wireless data networks. A further goal is the redesign and simplification of the network architecture to a system with significantly reduced transfer latency compared to the 3G architecture. The LTE wireless interface is incompatible with 2G and 3G networks, so that it must be operated on a separate wireless spectrum.

The LTE specification provides downlink peak rates of 300 Mbit/s and uplink peak rates of 75 Mbit/s. LTE has the ability to manage fast-moving mobiles and supports multi-cast and broadcast streams.

2.1.2 Exposure assessment and dosimetry

Electromagnetic waves that are produced by sources far from the body, such as base stations (Fig. 2-3), are characterised by their carrier frequency, their direction and their incident power, S, expressed in watts per square metre (W/m^2).

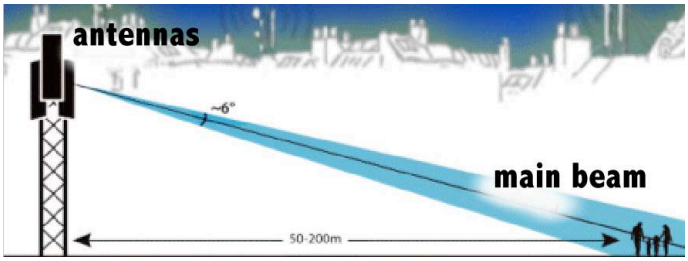

Figure 2-3: RF field emitted by a mobile telephony base station.
The main beam hits the ground 50-200 m from the base station.

These waves propagate at the speed of light and the power they transport decreases with the square of the distance. They are both reflected by the organism (around 50 % of reflection around one GHz) and absorbed inside the tissues.

When waves are absorbed by biological tissue, they interact mainly with water (around 60 % of the mass of tissues). As long as the body can dissipate the heat through thermoregulation, thanks to blood circulation in particular, there is no rise in temperature. If the power is sufficiently high, as in a microwave oven, the absorption leads to consequent heating via dielectric relaxation (Fig. 2-4), which is also profitably used in medical and industrial applications.

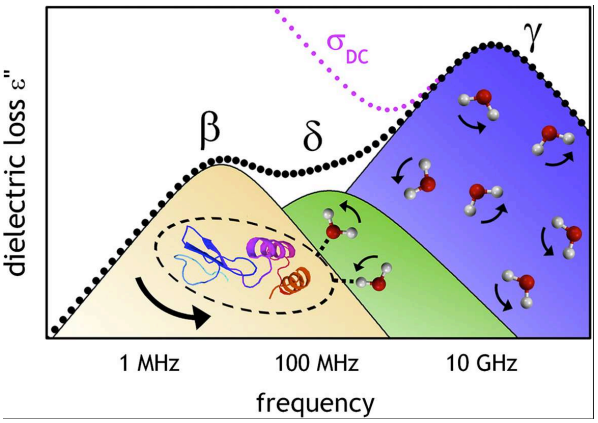

Figure 2-4: Schematic of the dielectric relaxation phenomenon.

RF waves propagate in biological tissues and are rapidly attenuated therein in an exponential manner. At frequencies of around one GHz, the penetration depth is approximately 3 cm. Propagation inside tissues (absorption and reflection) depends to a large extent on the electrical properties, or more precisely the “dielectric” properties, of the tissues, themselves a function of the water content and the frequency. Thus, biological fluids such as blood absorb more than bones, which contain little water.

The absorption of RF waves is quantified with the specific absorption rate SAR, a metric expressed in watts per kilogramme (W/kg). This represents, either at the level of the whole body or locally, the absorbed power per unit of tissue mass.

Existing exposure standards are based on acute effects recognised as being due to heating above a

certain power level. In particular, alterations in the behaviour of small animals exposed to levels exceeding 4 W/kg have served as reference.

The positioning of the mobile telephone against the head during communications has led to a large number of dosimetry studies (Fig. 2-5). Measurements on experimental phantoms suggest that half of the energy is emitted away from the head while the other half is absorbed by the head (half of it by the skin). For a typical mobile phone the maximum power absorbed by the head over 10 g is around 1 W/kg. In normal use, the absorbed power drops to around 0.3 W/kg in the GSM case and 1/100 of that level for a 3G phone to be compared to the exposure limit of 2 W/kg over 10 g [ICNIRP 1998].

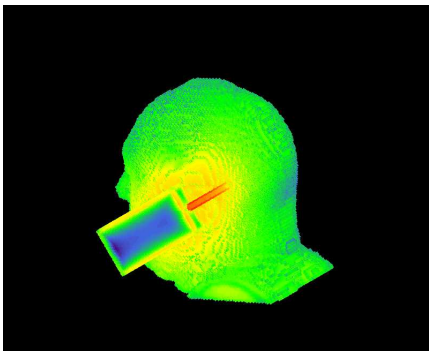

Figure 2-5: dosimetry studies of the energy absorbed by the head during mobile telephone communications.

For distant sources such as base stations, electromagnetic field measurements are carried out to check that the levels of whole-body exposure of users are below the limits recommended by regulations (4.5 W/m^2 for the general public at 900 MHz). Antennas are used along with spectrum analysers to determine, at a given site, the instantaneous field level as a function of frequency.

Calculations have been performed on numerical models of heads and bodies (animals, humans), as a function of sex and age, which make it possible to determine the deposition of energy in the tissues. The quality of such calculations has improved to a great extent over the last few years thanks to the better accuracy of models (using 0.5 mm voxels), the use of sophisticated software and mathematical methods, and greater computing power.

2.1.3 Interaction with living matter and biological effects

Heating within the tissues is negligible during the exposures linked to wireless communications applications: exposure limits are set 50 times below the critical level which corresponds to the lowest known thermal effects (4 W/kg for whole-body exposures and 100 W/kg for local exposures). Typical levels encountered in mobile telephony are ca. 1/10000 below the exposure limit for the distant base stations and 1/100 for 3G phones next to the head). Therefore, research into the health effects of RF needs to focus on the possible non-thermal effects.

Health risk assessment, which is based on the analysis of the results published in scientific reviews, has shown the importance of replication studies to ensure that the biological effects described by one

research team are reproduced by one or more independent teams. Results that cannot be reproduced after several attempts are no longer taken into account in the risk analysis. This is not specific to bioelectromagnetics, but common to all studies that aim to highlight the effects of low-level exposures to chemical or physical agents. The quality of the research and evaluations has progressed very significantly over the last ten years, particularly thanks to the progress made in the management of exposure systems and dosimetry.

The research activity is divided into several approaches in terms of biological integration, i.e., studies on populations (epidemiology), humans, animals and cells.

The study of biological effects and health effects in the RF range addresses several topics usually classified as cancer and non-cancer endpoints. The present work belongs to non-cancer research and more specifically to the RF interaction with the nervous system. Therefore the review below concerns only the state of the science related to this research topic.

2.1.4 State-of-the-art: RF and Central Nervous System

Epidemiology

Besides the epidemiological studies on tumours of the head affecting the central nervous system (CNS), there are no published reports of effects on the nervous system *per se*.

Electrosensitivity

Some people claim that their health is affected by exposure to man-made electromagnetic fields (EMF). They report that exposure to EMF causes any one of a number of symptoms, including headache, vertigo, sleeping problems, diminished concentration, and itching or tingling feelings. While the type of symptoms that are reported is similar to the type of symptoms commonly experienced by many people in their day-to-day life, people who attribute symptoms to EMF often report more symptoms, or more severe symptoms, than other people [Rubin et al., 2011; Baliatsas et al., 2012].

People who attribute symptoms to EMF exposure often describe themselves as being sensitive or hypersensitive to EMF. As a result, patients, self-help groups and the media often call the condition ‘electrosensitivity,’ ‘electromagnetic hypersensitivity’ or other similar names. Because it is not scientifically proven that EMF exposure can cause these types of symptoms, scientists and others working in the area often use the term Idiopathic Environmental Intolerance attributed to EMF (IEI-EMF; WHO, 2005). “Idiopathic” means that the mechanism and triggering factors for the symptoms are unknown. “Environmental Intolerance” refers to the fact that it is a factor in the environment that is reported as triggering the symptoms.

Human studies on cognitive function, sleep, hearing, and EEG.

Investigations on the EEG can be divided into three approaches: 1) resting EEG measured by

assessing the power in each frequency band, 2) EEG during sleep which, among other things, monitor the various sleep phases, most studies being conducted by exposing volunteers to RF before sleep, 3) evoked potentials, which correspond to the change in electrical potential generated by the nervous system in response to external stimulation, sensory or cognitive activity, that can be recorded using EEG.

Many quality articles (i.e., with proper dosimetry and biological protocol) have been published on the effects of radiofrequency (RF) fields from mobile phones on sleep and EEG in humans [reviewed in: Kwon et al, 2011; Regel & Achermann. 2011; AGNIR 2012; SSM 2013].

Most of the research has been carried out by the groups of Hämäläinen [Haarala et al, 2004, 2007] and Hietanen in Finland, Achermann in Switzerland [e.g., Regel et al, 2007], Thuroczy in Hungary [e.g Stefanics et al, 2008], Croft in Australia [eg. Croft et al, 2010] and Danker-Hopfe in Germany [Sauter et al., 2011]. In Italy several groups have performed studies on EEG [Curcio et al, 2005; Vecchio et al, 2010]. In France, few studies have been done on the EEG in humans. The group of G. Faucon in Rennes in collaboration with R. Seze of the INERIS had studied the effects of RF on the auditory evoked potential [Maby et al., 2005].

From a thorough analysis of the literature we can conclude that: 1) no effect on cognitive function and hearing has been established, 2) effects on sleep have been reported but are not consistent among research groups and 3) studies show effects of GSM signals on the intensity of the alpha band of the EEG, while an unmodulated signal, continuous wave (CW), does not produce such effects.

Some recent studies, which have not been included in the review articles cited above are described below:

- In its study of the effects of RF on 'spindles' during sleep, the Swiss team of P. Achermann exposed 30 volunteers for 30 min before the night's sleep to a signal at 900 MHz, modulated at 14 or 217 Hz [Schmid et al., 2012]. Exposure at 14 Hz significantly increased the contribution of 'spindles' during non-REM (Rapid Eye Movement) sleep while only a tendency to increase was observed at 217 Hz. A large inter-individual variability was evident.
- These results were confirmed in an Australian study [Loughran et al., 2012] in which 20 volunteers were exposed to 900 MHz GSM signal at 0.6 W/kg. The spectral power of the EEG was increased in the range of spindles during non-REM sleep again. The importance of inter-individual variability was also highlighted.
- The team of P. Achermann has recently studied the effects of RF on 22 teenagers [Loughran et al., 2013]. The EEG recording was performed on vigil subjects after a 30 min exposure. No alteration of the EEG was observed.

- The same team conducted a sleep study involving 16 volunteers exposed to a RF signal modulated at 0.8 Hz [Lustenberger et al., 2013]. The goal was to observe the effects of RF on the slow-wave activity (SWA). The SWA activity was increased after exposure to the modulated signal but not in CW exposures. The spindle activity was not affected. The authors interpreted these results as an action of RF on the renormalization of cortical excitability during sleep.
- An Estonian study involved 20 volunteers exposed to 450 MHz modulated at 40 Hz, at two low SAR levels (3 and 303 mW/kg) [Suhhova et al., 2013]. The EEG recording on vigil volunteers with closed eyes was carried out with 10 cycles of exposure (ON-OFF) lasting 1 min each. A significant increase in power was observed in the beta2 (157%), beta1 (61%) and alpha (68%) bands at the highest SAR level.
- A new study by the Australian group of R. Croft [Perentos et al., 2013] contradicts the common observation of a greater effect of modulated RF signals at low frequency. In this protocol, 72 volunteers were exposed to successively (crossover design) modulated RF signals (average SAR 0.06 W/kg) or CW (average SAR of 1.95 W/kg). The EEG recording was performed on vigil subjects with eyes open showed that RF caused a weakening of the alpha band and CW signals were as effective as the modulated signals with a mean SAR that were 325 times larger!
- The Hungarian group of G. Thuroczy used the UMTS signal on 17 volunteers exposed for 30 min at a 10 g SAR of about 1 W/kg [Trunk et al., 2013]. No alteration of the EEG spectrum was observed. These results suggest that high quality "modulation" as is present especially in the GSM signal is required for obtaining an effect on the EEG, because the UMTS signal does not have a recurring spectral component.

There are several studies on the EEG in humans exposed to RF in the literature, but, because of the various experimental conditions, there are no well-established effects. However, the consensus is that the corresponding potential health effects are probably negligible. Nonetheless, it is important to understand how these non-thermal biological effects can be produced by low-level RF exposure.

The other conclusion is that the effects described in these studies are not generally associated with effects on cognitive function [Van Rongen et al, 2009; AGNIR 2012].

Animal studies

Brief descriptions of the published results are given in chronological order:

- In 1994, a Hungarian team [Thuróczy et al., 1994] published results on the effects of whole-body RF exposure on the EEG of anesthetized rats. In this study, the total spectrum of the EEG increased after a CW 10 min exposure at 2.45 GHz at 30 but not at 10 mW/cm^2 (SAR level not calculated but equivalent to about 10 W/kg, i.e., a thermal level). Power in the delta

band (0.5-4 Hz) was increased by a CW localized exposure of the head at 4 GHz and 42 W/kg (corresponding to a temperature rise of 2 °C). The beta band (14.5 to 30 Hz) was increased by exposure at 4 GHz, modulated at 16 Hz, and 8.4 W/kg (non-thermal level), while the equivalent CW signal did not alter the EEG. One limitation of this study showing positive results is that the animals were anesthetized.

- In the USA, Beason and Semm exposed birds (zebra finch) to a GSM 900 signal at 0.05 W/kg using a three-phase protocol (pre-exposure, exposure and post-exposure) of 10 min each [Beason & Semm 2002]. They recorded 133 active sites on 34 birds. Most sites (76%) saw their electrical activity increased by a factor of 3.5 as a result of GSM exposure. In this study showing effects, the animals were anesthetized.
- A Russian team reported effects of 1 min 800 MHz exposure of brains of anesthetized but not immobilized rabbits Chizhenkova 2004]. The power levels were 0.2 to 40 mW/cm^2 but the corresponding SAR level was not calculated. Electrodes were placed in the sensorimotor area of the cortex. Depending on the power level, the values of both recorded parameters (intervals between spikes and frequency of bursts) were modified by exposure. The main weakness of this study was the lack of accurate dosimetry.
- A French team has investigated the effects of exposure to GSM 1800 signals on unconstrained rats in an anechoic chamber at SAR levels of 71-530 mW/kg (in the head) [Crouzier et al., 2007]. The EEG recorded with implanted electrodes was not altered as a result of 24 h RF exposures.
- Rats were exposed by a Spanish team to a GSM signal and the action of picrotoxin which is an inhibitor of GABA ion channels and causes epileptic seizures [López-Martín et al., 2009]. Exposure to RF (30-260 mW/kg in the brain) caused a synergistic effect of picrotoxin with the GSM signal which was more effective than the CW signal.
- In Russia, eight rats were exposed to 945 MHz RF signal (0.1-0.2 mW/cm^2) modulated at 4 Hz for 10 min [Vorobyov et al., 1997]. The rats were implanted with electrodes in the cortex and the EEG was altered only during the exposure for the first 20 s in the range of 10-14 Hz. The authors suggested that this effect could be due to interference of the EEG electrodes with the RF. These results highlight the care that must be taken to eliminate such interference.
- In 2010, Vorobyov and his Serbian colleagues exposed ten free moving rats to an RF signal (915 MHz, 0.7 W/kg whole body, 10 min) [Vorobyov et al., 2010]. The power in the beta band of the EEG (from 17.8 to 30.5 Hz) was significantly increased in the hypothalamus compared to the cortex. The authors concluded that the effects of RF were clearly observable in the EEG.

Cell Studies

Brief descriptions of the published results are given in chronological order.

- Studies on excised neural studies began in the '70s in the USA by the Wachtel and the Guy groups who aimed at assessing the effects of pulsed and CW RF at high power (i.e., up to 100 W/kg time-averaged power). In most experiments large neurons were excised from rabbits [Courtney et al., 1975], Aplysia marine gastropods [Wachtel et al., 1975], cats and frogs [Chou and Guy, 1978]. Nerves were usually exposed inside waveguides, most investigations being performed at 2.45 GHz and others at 1.5 GHz. In overall conclusion, most of the positive findings were evidently thermally induced at high SAR levels. However, the electrophysiological techniques available at the time were not at all as sophisticated as they are now and therefore a lot of information was missing about the electrical activity of the neurons and *a fortiori* on neuronal networks. In some of these reports only the vitality of the neurons (refractory period as a function of exposure duration) was assessed [McRee and Wachtel, 1980, 1982].
- Rat hippocampal slices were exposed by a British team [Tattersall et al., 2001] at 700 MHz (CW, 5-15 min, low SAR of 1.6 to 4.4 mW/kg). The effect of RF was studied in the presence of aminopyridine which induces epileptic activity. Under exposure, the epileptic activity (burst type) were reduced or abolished in 36% of the slices tested. Any field-induced rises in temperature were too small to be detected even using sensitive measuring equipment. Imposed temperature changes of up to 1°C failed to mimic the effects of RF exposure. However, it was later reported that significant heating occurred at the tip of the metallic stimulating electrode at much higher SARs (7-10 °C at 0.4 W/kg) which may have influenced these results.
- The same British group investigated the effects of Terrestrial Trunked Radio (TETRA, 400 MHz pulse modulated at 17.6 Hz, 25% duty cycle) fields on intracellular calcium signalling in excitable cells (cerebellar granule cells and cardiac myocytes) using fluorescent probes [Green et al., 2005]. There was no change in calcium concentration at SAR levels from 5 mW/kg to 0.4 W/kg.
- Exposure of rat hippocampal neurons was made by a Chinese team (GSM 1800, 2.4 W/kg) [Xu et al., 2006]. Exposure decreased the excitatory synaptic activity as measured by the patch-clamp technique.
- Studies carried out by an Italian team on rat neurons were performed at 900 MHz (GSM and CW, 1 W/kg) and single potassium channel currents activated by calcium measured by patch-clamp [Marchionni et al. 2006]. No effect was observed under RF exposure.
- An Italian team exposed rat cortical neurons to a GSM 900 (2 W/kg) and to CW signals and

measured the barium currents through voltage-gated calcium channels using the patch clamp technique [Platano et al., 2007]. No effect was observed.

- An attempt was made to measure the activity of neural networks in RF exposure in Germany by the group of J. Gimsa in Rostock [Koester et al., 2007]. In this investigation, neurons were exposed to a UMTS signal in MEAs placed in a waveguide. Effects on the electrical activity were observed but, according to the authors, they were due to an increase in temperature. This project was not pursued due to lack of funding, but the authors have helped us with their advice during a visit to Rostock.
- More recently, the German group of C. Thielemann published an article describing the GSM exposure of 3D cell cultures on MEA [Daus et al., 2011]. The exposure system is similar to ours and was characterized in terms of dosimetry though the cells were excitable cardiac myocytes instead of neurons.

Current research is focused largely on the effects of RF non-thermal nature on the nervous system and therefore it becomes necessary to use cell and animal models to determine if effects exist and can be characterized and complement human observations. Moreover, the observed effects are at the macroscopic scale (e.g., EEG) where observations are "averaged" over the cortex and it is desirable to decrease the scale of complexity.

In this context our project may bring a substantial improvement in the understanding of the real-time response of electrical activity of neuronal networks to RF exposure, at non-thermal levels.

In our system, a mobile telephone GSM signal is applied to study neurons in culture, using an extra-cellular electrophysiology technique. The aim is to observe whether potential effects exist and to determinate their mechanism.

Our exposure system is well defined, with detailed dosimetric characterization, as recommended by the World Health Organization (WHO) in its EMF Project 2006 RF research agenda and recently reconfirmed in the 2010 update.

2.2 The Central Nervous System

The nervous system is divided into the central nervous system (CNS) and peripheral nervous system (PNS). The whole system is responsible for receiving, interpreting and sending information from and to all reachable parts of the body. The nervous system monitors and coordinates internal organ function and responds to changes in the external environment.

The close proximity between the mobile phone and the brain and the fact that neurons are excitable cells make the CNS the most likely target of RF exposure. Experimental studies in humans on EEG and sleep under RF exposure support this hypothesis and foster the need for understanding the

interaction mechanisms of RF effects on neuronal networks.

The CNS is the processing centre for the nervous system. The two main organs of the CNS are the brain and the spinal cord. The brain processes and interprets sensory information sent from the spinal cord. Neurons are the basic unit of the nervous system and are described below.

Glial cells compose a voluminous support system that is essential to the proper operation of nervous tissue and the nervous system. Unlike neurons, glial cells do not conduct nerve impulses. Glia performs a plethora of functions in the nervous system, which include providing mechanical support for the brain, assisting nervous system repair, development, and providing metabolic functions for neurons. There are several types of glial cells (Fig. 2-6). Astrocytes have important functional roles: they contribute to gliosis, which is a healing process for the nervous system. They are also present at synapses to capture the neurotransmitters, or at the capillaries to form the blood-brain barrier. They also have a role in transport of molecules and supply neuron with lactate. Microglial cells have the potential to regulate the development, structuring, and function of neuronal networks. They monitor the status of synaptic contacts and receive information from the networks. Microglial cells may also be able to remodel neuronal connectivity and participate in physiological processes within neuronal networks. The multiple activation states of microglial cells may explain the existence of "resting active" microglia, or even "active" compartments in the processes of surveillance microglia, which dynamically interact with neuronal circuitry and contribute to their plasticity. Oligodendrocytes are central nervous system structures that wrap some neuronal axons to form an insulating coat known as the myelin sheath which allows faster electrical signal transmission.

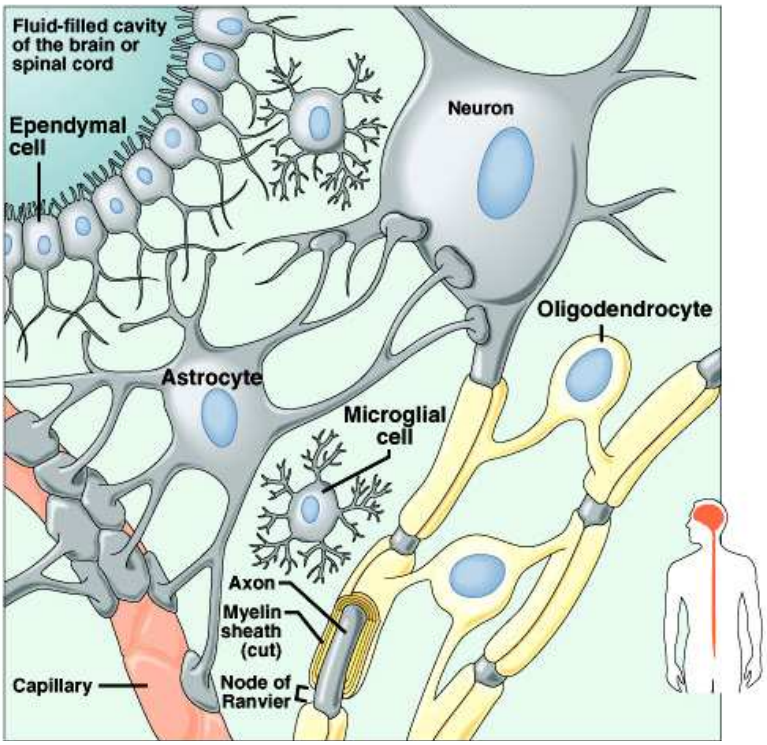

Figure 2-6: Types of glia cells around a neuron [Shier, Butler and Lewis – Human anatomy and Physiology, McGraw-Hill, 2007].

2.2.1 Basic morphological features of neurons

In the brain, neurons share a number of common features. They are different from most other cells in the body in that they are polarized and have distinct morphological regions, each with specific functions (Fig. 2-7). Dendrites are the region where one neuron mainly receives connections from other neurons. The cell body or soma contains the nucleus and the other organelles necessary for cellular function. The axon is a key component of nerve cells over which information is transmitted from one part of the neuron (e.g., the cell body) to the terminal regions of the neuron. Axons can be rather long, extending up to a meter or so in some human sensory and motor nerve cells. Chemical synapses are terminal region of the axon where one neuron forms a connection with another and conveys information through the process of synaptic transmission. One cortical neuron can receive contacts from up to 10,000 other cells. Consequently, the potential complexity of the networks is enormous.

A presynaptic cell is not directly connected to the postsynaptic cell. The two are separated by a gap known as the synaptic cleft. Therefore, to communicate with the postsynaptic cell, the presynaptic neuron needs to release a chemical messenger. That messenger is found within the neurotransmitter-containing vesicles. An action potential in the presynaptic terminal causes these vesicles to fuse with the inner surface of the presynaptic membrane and release their contents via exocytosis. The released transmitter diffuses across the gap between the pre- and the postsynaptic cell and very rapidly reaches the postsynaptic side of the synapse where it binds to specialized receptors that "recognize" the transmitter. The binding to the receptors leads to a change in the permeability of ion channels in the membrane which leads to a change in the membrane potential of the postsynaptic neuron known as a postsynaptic potential (PSP). Therefore signalling among neurons is associated with changes in the electrical properties of neurons.

The ability of the connection, or synapse, between two neurons to change in response to transmission over synaptic pathways is called synaptic plasticity. Plastic changes also result from the alteration of the number of receptors located on a synapse. There are several underlying mechanisms that cooperate to build up synaptic plasticity, including changes in the quantity of neurotransmitters released into a synapse and changes in how effectively cells respond to those neurotransmitters. Since memory works via vastly interconnected networks of neurons in the brain, synaptic plasticity is one of the important neurochemical foundations of learning and memory [Hebb, 1961].

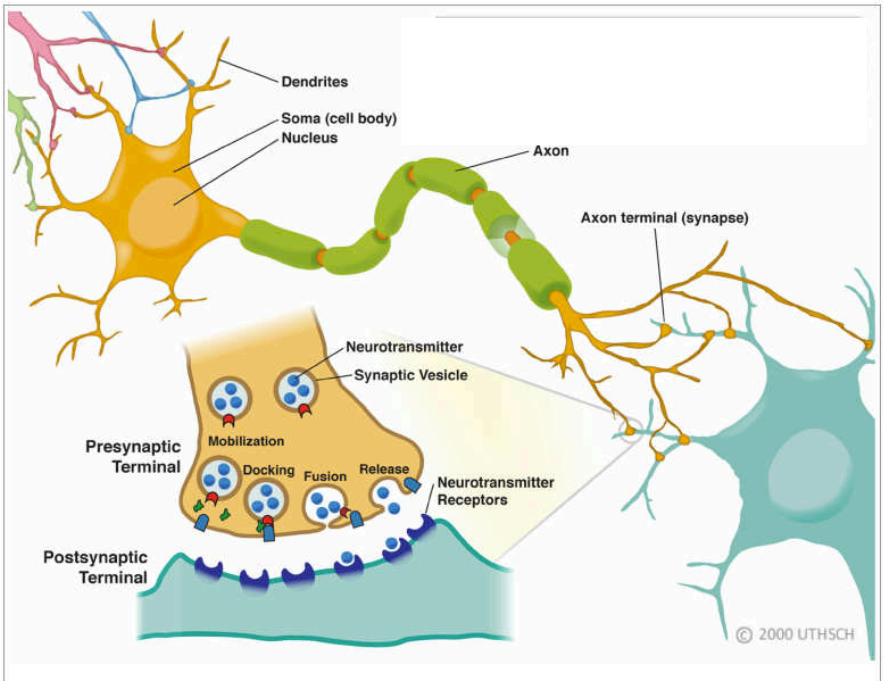

Figure 2-7: Neuron with synaptic input and connected to a postsynaptic neuron. Bottom left: expended view of the synapse [http://neuroscience.uth.tmc.edu/s1/introduction.html].

2.2.2 Resting Potentials and Action Potentials

A potential of about –60 millivolts inside, negative with respect to the outside, is recorded. This potential is called the resting potential and is constant for indefinite periods of time in the absence of stimulation. All cells in the body have resting potentials. What distinguishes nerve cells and other excitable membranes (e.g., muscle cells) is that nerve cells membrane potential can change thus integrating and transmitting information while in the case of muscle cells, it produces muscle contractions.

Neurons are electrically active cells. This stems from the fact that the ionic distributions across the membrane can be modified by fluxes through channels the opening of which depend on the transmembrane potential.

The main ions to be considered are sodium (Na^+), potassium (K^+), calcium (Ca^{2+}) and chloride (Cl^-). Ion pumps (for sodium-potassium and calcium ions) ensure that there is a gradient between extracellular and intracellular concentrations: the cell contains higher concentration of K^+ ions and lower concentrations of Cl^-, Na^+ and Ca^{2+} with respect to the extracellular medium. Taking into account the selective ion permeability through the cell membrane, these concentration gradients build up an electrical potential, i.e. the resting potential, of about -60 mV (fig. 2-8).

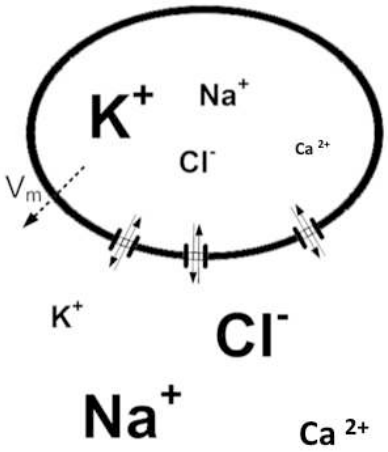

Figure 2-8: schematic representation of main ion concentrations inside and outside the cell.

In 1952, Hodgkin and Huxley discovered the existence of selective ion gates (channels) in the cell membrane. Furthermore, they discovered that the conductance of these gates changes depending on the voltage across the membrane. In the resting state these ion gates are closed.

Some extracellular event (i.e. a stimulus) can change the cell membrane potential. When the voltage across the membrane reaches a certain level, the Na^+ channels open, setting off the influx of Na^+ ions into the cell. The membrane is depolarized, i.e. the voltage rises from –60 to 30 mV. This is followed by repolarization which is the result of the opening of the voltage-sensitive K^+ channels and the efflux of K^+ ions and the inactivation of the Na^+ channels. Figure 2-9 shows a typical shape of a neuronal membrane potential. After each fired action potential there follows a silent period (i.e. refractory period) during which another impulse cannot be fired. The "typical" action potential is a transitory event lasting about 1 ms with a refractory period of 2 to 3 ms.

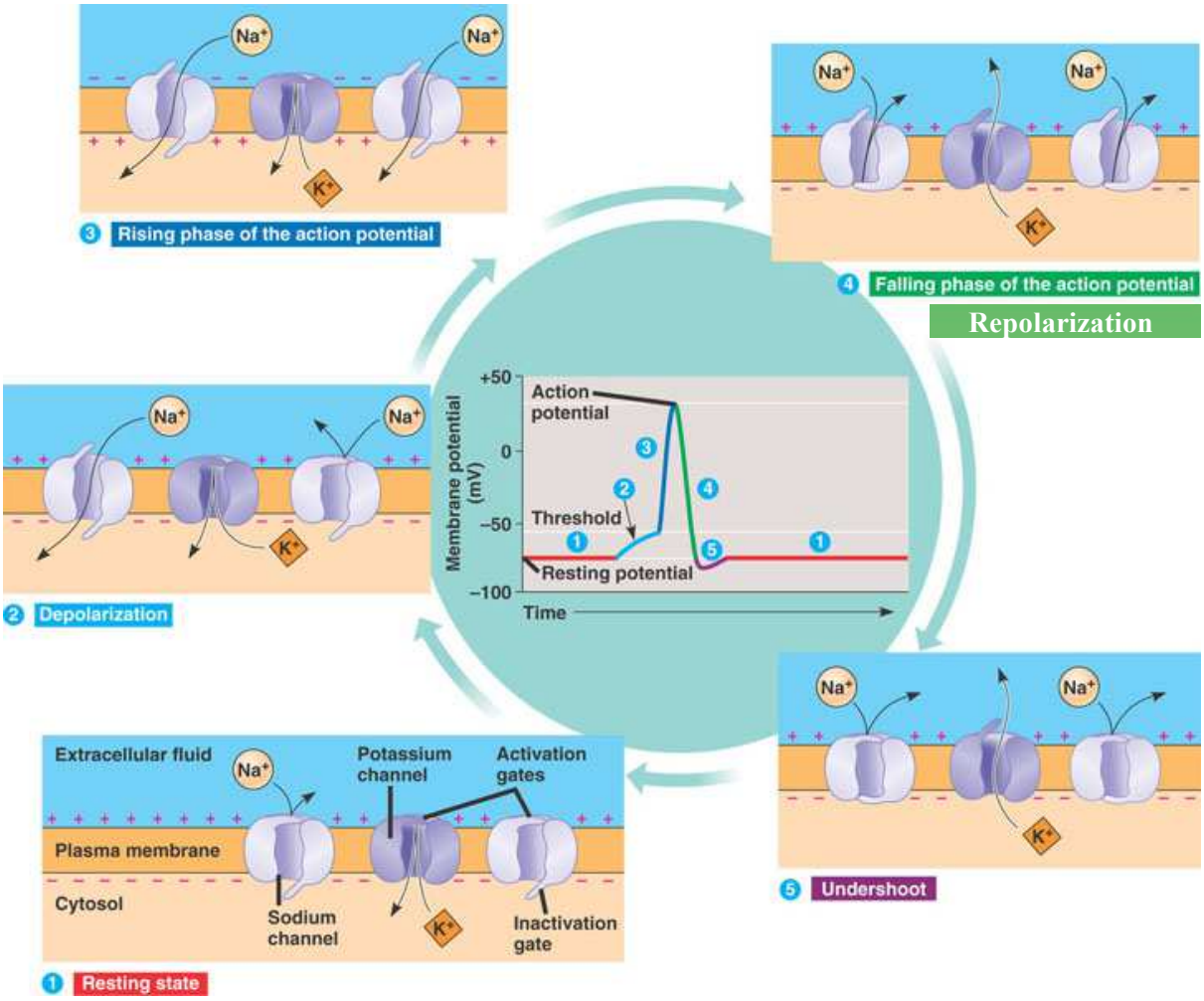

Figure 2-9: Neuronal membrane potential and expanded views of each phase [http://home.sandiego.edu/~gmorse/2011BIOL221/studyguidefinal/Studyguide_final.html]

2.2.3 *In-vitro* neuronal network

Our main motivation for using *in-vitro* neuronal networks is the assumption that the organizing principles operating at the level of neuronal populations *in vivo* are intrinsic to neurons and therefore manifested in *in-vitro* cultured networks.

Spontaneous neuronal activity refers to the activity that is not attributable to specific sensory inputs or motor outputs; it represents neuronal activity that is intrinsically generated by the brain. Its most obvious manifestation is during sleep where the main sensory inputs and motor outputs are absent. But neuroimaging studies indicate that, even during waking states, brain regions unrelated to a specific task or function are active [Fox & Raichle, 2007].

Spontaneous activity emerging from cultured networks usually appears at the end of the first week in vitro and fast sequences of spikes, named bursts, emerge during the second week (van Pelt et al., 2004). Once the network has reached its mature state (from the third week *in vitro* on), it exhibits

network bursts, sequences of synchronized single-channel bursts, which spread across all or part of the MEA [Eytan et Marom, 2006; Chiappalone et al. 2007]. These pattern structures are hypothetically correlated with the activation of different functional groups of cells in the network [Baruchi et al. 2008, Pasquale et al. 2010].

In the intact brain or spinal cord, bursts can be observed as motor patterns, sensory gates, sleep spindles, UP-states, developmental signals, epileptiform activity, or memories [Steve M. Potter, 2008]. Bursting behaviour is influenced by the age of the culture, chemical/electrical stimulation or environmental conditions.

Differently from the *in-vivo* condition, where bursts usually are 'rare' events, with features strongly correlated to the experimental subject and to the portion of the brain in which the electrode is placed [Cocatre-Zilgien and Delcomyn 1992; Metzner et al. 1998; Reinagel et al. 1999], the *in-vitro* bursts are a dominant element of recordings, whose main features, in the mature state, are quite homogeneous also among different labs [Marom and Shahaf 2002; van Pelt et al. 2005; Wagenaar et al. 2006].

2.3 Electrophysiology techniques

Electrophysiology involves measurements of voltage or electric current on a wide variety of scales from single ion channel proteins to whole organs like the heart. Recordings of large-scale electric signals from the nervous system such as electroencephalography (EEG) may also be referred to as electrophysiological recordings. It includes measurements of the electrical activity of neurons, and particularly action potentials. At the cellular level, there are two complementary electrophysiological approaches: intracellular and extracellular. Intracellular recordings form a group of techniques used to measure with precision the voltage across, or electrical currents passing through, neuronal or other cellular membranes by inserting an electrode inside the cell.

To make an intracellular recording, the tip of a fine (sharp) microelectrode must be inserted inside the cell, so that the membrane potential can be measured. Typically, the resting membrane potential of a healthy cell is -60 to -80 mV, and during an action potential the membrane potential may reach +40 mV. A disadvantage of intracellular technique is that the recording device may damage the cell, and therefore, affect the neuron's real spiking activity.

In the extracellular approach, the electrode is in contact with the cell exterior or extracellular medium so the membrane potential is measured indirectly through the induced electrical field.

An example of extracellular recording device is the MEA (microelectrodes array): a set of metallic electrodes that measure the extracellular potential of neurons that are at or in a near proximity of an electrode.

In comparison to intracellular measurement techniques such as patch-clamp, the MEA-based

techniques are non-invasive, greatly simplify the experimental setup and importantly, allow simultaneous monitoring and stimulating of many neurons over extended periods of time.

The major disadvantage of extracellular measurements with respect to intracellular ones is the three orders in magnitude decrease of the signal amplitude, as shown in figure 2-10. Typical signal amplitude of an extracellular potential is in the order of a few tens to a few hundreds of microvolts, depending on the cell type and the quality of cell/electrode interface.

The MEAs bridge the gap in the understanding of the brain from a single neuron (i.e. by patch-clamp) to the high level behaviour of the whole brain (i.e. EEG, functional imaging, etc.).

For these reasons, over the last decade MEAs have been widely used for studying neuronal networks in culture.

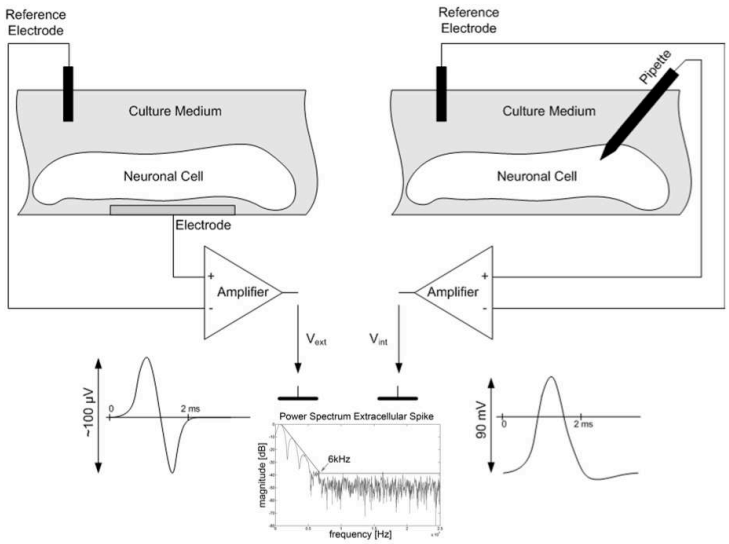

Figure 2-10: Extracellular measurement (left), intracellular measurement (right). The difference in shape and amplitude of the recorded signal can be seen. Moreover, the extracellular technique is non-invasive which can enable long-term recordings (PhD thesis of K Imfeld, Univ. Neuchâtel, 2008).

2.3.1 MEA

MEAs are devices with fixed geometric arrangements of microelectrodes for multisite, parallel electrophysiological recording. MEAs can be divided into subcategories based on their potential use: *in-vitro* and *in-vivo* arrays.

The *in-vitro* use of MEAs for extracellular measurements of dissociated neuronal cells cultures has been a fruitful methodology for investigating learning and memory processes, and effective and rapid screening in pharmacology and toxicology for drug testing.

An overview of *in-vitro* MEA technology is given is Figure 2-11. MEAs may be either purely passive, containing only an array of conductors devoid of active circuitry, or active having on-chip integrated circuitry to carry out on-site computations, multiplexing, and/or pre-amplification. MEAs

with active electrodes are fabricated using C-MOS or EOS-FET technologies. These devices can overcome some of the limitations of passive MEAs, in particular by performing measurements at high spatial and temporal resolutions.

In order to study the effects of RF exposure on neuronal cultures we chose to use passive MEAs to avoid potential interferences of RF fields with the on-board electronic components that are present in active MEAs. Our experimental requirements were fulfilled using passive MEAs.

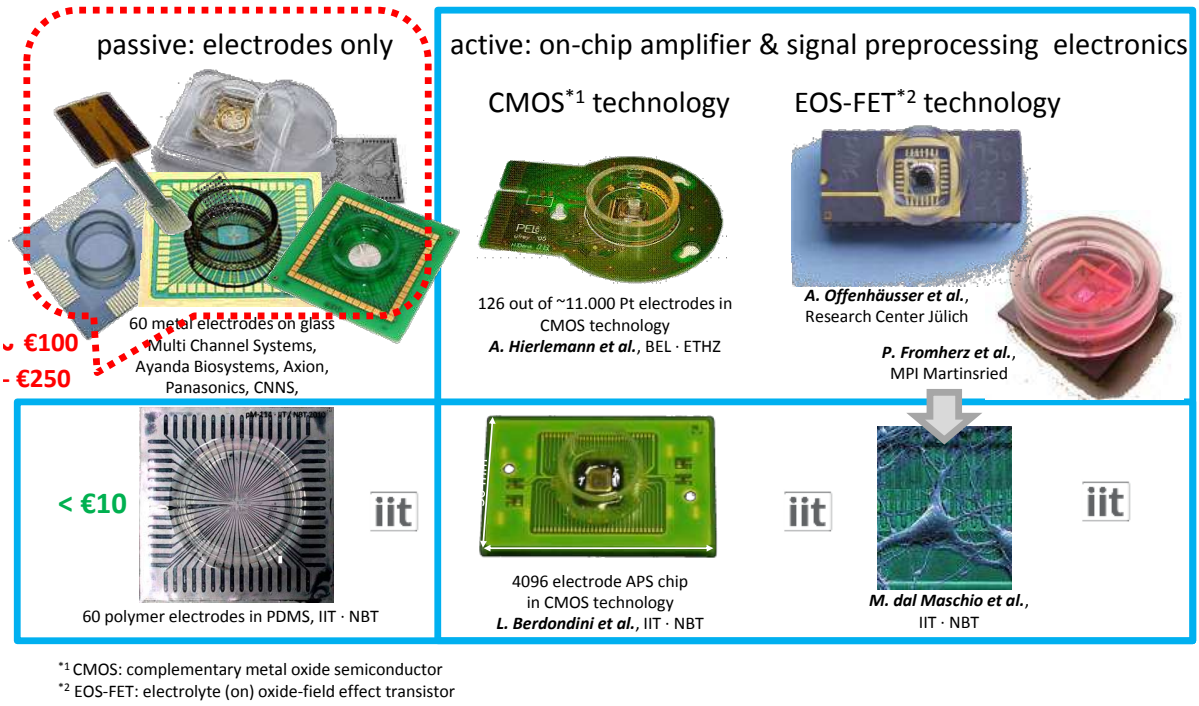

Figure 2-11: Examples of *in-vitro* MEA with their main features and manufacturers [A. Blau]

A typical passive MEA consist of a glass slide onto which an integrated array of extracellular microelectrodes has been photo-etched. Electrode materials are indium-tin oxide (ITO), palladium, platinum, or gold and electrodes tracks are coated with silicon nitride, polyimide (kapton) or SU-8 photoresisit. (Fig 2-12).

The diameter of each electrode ending ranges from 10 to 70 µm, and the electrodes are often set up as a grid with an area of 0.2–2 mm^2. However, the number, size and arrangement of the electrodes can all be custom designed, depending on the application.

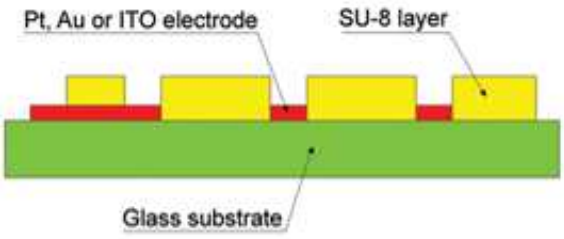

Figure 2-12: Schematic of the cross-section of a microelectrode array chip composed of a glass substrate, patterned platinum electrodes and an SU-8 epoxy insulation layer [www.qwane.com].

Each electrode extends to the periphery of the chip, and makes contact with an external amplifier, which relays the electrical signals to a computer for analogue-to-digital conversion, filtering, signal detection, storage, and analysis. The spatio-temporal pattern of electrical activity (action potentials) is provides important information on network structure and function that is difficult or impossible to obtain using other electrophysiological techniques. Currently, seven manufacturers provide hardware and software for MEA systems (in alphabetical order: Alpha MED Sciences, Osaka, Japan (MED systems formally manufactured by Panasonic); Axion Biosystems, Atlanta, GA; Qwane Qwane Biosciences, Lausanne, Switzerland; 3-Brain, Landquart, Switzerland; MultiChannel Systems, Reutlingen Germany; Plexon, Inc., Dallas TX; Tucker-Davis Technologies, Alachua, FL).

MEA systems offer a great deal of flexibility regarding biological tissues and experimental designs. For example, the electrodes may be planar to allow for a cell monolayer to be grown on top of them, or they may have a three-dimensional arrangement that allows penetration of the electrodes through outer layers of tissue slices thereby enhancing the cell-electrode coupling to cells. In all cases, following use, biological tissues are removed from the MEAs, thereby allowing for multiple reuses.

2.3.2 Cell-electrode interface

MEAs measure the extracellular potential changes that arise at the cell-electrode interface. This electrochemical interface is very complex and many studies have been carried out to understand and model its behaviour. A simplified, but widely used model of the electrochemical interfaces electrode-electrolyte-cell is shown in Figure 2-13.

R_{met} (metallic resistance) models the resistance of the connection path of the microelectrode; C_e models the capacitance of the microelectrode–electrolyte interface; R_e (leakage resistance) accounts for the charge carriers crossing the interface; C_{sh} (shunt capacitance) accounts for all the shunt capacitances to ground. R_{seal} (seal resistance between cell and microelectrode) models how much the cell is attached to the microelectrode, that is, it describes the separation of the cell and microelectrode which results in an extended cleft of electrolyte; it is in parallel to the microelectrode surface (cellular membrane). R_{spread} (spreading resistance) models the signal loss due to the distance between the microelectrode and the cell; it is placed perpendicularly to the microelectrode surface (cellular membrane). C_{hd} (cell membrane–electrolyte interface capacitance) models the polarization layers of the electrolyte solution in front of the cell. H-H model is the Hodgkin-Huxley-Model, a well-known

biophysical model of a neuronal cell [Hodgkin and Huxley ,1952]. Models and measured values can be found in literature [Massobrio et al., 2007]:

R_{seal} = 5 MΩ

R_{spread} = 11.7 kΩ

C_{hd} = 17.45 pF

C_e = 1.14 nF,

R_e = 100 kΩ.

R_e = 0.14 MΩ

R_{met} = 1.5 Ω,

C_{sh} = 5 pF

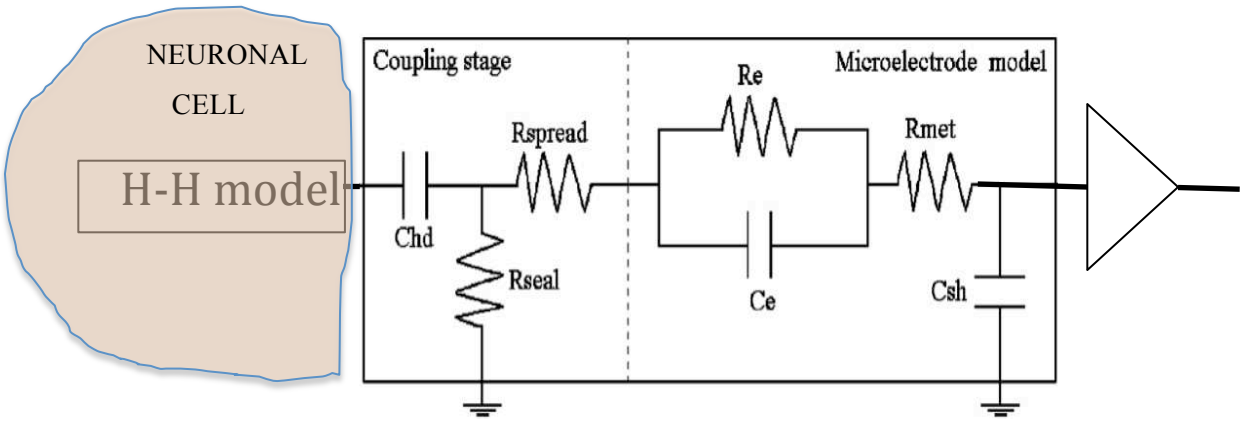

Figure 2-13: Schematic representation of the neuron-electrode interface [Massobrio et al, 2007].

3 MATERIAL & METHODS

We have developed a dedicated experimental setup in the GHz range for the simultaneous exposure of neuronal networks and monitoring of their electrical activity. To collect the electrical activity, primary neurons were cultured on MEA.

Due to the lack of such MEA-based exposure setups and growing interest in neuronal investigations, a new MEA-based system for electrophysiological recordings was developed based on an open transverse electromagnetic (TEM), cell in collaboration with the group of Philippe Lévêque at XLIM in Limoges [Merla et al., 2011].

3.1 Cortical neuronal culture

Initial cell culture protocol

To perform successfully the neuron cultures on the 60-channel planar MEA, dedicated protocols were used. The MEA active area was successively coated with Polyethyleneimine (PEI) and Laminin. Primary neuronal cell cultures were obtained from the cortex of embryonic (E18) Sprague-Dawley rats. Cortices were dissected in DMEM (Dulbecco's Modified Eagle Medium) - Glutamax and treated with trypsin for 25 min. The fragments were subjected to mechanical dissociation using Pasteur pipettes and briefly centrifuged. The supernatant was transferred in a new tube and centrifuged at 140 g for 5 min. The pellet was then successively treated with trypsin, soybean trypsin inhibitor, DNase, and finally centrifuged at 140 g for 5 min. Pellet dissociated cortical cells were suspended in culture medium (neurobasal medium supplemented with 2% B-27, 1% Glutamax, and 1% penicillin/ streptomycin). Each MEA was plated with a suspension of 10^5 cells in a 100 µl volume and kept in a 5% CO_2 incubator at 37 °C in a humidified atmosphere until recording. The culture medium was half-exchanged twice a week (see appendix A for a full description of the protocol).

Coating materials

Various materials were tested for MEA coating in order to find the best attachment and growth of cell cultures conditions.

Two different coatings were tested:

- PEI diluted in borate tampon (PH 8.4) + laminin
- Poly-D-lysine+ laminin

PEI is a synthetic polycation that readily attaches to the slightly negatively charged glass substrate of the MEA. Laminin is a protein that can be found abundantly in the extracellular matrix and binds to specific receptors on the surface of the cells, thereby providing focal points of adhesion.

No remarkable differences was obtained between the 2 coatings, therefore we finally adopted PEI diluted in borate tampon (PH 8, 4) + laminin for practical reasons, as it was the simplest and cheapest approach.

Improve culture protocol on MEA

Overtime cell cultures in MEA did not provide a satisfactory percentage of exploitable cultures so the next step was to improve the experimental conditions.

One prerequisite for recording extracellular signals from planar MEAs is that the neurons must be located in close proximity to the electrodes [Claverol-Tinture and Pine, 2002]. This can be achieved with cells plated at high density (2000 cells/mm^2), which is also required to ensure a healthy culture. To achieve a high-density of neuron growth in the central electrode region of the MEAs we decreased by half the cellular suspension volume deposited, from 100 µl according to the standard protocol to 50 µl, while maintaining constant the final number of cells. This change increased the number of active cultures, and in one case up to 100% of exploitable cultures.

Furthermore, in a second phase, inspired by [Mok et al. 2009], we used 5 mm diameter Teflon tubes to constraint the suspended cells to settle in the MEA electrode region during the seeding, and for the two following hours, before adding 1 ml cell medium after removing the Teflon tubes. This process eliminated definitely the cells not centred in the central electrode region of the MEA.

Moreover, after repeated attempts without successful cultures, we speculated on a possible degradation of the MEA components that prevented the use of each MEA for more than 3-5 times.

A new batch of MEA was bought and tested using simultaneously the previous protocol and another one based on the use of a papain-dissociation protocol (annexe B). This new protocol led to a higher proportion of exploitable cultures.

Recording environment

Recording the neuronal electrical activity was carried out in a dry incubator at 5% CO_2, to avoid damaging the electronics in a humidified atmosphere. In this experimental dry environment, evaporation of the cell medium in the MEA chamber (~ 1 ml) was monitored.

The whole cell medium evaporation took 7 hours, while, in the presence of a PVC membrane sealing the MEA culture chamber, this duration rose to 60 hours. A removable sealing membrane made of fluorinated ethylene-propylene [ALA Scientific Instruments, New York, USA] was finally used, preventing evaporation while allowing for gas exchange.

3.2 Exposure system

3.2.1 Customized MEA

The electrophysiological interface that we used was a custom commercial MEA from Qwane

Biosciences [Qwane, Lausanne, Switzerland].

Unlike the typical MEAs fabrication, which has a single component, our customized MEA are composed of two pieces developed separately: MEA chips and the printed circuit boards (PCB).

The MEA chips (15 x 15 mm) are fabricated using standard photolithography. They are composed of a glass substrate, thin film platinum electrodes and a 5 µm thick SU-8 epoxy insulation layer. The MEA chips are then glued onto PCB by a screen-printing technique (Fig. 3-1). The PCB is a 50 x 50 mm large device that fits into an external data acquisition. In our application, the pre-amplifier [MEA1060-Inv, MCS, Multi Channel Systems, Reutlingen, Germany] had to be placed underneath the MEA to allow for the insertion of the culture chamber inside the exposure system; we thus had custom MEAs, in which the contact pads were placed on the lower side of the PCB (Fig. 3-2 b).

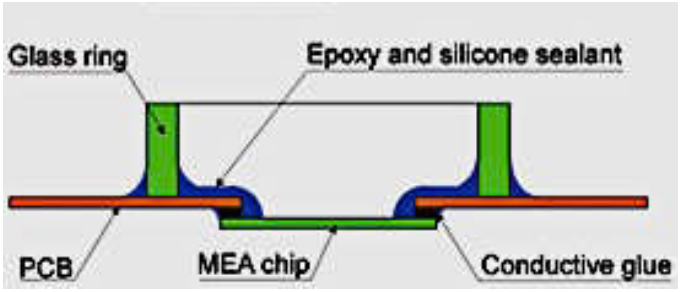

Figure 3-1: Schematic cross-section of our customized MEA [www.qwane.com].

The MEAs have 60 platinum electrodes, 200 µm spaced, with 40 µm diameter tips (see datasheet, Appendix B). There are 59 recording electrodes and one larger electrode used as internal reference electrode for grounding the bath (Fig 3.2c). In our case, the reference electrode was always set as the 78th channel. No external reference using a silver wire was necessary to ground the bath.

The first version of the MEA was extremely fragile: the glass substrates mounted on the PCB came out easily. Therefore, in the second version, an epoxy seal was added to the external lower side of the glass substrate. No further problems were observed thereafter. In this second MEA version, a metal layer was inserted within the PCB and connected to the reference electrode for improving the mechanical rigidity of the MEA and increasing the electrical insulation (fig 3-2a).

In summary only three cultures were successful enough to be exploited in tests.

Preliminary tests with single 3 min GSM exposures were done using the first MEA version and the initial culture protocol described above.

The cultures used for the other GSM protocols (3 min GSM exposures repeated 3 times and 15 min GSM exposures) were carried on MEAs reinforced with an epoxy seal at 1st or 2nd use of the MEA), with a cellular suspension volume of 50 µl.

The cultures used for the CW exposure were grown on MEA at first use with the papain protocol and the initial protocol.

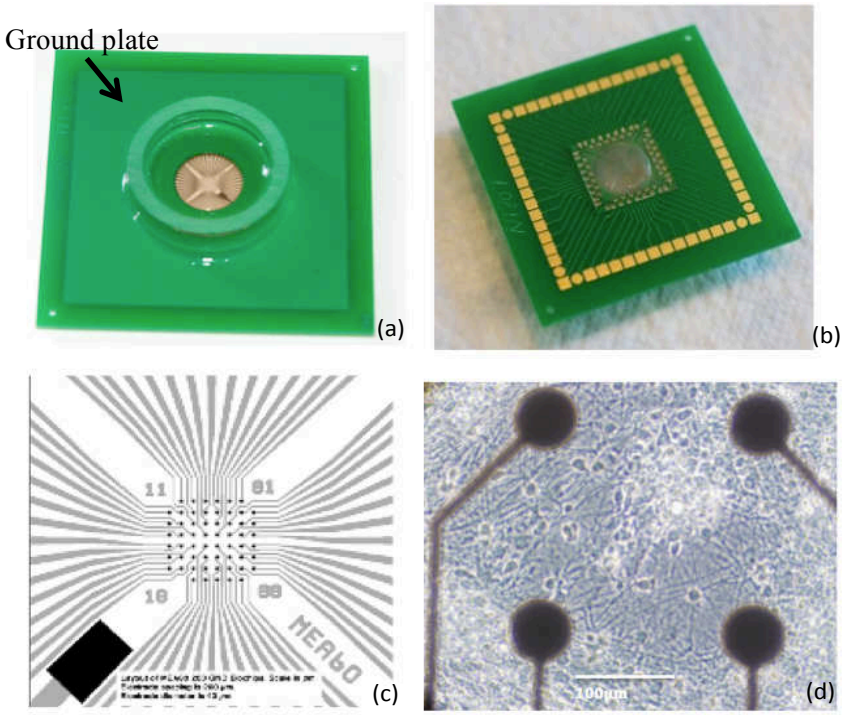

Figure 3-2: MEA views. (a): upper side of MEA with the culture chamber and (b) lower side; (c) electrode layout grid, (d) zoom on electrode tips and neurons in culture.

3.2.2 Open transverse electromagnetic cell

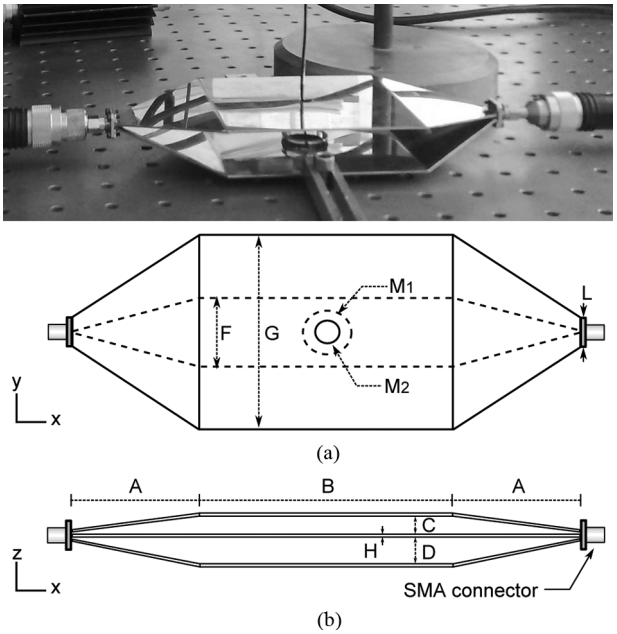

TEM cell dimensions (mm)	
A	51
B	100
C	8
D	12
H	1
F	30
G	85
H	1
I	37
L	14
M_1	14.5
M_2	10

Figure 3-3. TEM cell geometry. (a) Top view. A circular hole in the TEM cell ground plate to accommodate the MEA system is shown. (b) Side view. On the right TEM cell dimensions [Merla et al., 2011].

The exposure setup for electrophysiological recording comprised the MEA and an open transverse

electromagnetic cell (TEM) which consists of a rectangular coaxial transmission section which is tapered with the coaxial connectors of both sides, as shown in figure 3-2. The inner conductor, the septum, acts as the positive conductor or the hot line. The outer conductor acts as the ground. The impedance along the TEM cell is 50 Ω. Therefore, a matched 50 Ω is placed at the output port.

The TEM cell is connected to a RFPA (Artigues-près-Bordeaux, France) RF generator-amplifier as a source of GSM and CW signals at 1800 MHz. This generator was calibrated in terms of input power into the TEM cell.

The TEM cell exposure system satisfies the main biological requirements for experimental investigations such as easy access to biological samples, good air and CO_2 circulations and real-time temperature monitoring, thanks to the open structure of the TEM cell.

A circular hole into the TEM cell ground plate (diameter M figure 3-3) allows for the insertion of the MEA glass cylindrical chamber into the cell.

An important EM requirement is fulfilled by this system as suggested in [Liberti et al, 2004] and [Paffi et al, 2007] as electric field lines in the TEM cell are orthogonal to the MEA electrodes surface, thus minimizing their coupling and interferences with the RF field. The TEM cell was designed for operating from 0.8 to 3 GHz. The electromagnetic field is propagating through the TEM cell and there are no standing waves.

3.2.3 Numerical and experimental dosimetry

An accurate numerical and experimental characterization of the global structure (TEM cell and MEA) was carried out at a frequency of 1.8 GHz [Merla et al., 2011]. Numerical dosimetry, done using FDTD method (Finite Difference in the Time Domain), realistically took into account the metallic lines and recording electrodes. The optimization of the exposure system was considered and the proposed solution was a compromise between the coupling of the wave with the MEA and the homogeneity of the SAR in the solution.

The analysis revealed a great inhomogeneity of SAR distribution near the recording electrodes, which strongly concentrated the electric field lines.

Experimental dosimetry was carried out by measuring 2 experimental parameters: the scattering parameter S_{11}, index of the adaptation of the system in its working range, and the temperature. S_{11} values were in good agreement with the simulated ones, thus confirming the transmission behaviour and adaptation of the MEA within the TEM cell.

Six different configurations were studied: isolated electrodes without connections, metal connexions, no electrode, 40 µm and 80 µm electrode diameters.

The SAR value is in agreement with the simulated value for the modelling strategy of isolated electrodes in case of 40-µm electrode diameter (fig.3-4), therefore confirming the suitability of the numerical analysis and the relevance of proper electrodes dimensioning for system characterization.

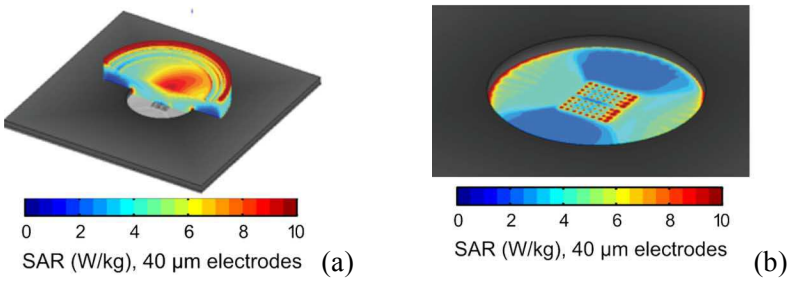

Figure 3-4. Configuration isolated electrodes without connections, 40 µm electrode diameter (a) SAR distribution in the whole biological sample volume (SAR visualized in the half of structure). (b) SAR distributions at the interface between the recording electrodes and the biological solution [Merla et al., 2011].

A good system efficiency was obtained from both numerical analysis and temperature measurements. A temperature elevation of about 0.3 °C for an input power of 1 W was evaluated corresponding to a local SAR value of 3.2 W/kg. This level was used in our experiments and based on the estimation of a time constant of 13 min for temperature elevation from Fig.3-5, the rise in temperature in our experiments with exposure lasting 3 min was 0.06 °C.

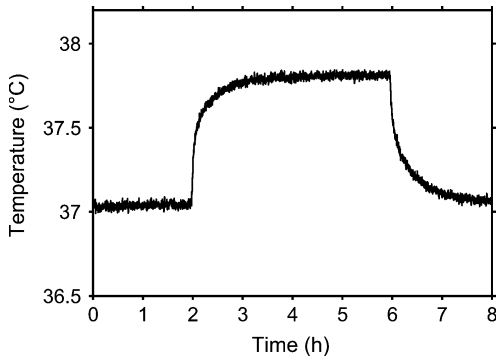

Figure 3-5 Temperature measurements with a 2.3 W input power, before (2 h), during (4 h), and after (2 h) RF exposure [Merla et al, 2011].

At this SAR level, the peak electrical field in the medium at 1 mm over the central recording zone is E = 112 V/m,

considering that: SAR = 3.2 W/kg, $SAR_{GSM\ 1/8} = 8 \times 3.2 = 25.6$ W/kg

$$SAR = \frac{\sigma E^2}{\rho}$$

where E is the RMS electric field, σ the biological medium conductivity at 1800 MHz = 2.1 S/m, and ρ the biological medium density = 10^3 kg/m^3. The dielectric properties of the biological solution at 1.8 GHz are those of the standard culture medium. These are 71 and 2.1 S/m for relative permittivity (ε_r) and conductivity (σ), respectively. While performing simulations, 3 ml of RPMI solution filled the culture chamber. A medium density ρ of 1000 kg/m^3 was used for SAR calculation.

3.2.4 MEA positioning within the TEM cell

In an ideal configuration, the MEA electrodes should be at the level of the TEM cell ground plate to guaranty the continuity of the electrical field. As the pre-amplifier had to be placed underneath the MEA and the contact between the pre-amplifier input pins and the MEA electrode pads had to be secured using a mechanical holder. Three designs (fig. 3-6) were analysed in terms of placement of the MEA with respect to the TEM cell.

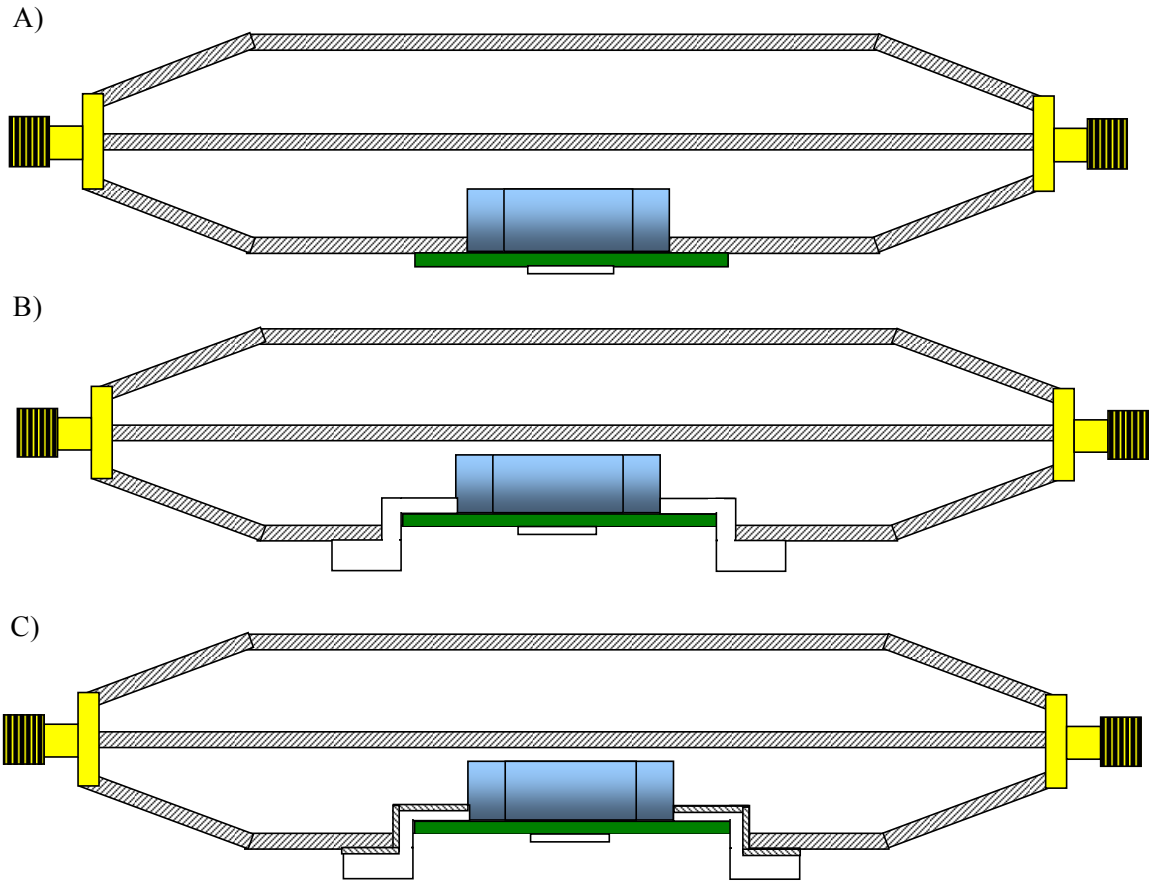

Figure 3-6: Three possible designs for the placement of the MEA within the TEM

The first setup is the simplest of the three and the MEA chamber is shielded. Even if the neurons are slightly underneath the ground plate, this setup is similar to the simulation conditions in the dosimetry studies. In the other two setups, the neuronal networks are precisely at the same level as the ground plate but they present other drawbacks: in the B configuration there is a gap (Teflon, white material in figure 3-6 B) between the ground plate of the TEM and the MEA PCB and moreover there is no shielding of the MEA chamber. In the C configuration there is a discontinuity of the ground plane which constitutes an obstacle for the propagation of the incoming waves.

The preferred solution was thus the first design which was finally selected (fig 3-7).

The design and building were performed by A. Curutchet (ADV-TECH, Mérignac, France).

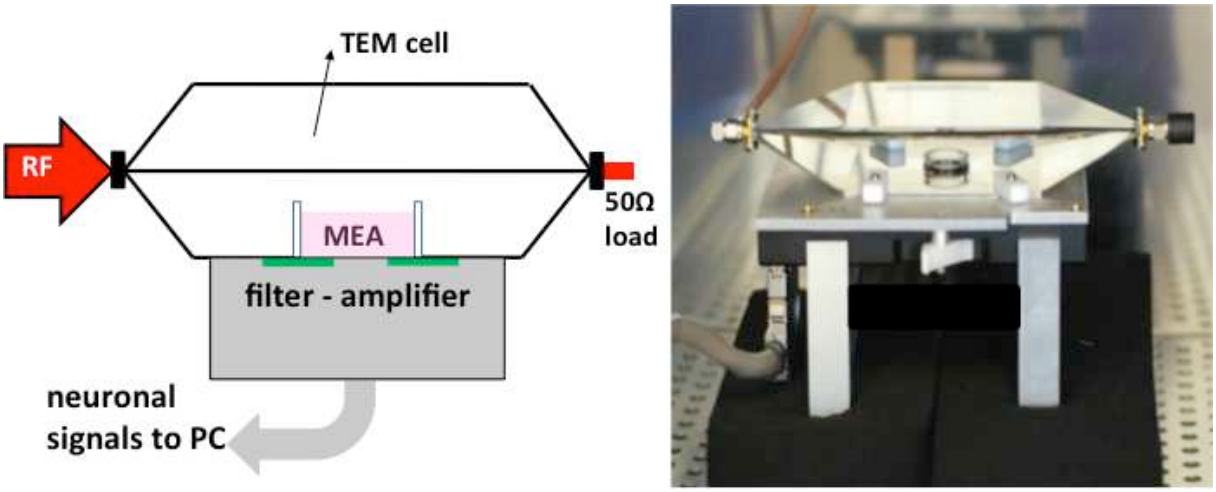

Figure 3-7 Experimental setup. Left: schematic representation.
Right: location inside the incubator at 37 °C and 5% CO_2.

3.3 Acquisition system

The electrical signal from the MEA 60 electrodes was amplified using the 60 channels amplifier system (MEA1060-Inv, MCS, MultiChannel Systems, Reutlingen, Germany) built using SMD (Surface Mounted Devices) technology. These small-size MEA amplifiers combine the interface to the MEA probe with signal filtering and amplification of the signal. The compact design reduces line pick-up and keeps the noise level down.

The MEA is placed directly onto the MEA amplifier system. When the MEA is secured within the TEM cell to the amplifier using four mechanical “clips”, the contact pins of the amplifier are pressed onto the MEA contact pads. The very close location of the amplifier to the MEA sensor is very favourable in terms of signal-to-noise ratio.

The MEA amplifier has a band pass from 1 to 3000 Hz for recording action potentials. The gain is 1200. The amplifier, inside the incubator, is connected to the external data acquisition computer via a single 68-pin MCS standard cable. The analogue output signals of the MEA amplifier are then acquired and 16 bit digitized by the MC_Card 64 (MEA-System) [MEA1060-Inv_Manual]. Raw data were sampled at 25 kHz/channel.

The layout of standard MEA electrodes follows the scheme of a standard grid: the first digit is the column number, and the second digit is the row number.

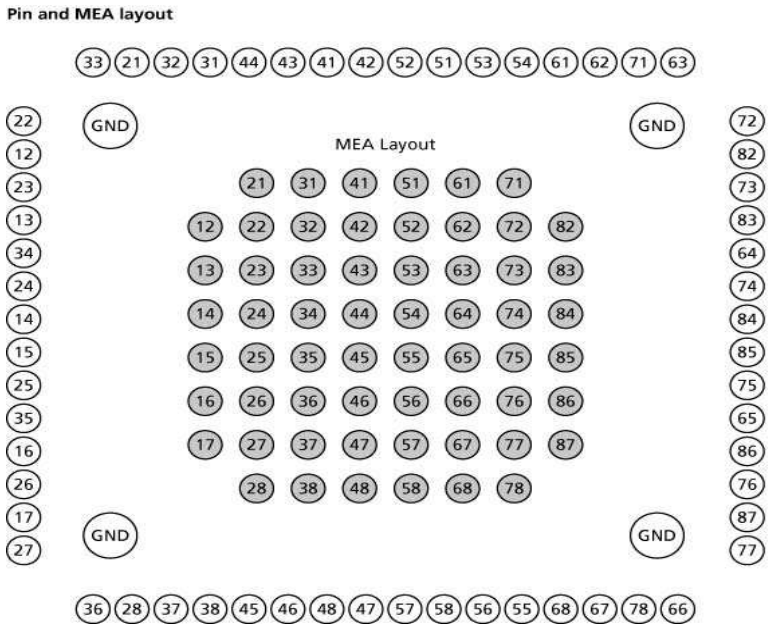

Figure 3-8: this illustration shows the standard pin layout of the socket on the amplifier.

MC-Rack is the acquisition and control software. It allows to visualize simultaneously the 60 channels signals displayed in a grid analogous to the MEA electrodes layout in figure 3-8. A screen shot during a recording session is shown in figure 3-9.

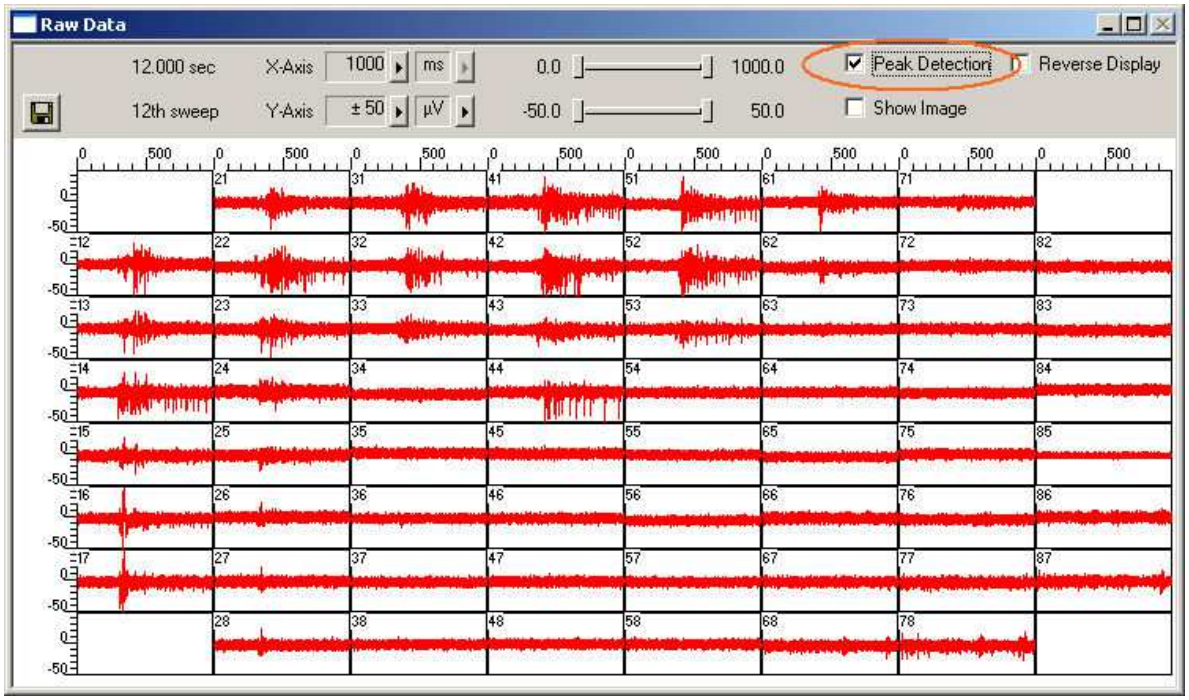

Figure 3-9: a screen shot from a recording session with the MC_Rack software.
The number of the electrode is reported on the top-left on each window.

To test the amplifier we used the test model probe (Test-MEA, MCS) mounted on the amplifier. This test fixture simulates MEA recording condition with a resistor of 220 kΩ and a 1 nF capacitor as electrical model of bath–electrode interface.

We obtained a signal with a maximum noise level of ± 7 μV in agreement with the amplifier datasheet (maximum noise level of ± 8 μV). On a 500 ms time window, the signal mean is zero and the standard deviation is around 1 μV. This estimation represents the electronic noise caused by random thermal motion of charge carriers.

3.4 Analysis software

Signals were recorded and monitored using the MC Rack software provided with the acquisition system. Data were stored in a proprietary MCS ".mcd" format. In preliminary studies we used the MC Rack as analysis software, but it has limited possibilities for incorporating new tools or modifying existing ones. In particular it is not possible to add a customized filter, which is a fundamental request in our case due to GSM interferences during exposure. For these reasons, other programs were considered: Openelectrophy[1], Neuroexplorer[2], and SPYCODE [Bologna at al., 2010]. Only the last one of those answered our specific needs to add a customized off-line filter for the signal processing. We thus adopted SPYCODE as analysis software to carry out all operations: conversion from .mcd to .mat files, filtering, calculation of the different metrics, plotting data, etc.

SPYCODE presents other specific advantages:

(i) implementation of the 'multiple analysis' is a main feature of SPYCODE. This approach allows the automatic batch computational operations of 'multiple' recording streams (even from different experiments) without manual intervention, except for the initial setting of the parameters needed to retrieve the recordings. This feature permits to operate speedily and easily, thereby reducing potential human errors.

(ii) a rich repertoire of algorithms for extracting information both at a single channel and at the whole network level (e.g. self-adapting burst and network burst detection). In the following paragraphs, the algorithms used to extract the metrics analysed are described in detail.

SPYCODE was written in MATLAB. To have access to whole SPYCODE tools it is necessary to have the following MatLab toolboxs: Signal Processing toolbox, Curve Fitting toolbox, Image Processing toolbox and Statistics toolbox.

The SPYCODE software package has been developed through a user-friendly Graphical User Interface (GUI) in which also a non-experienced MATLAB user is able to perform data analysis without knowing the details of the source code.

[1] http://neuralensemble.org/ [2] http://www.neuroexplorer.com/

The GUI gives access to a comprehensive menu bar through which the user can choose the analysis to perform. This choice was taken to allow the developers to add new functionalities to the software by simply adding new menu or submenus to the main interface. Hence, SPYCODE is a dynamic tool which can be easily modified and integrated with additional algorithms, though keeping its core structure unchanged. The GUI menu is split into sections oriented by function type. Fig 3-10 shows schematic overview of the data analysis procedure implemented within SPYCODE. The first level consists of eleven menus, namely, 'Data Conversion', 'Pre- processing', 'Spike Detection', Plot', 'PSTH', 'Spike Analysis', 'Burst Analysis', 'Cross Correlation', 'Additional Tools', 'Multiple Analysis' and 'Help'. The data flow starts with the data conversion procedure, after which raw data are available in Matlab internal format (i.e. *.mat). A filter can then be applied to de-noise the data (optional) and the spike detection procedure then reduces greatly the size of the data (raw signal to timestamps, e.g., from ca. 500 Mb to 300 kb) and prepares them for activity analysis.

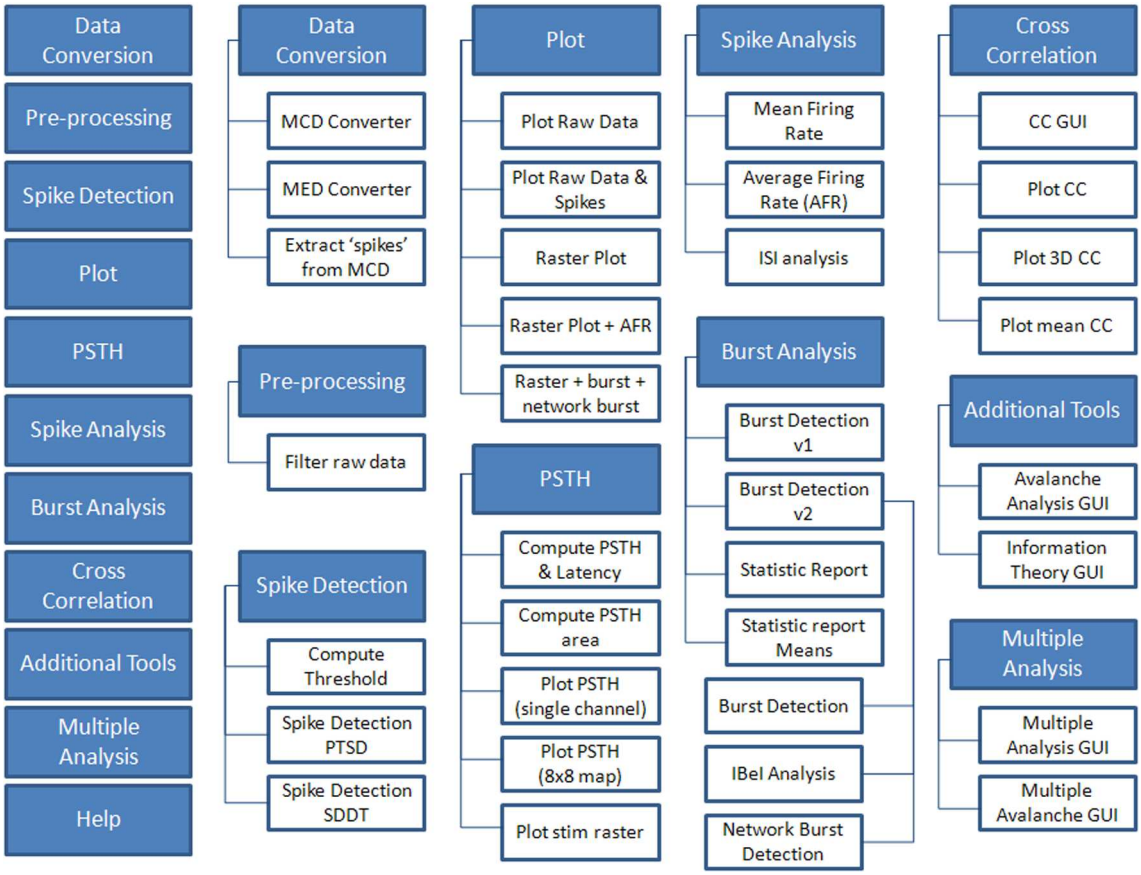

Figure 3-10 Schematic overview of the data analysis procedure implemented within SPYCODE [Bologna et al., 2010].

3.5 Noise evaluation and filtering

The amplitude of the recorded spikes can vary widely from one electrode to the next depending on the relative position and orientation of the recording site and the neurone carrying the impulse.

Moreover, background noise caused by distant neuronal activity, electrode noise, and electronic noise in the preamplifier can vary with time, temperature, and electrode position.

As described in the literature [Maccione et al, 2009; Harrison, 2008] we define the background noise (also called biological noise) in terms of standard deviation, σ, in a short time window (i.e. 500 ms for MC_Rack) from actual neuronal recordings with the assumption that the distribution of the noise is Gaussian. Based on a measurement of σ for the background noise, we can then set a detection threshold to some multiple of σ and reject a fraction of the background noise. For example, with a threshold of 5σ, the probability of Gaussian noise triggering the spike detector is approximately 3×10^{-7}.

The amplitude of the electronic noise in our experimental setup is around 7 μV, as explained in paragraph 3.4. Recordings from culture on MEA show a biological noise, respectively for each channel, with a maximum level of ca. 20 μV with $\sigma \leq 5$ μV. Following the application of the two filters that they are routinely used in the pre-processing phase explained below, the Gaussian noise hypothesis is verified.

We used a thick layer of conductive foam under the amplifier to eliminate mechanical vibrations and consequently potential source of noise.

In order to eliminate the fluctuations of the signal baseline it was necessary to use a high-pass (HP) filter. Following tests at several frequencies we concluded that a 50 Hz cut-off frequency was optimal in terms of removal slow fluctuations and absence of impact on spike detection.

3.6 Spike Detection Method

The study and extraction of relevant parameters from neuronal populations involve long-term measurements (from minutes to hours); therefore several Gigabytes of data are recorded in a single experiment and usually more than one file for each experimental phase is recorded. To trim this huge amount of data, without losing too much information there are two complementary techniques that are used in the analysis of electrophysiological data: spike sorting and spike detection. Spike sorting is the grouping of spikes into clusters based on shape similarity. Given that, in principle, each neuron tends to fire spikes of a particular shape, the resulting clusters correspond to the activity of different neurons. The end result of spike sorting is the determination of which spike corresponds to which of these neurons.

In the spike detection technique, spikes are stored on a time basis. All metrics related to the activity of a neuronal network (e.g., Firing Rate, Inter Spike Interval, burst detection, Bursting Rate) are computed from the spike timestamps.

Spike timestamps originated by the spike sorting are relative to single neuron while spike timestamps by a simple detection are originated by some neurons around the electrode.

In all our data analysis we applied the spike detection approach for the following reasons:

In view of the size of the electrodes and inter-electrode distances, the recorded signal comes potentially from several neurons located either on a given electrode or in its proximity. Moreover, we used cultures with random spatial distribution and not patterned cultures for which we would control the neuronal network architecture, so that no a priori hypothesis on the position and number of neurons with respect to the electrodes was made. Many neurons contribute to the spike train at each electrode and a variety of spike waveform shapes were observed. During bursts, the overlapping of waveforms was a common feature, making spike sorting problematic.

Therefore, spike sorting was not attempted, and all results in this work are based on multiunit data with spike detection.

The detection of spikes (single or organized in bursts) was the first and most important step in the analysis of the data. For this reason, we evaluated different spike detection methods in order to find the best compromise in terms of false positive.

The spike detection methods presented below are based on the amplitude threshold approach. In each case the threshold is set independently for each channel and determined on the basis of the standard deviation of the noise.

3.6.1 Hard Threshold method

The Hard Threshold method (HT) is based on the definition of a positive/negative threshold for each considered channel. If the signal overcomes the threshold, a spike is detected. The threshold is defined as *n* times the standard deviation of the basal signal noise and is separately defined for each recording channel. In MC_Rack a time interval of 500 ms is used to calculate the standard deviation.

In order to count univocally a spike event with one spike timestamp is necessary to introduce the dead time (*dt*) parameter defined as the spike latency during no new event can be detected after a detected event (fig. 3-11).

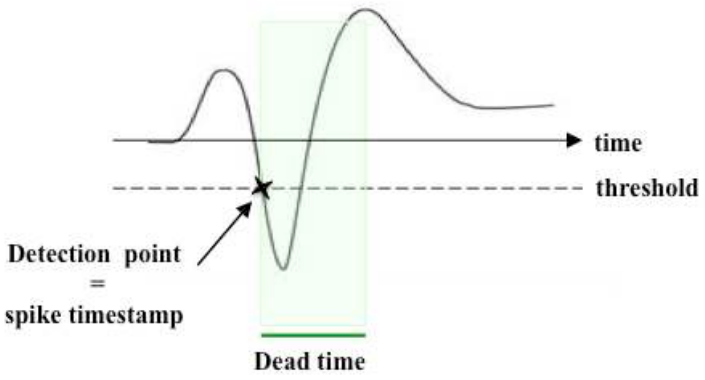

Figure 3-11: Hard threshold method.

Considering that the spike lasts around 1 ms, this value was used to set the *dt* for spike detection

using the HT method.

To find the optimal threshold, we calculated the number of spikes detected as a function of $n\,\sigma$, for n = 3–5, step of 0.5. The test was carried out on 5 cultures for 30 seconds recording without signal baseline fluctuation, so no off-line filter was used. The total number of spikes was computed for the 6 most active electrodes in two experimental conditions: spontaneous activity (SC) and after KCl chemical stimulation (addition of this salt causes immediate neuron death and as a consequence a total disappearance of electrical activity). The threshold was computed for each experimental condition: spontaneous activity under standard conditions and after KCl stimulation. The detected spikes in the KCl recordings were considered as false positives. This method does not allow to quantify for false negatives.

The relative error was defined as: $(\Sigma\ \text{Spike}_{SC} - \Sigma\ \text{Spike}_{KCl})/\Sigma\ \text{Spike}_{SC}$ Increasing the factor n, reduced the number of spikes detected due to the loss of false positives and the addition of false negatives. In Figure 3-12 the mean of this relative error reaches an optimum value at 5σ where the false positives become negligible. Considering this result as optimal for minimizing the false positives and the impossibility to evaluate false negatives as a function of n, we took 5 as the best value.

In conclusion, a threshold equal to 5σ with a dead time equal to 1 ms were used for the HT method in a good agreement with the practice found in the literature [Madhavan et al, 2007]

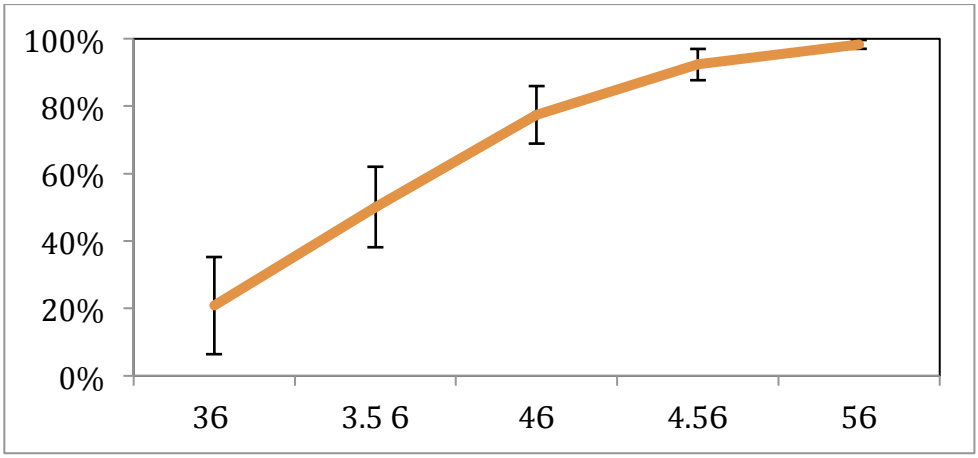

Figure 3-12: relative error mean and his error (the error is the standard error of mean (SEM)).

3.6.2 Spike Detection Differential Threshold

The Spike Detection Differential Threshold (SDDT) consists in defining a peak-to-peak threshold, set as a multiple of the signal standard deviation (i.e. thresh = $n\,\sigma$). The default value of the multiplying factor n can be set between 5 and 8, as reported in the literature [Jimbo et al, 1998; Shahaf et al., 2001]. The raw signal is processed by means of a shifting window (Fig. 3-13), fit to hold at most one single spike (typically 2 ms). A peak is detected when the absolute distance between the maximum and the minimum within the window reaches the differential threshold [Maccione et al, 09].

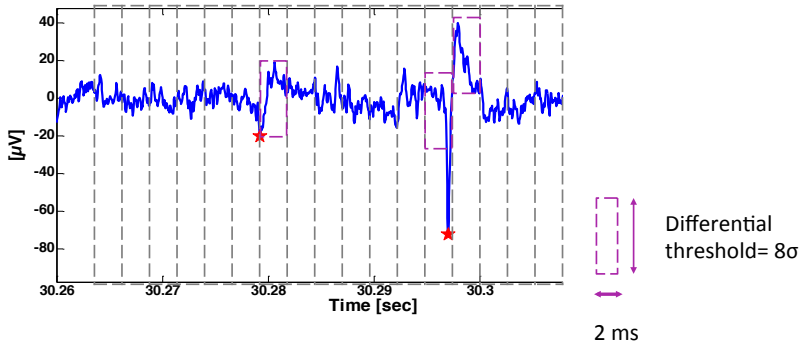

Figure 3-13: Raw signal processing using SDDT method, the signal is split in 2 ms shifting windows (grey squares) and if the differential threshold is reached a spike is detected.

3.6.3 PTSD

The Precision Timing Spike Detection (PTSD) method has two main issues: the reliability of the method and the precise positioning of the detected peaks in the spike train [Maccione et al, 2009]. Moreover, the PTSD provides a good trade-off between performance and computational costs.

The algorithm requires three parameters: (1) the differential threshold (DT), (2) the peak lifetime period (PLP) and (3) the refractory period (RP). The threshold, set independently for each channel, is determined based on the standard deviation of the biological and thermal noise. The peak lifetime and the refractory period are related to the duration of a spike and the minimum interval between two consecutive events (Fig. 3-14).

The algorithm computes the Relative Maximum or relative Minimum (RMM) of the raw data signal. When the RMM is a Minimum, the algorithm looks for the nearest Maximum within the peak lifetime (PLP) window, and vice versa. If the difference between the two RMM (differential value) overcomes the differential threshold (DT), the spike is identified and its timestamp is stored. If the refractory period (RP) is set, no other RMM within that time lag can be computed (Fig.3.14-a).

In order to increase the accuracy of the temporal detection (assuming that the time stamp of an event corresponds to the higher absolute value of the spike), the algorithm implements the following rules:

1. If the higher value corresponds to the last point of the peak life-time period, a further time interval named “overshoot” is used to find the correct peak value (Fig.3.14-b).

2. All the RMM inside the peak lifetime period are taken into account in detecting the precise time stamp of the event, even if they have not been used to find the spike (Fig.3.14-c).

It is worth noting that the algorithm does not use a sliding window moving on the entire recording [Borghi et al., 2007; Vato et al., 2004], but it only takes into account the RMM of the signal, providing a sort of “undersampling” of the raw data that boosts the computational speed.

The main difference of SDDT method with respect to PTSD is that the window can only move by

fixed steps and no additional checks on the detected peak are done.

In addition, in SPYCODE, the algorithm is implemented in C# (a C-based language which performs well with "for" loops needed to "scan" the signal) through the use of pointers for a fast access to memory.

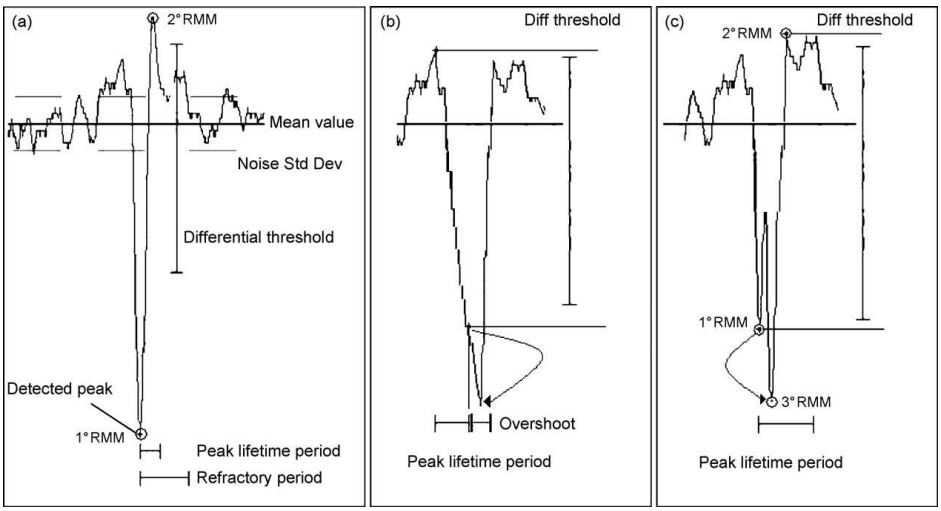

Figure 3-14: Schematic representation of the main feature of the PTSD method [Maccione et al., 2009].

3.6.4 Comparison among: HT, SDDT, PTSD

The lack of ground data is a crucial issue in comparing different spike detection methods. On one hand, even if in the literature some models or techniques to synthesize spike trains have been presented [Borghi et al., 2007; Smith and Mtetwa, 2007], it is difficult to generate a signal presenting reliable critical events such as the fast and noisy variation of the signal during bursting activity. On the other hand using real raw data with complex dynamics makes very difficult the *a priori* identification of the spikes.

Based on the work published in [Maccione et al., 2009], a series of spikes was detected using the PTSD algorithm as a reference sequence to be compared with the output of the HT and SDDT detection methods. The test was carried out in two recordings showing activity in terms of spikes and bursts, one under standard recording conditions (without RF exposure) and one during GSM exposure after application of a spectral filter to remove GSM signal interferences, as explained in detail in paragraph 3.10. The PTSD is the most precise method in terms of detection of spikes, as already known from the literature. It yields the smallest number of false positives and negatives.

Firstly, we evaluated the performances of the three methods by comparing the respective spike counts and by visual assessment. Table 3-1 shows that results are globally similar. Figure 3-15 shows that while the SDDT method has good performances, similar to the PTSD method, it yields false positives because of double detection of single events (Fig 3-15, green lines under the spike). The HT method has the worst performance in terms of false positives (Fig 3-15, grey stars under the spike) and

spike timing accuracy due to the high sensitivity of the method to the signal/noise ratio.

The outcome of this comparison is in agreement with the literature in terms of spike timing accuracy: the PTSD and SDDT are, on average, five times more precise than the commercially available spike detection methods [Maccione et al, 2009]. The accuracy of the spike detection influences heavily the quality of the analysis, as for example burst detection is computed from the spike timestamps.

Methods based on the hard threshold approach are good from a computational point of view, especially in real-time analyses.

In our case, the accuracy of the spike timestamp is an important feature (ISI, burst detection method, etc.) and the spike detection can be performed off line with no constraint on the computational cost. Therefore, the PSTD method was selected.

# channel	PTSD*	SDDT **	HT***	(PTSD-SSDT)/PTSD	(PTSD-HT)/PTSD
37	1248	1419	1217	-14%	2%
73	216	212	222	2%	-3%
28	183	178	156	3%	15%
65	258	270	263	-5%	-2%
75	109	108	121	1%	-11%

Table 3-1: 5 most active electrodes were considered.
* PLP=RP=1ms, differential threshold = 8σ;
** sliding window length = 2ms; differential threshold = 8σ;
*** dead time=1ms, threshold= -5σ.

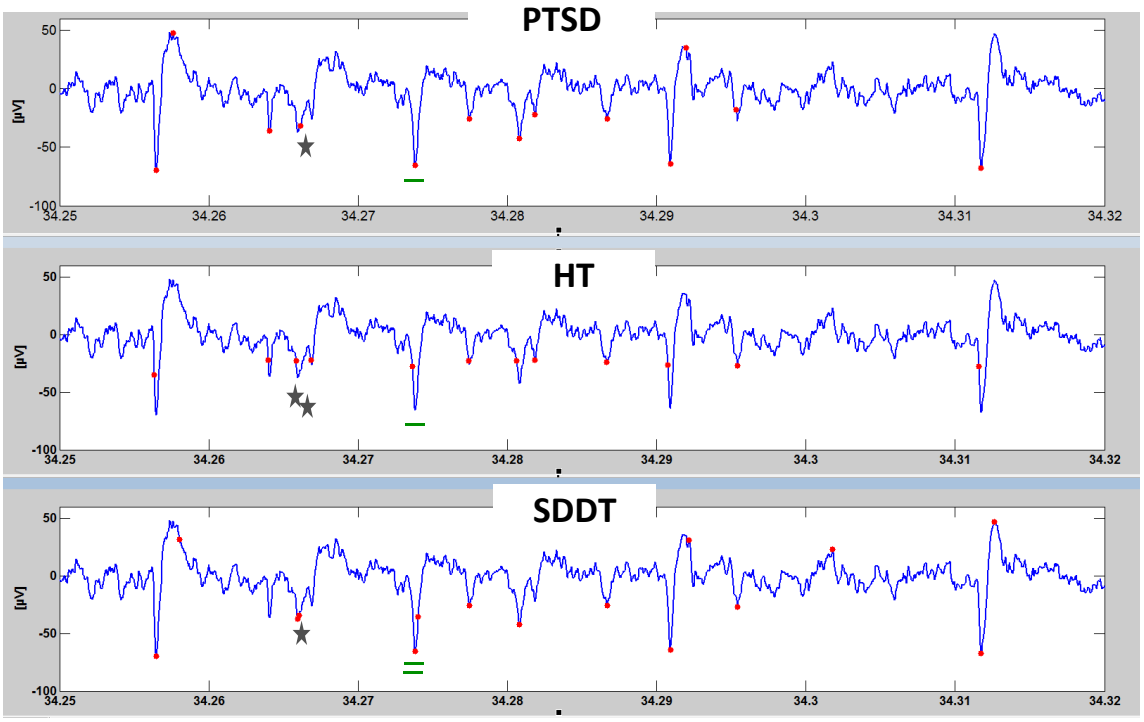

Figure 3-15: Spike detection results obtained by PSDT, HT, and SDDT method, respectively.

3.7 Inter Spike Interval

The ISI distribution is the probability density of time intervals between consecutive spikes and it is a useful statistics for describing spike trains.

The formula to calculate the ISI histogram is reported below:

$\mathrm{ISI}(\tau) = \sum_{s=1}^{N-1} \delta(t_{s+1} - t_s - \tau)$

where τ represents the values of ISI and δ the Dirac function.

As reported by the literature [Perkel et al, 1967], for finite samples of data, such as the observed neuronal spike trains, the ISI histogram (ISIH) serves as an estimator of the actual probability density function. The ISIH provides a detailed way to classify the dynamic pattern of neurons, e.g. 'spiking' or 'bursting', since bursting neurons usually display ''bimodal'' ISI histograms [Cocater-Zilgien & Delcomyn, 1992; Tateno et al, 2002]. Plotting histograms of logarithmic ISI instead of linear ISI can be useful in better discriminating between intra-burst and inter-burst intervals.

The occurrence of in vitro network bursts usually lead to bimodal ISI histograms, in which intra-burst ISIs correspond to shorter values, whereas inter-burst ISIs assume [Pasquale et al, 2010].

3.8 Burst Detection

Bursts are an important feature to describe *in vitro* neuronal activity.

Generally, a burst consists of a fast sequence of spikes with a duration equal to the sum of the inter-

spike intervals (ISIs) within the burst itself and separated by an interval relatively long compared to the burst duration [Tam, 2002].

A population burst consists of episodes of activity (i.e. densely packed spikes) occurring simultaneously at many channels, spread over the entire network. The spikes belonging to a given burst are separated in time by a few milliseconds; these bursts generally last from hundreds of milliseconds up to seconds with long quiescent periods (Inter Burst Interval: IBI).

Most of the burst detection methods are user-dependent and require the setting of several parameters (e.g., minimum number of spikes within a burst, maximum ISI within a burst, minimum burst distance).

If those parameters are not modified within a given experiment, even though the cultures undergo several pharmacological or electrical treatments we talk of a parametric method. The choice of these parameters is fundamental for burst detection as burst features may depend on the experimental conditions (age, pharmacological or electrical treatments). Therefore the choice of the parameters may affect the interpretation of the results. On the contrary, non-parametric methods automatically determine the best parameters for burst detection for each recording.

3.8.1 Parametric methods

The MaxInterval method

To detect bursts MC-Rack proposes a simple non-parametric method: the Max Interval Method based on [Legendy C.R. and Salcman M, 1985].

At first it is necessary to set the 5 parameters (fig. 3-16):

- maximum ISI to start the burst : Max Start Interval (MaxSI).
- maximum ISI to end the burst : Max End Interval (MaxEI).
- minimum ISI between two bursts : Min InterBurst Interval (MinIBI).
- minimum burst duration : MinBD.
- minimum number of spikes in a burst : MinNSB.

The algorithm scans the spike train until an ISI is found that is less than or equal to max interval. While the ISI are less than MaxEI, they are included in the burst.

If the ISI is more than MaxEI, the burst ends. The bursts that are less than MinIBI are merged apart. The bursts that have duration less than MinBD or have fewer spikes than MinNSB are removed.

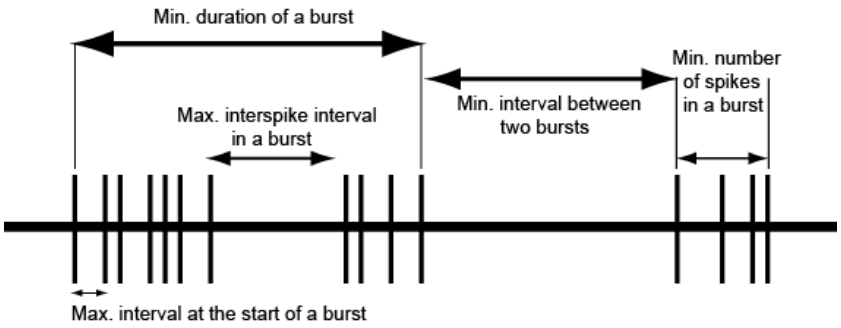

Figure 3-16: MaxInterval method to detect burst: parameters to set [MC_Rack_Manual, pg. 151]

The String method

The String method is a simple method for defining bursts as strings of spikes [Turnbull et al, 2005] with only two parameters: a minimum number of spikes per burst and a maximum ISI. These two values represent a simple parameterization that is adequate for the description of temporal grouping in spike trains. Because this method has a minimal computation time, it allows implementation of burst analysis in real-time, including statistical changes in burst variables, histograms of burst types, and combination patterns of burst variables.

The Chiappalone method implemented in SPYCODE, is analogous to the String method, with a default value of at least 5 consecutive spikes with a maximum ISI of 100ms.

3.8.2 Non-parametric method

The Pasquale group has developed a self-adapting method for detecting both bursts and network bursts from electrophysiological activity recorded by means of microelectrode arrays.

The Burst Detection (BD) algorithm is based on the evaluation of the logarithmic ISI histogram (logISIH) in order to look for the best threshold between intra-burst (i.e. spikes within bursts) and inter-burst (i.e. between bursts and/or outside bursts) activity for each recording channel of the array [Pasquale et al., 2010]. This algorithm considers the fact that the firing rate within bursts is usually quite variable in neuronal cultures in vitro. Thus, the intra-burst ISI threshold (ISIth) cannot be fixed a priori, but it has to adapt to the actual experimental condition.

If ISIth is lower than 100 ms, the default value, (fig 3-17 a, b, indicated by the red dashed line), the BD method uses the ISIth value to determine the maximum ISI allowed within a burst. (fig 3-17 c, d.) On the contrary, if ISIth is higher than 100ms, the newBD method uses two different thresholds: the first one (i.e. 100 ms) is used for detecting burst cores, whereas the second one (i.e. ISIth) is used to extend burst cores at the boundaries to include all spikes whose ISI is lower than ISIth.

In the following data analysis the BD is performed using this Pasquale method in view of its good performance compared to other algorithms. It is already integrated in SPYCODE (Burst Detection—v2), which is the analysis software we have chosen.

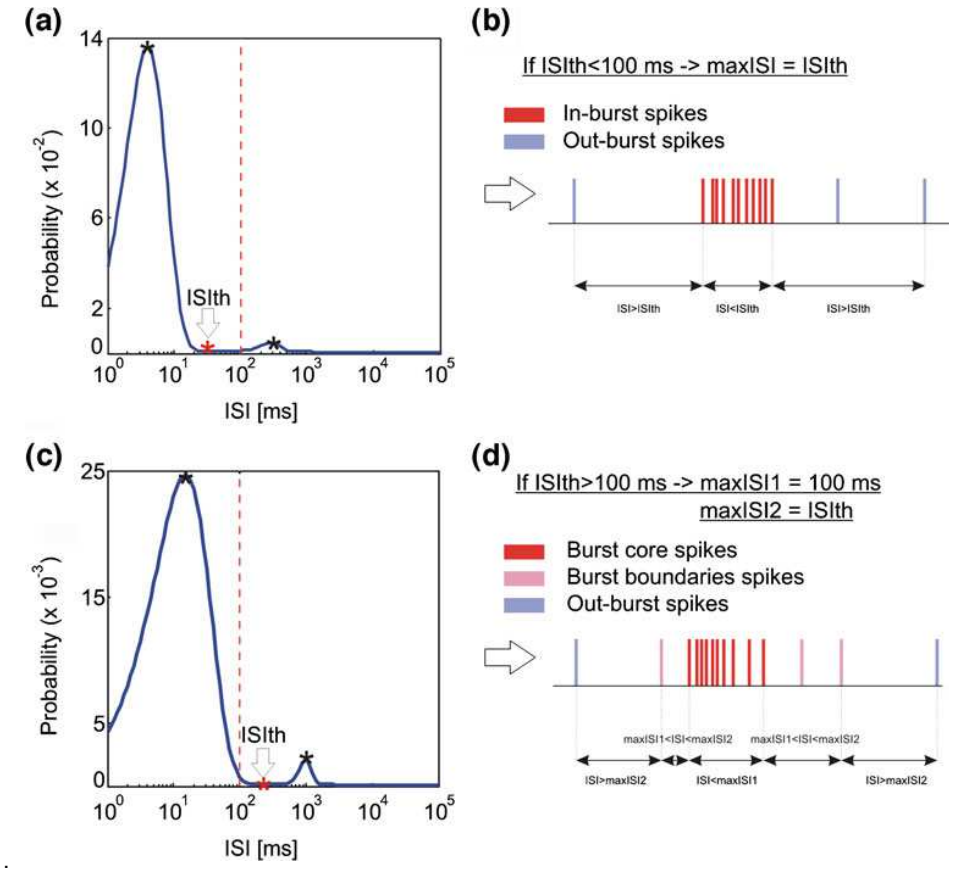

Figure 3-17 Sketch illustrating the BD method [Pasquale et al., 2010].

3.9 Network Burst Detection

Network bursts (NB) can be seen as a third feature, after spikes and bursts, to describe a neuronal network.

The NB detection (NBD) methods developed by Pasquale is analogous to the burst detection algorithm and is based on the Logarithmic Inter-Burst event Interval Histogram (logIBeIH)

In order to study the spatio-temporal patterns of activity propagation within network bursts, we would like to cluster single-channel bursts in network bursts according to the initial spike's time. If one considers the sum of all the 60 burst event trains recorded from a MEA, namely the cumulative burst event train, network bursts appear as clusters of closely packed burst events separated by relatively long periods. In other words, a network burst can be viewed as a burst of burst events in the cumulative burst train. Hence, the same approach developed for the detection of bursts can be potentially applied to the NBD: we have only to set two thresholds, firstly the maximum Inter-Burst event Interval (IBeI) for burst events within a network burst (maxIBeI) and secondly the minimum percentage of recording electrodes involved in a network burst (minPercElec).

As the ISI distribution, also the IBeI distribution can be computed by binning data in equally

spaced logarithmic bins (sized 0.1 in log10(IBeI) units), highlighting the presence of two or more distinct peaks, the first one corresponding to short intervals within network bursts and the others to long intervals between network bursts. By using the same algorithm described above (see section 3.8.2) an IBeI threshold (IBeIth) can be extracted from the logIBeIH and this value can be used to perform the NBD starting from the cumulative burst event train.

NBD is implemented in SPYCODE.

Two parameters have to be set by the user: the short interval within network bursts (usually set a 100 ms) and the minimum percentage of channels involved in a network burst (usually set at 20% of the total number of channel active in term of bursts.

The main limitation of NBD algorithm is that it relies on the bimodality of the logIBeIH.

This algorithm needs at least 10–20 min of recording to run the analysis tools. Characterizing of such events in our case with recording phases of 3 min was hardly possible. Furthermore our cultures were studies after 2-3 weeks in vitro, and NBs usually appear from the third week. Therefore, the NB analysis has not been a leading analysis for our studies.

3.10 GSM Interference

Recordings of spontaneous activity during GSM exposure show artefacts caused by interference with the GSM signal. As shown in Figures 3-18 and 3-19, the GSM interference produces negative synchronized “spikes” at 217 Hz (GSM frame), with the same duration of a GSM impulsion, i.e., a time slot of 0.57 ms.

The amplitude of the interference depends on the electrode position (Fig 3-18) and it has a range between zero and –450 μV (electrode 43). The low artefact amplitude guarantees that the amplifier operated in its linear range ([–4 mV, 4 mV]).

Three off-line methods were examined for removing the GSM interference to access to neuronal activity.

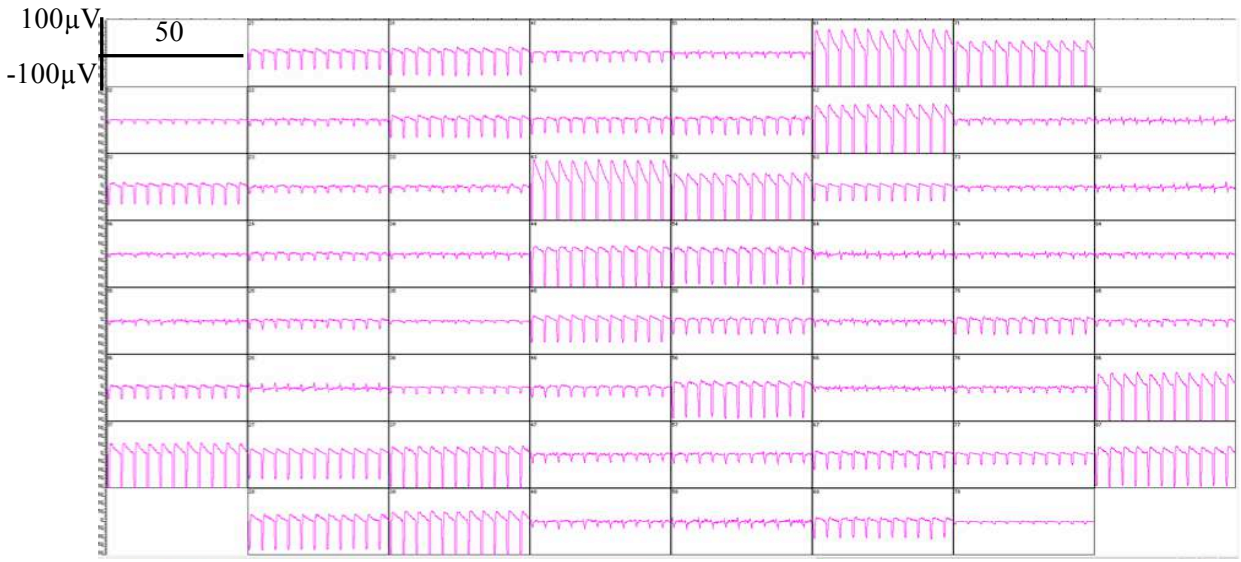

Figure 3-18: recording from the 60 channels under GSM exposure. The neagative peaks have a frequency of 217 Hz.

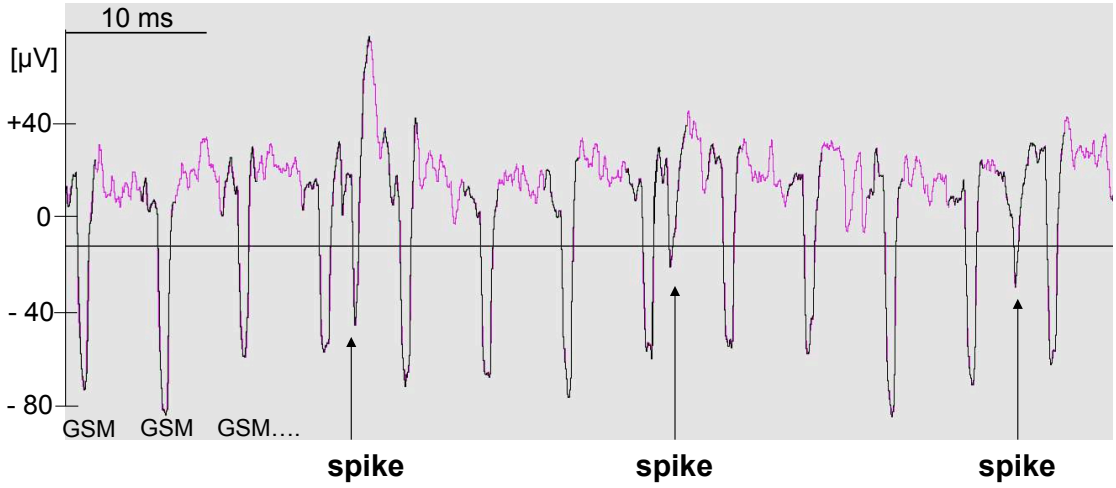

Figure 3-19: example of a recording under GSM exposure. The biological spikes are overlapped to the GSM interferences, synchronized at GMS frequency frame, (a period of 4.6 ms and active slot of 0.5 ms).

3.10.1 Subtraction method

The identical shape of the recurring event in the GSM artefact suggested at first an intuitive method to remove the artefact: subtracting a recording with GSM interference but without biological activity from a signal that contained both, to extract the biological signal.

However, the area under each artefact (GSM pulse) was not strictly constant and the slight differences produced other artefacts when doing the subtraction. This method was therefore abandoned in spite of its simplicity.

3.10.2 Time selection method

Another simple method was able to give access to 7/8 of the recording, by ignoring (blanking) all events during the active timeslot. Even though the lack of an eighth of the information was not quantitatively very limiting, we had to take into account the fact that this interval corresponds to the

critical ON timeslot, when the energy is deposited with a power 8 times the average power (3.2 W/kg). This second method was thus also abandoned.

3.10.3 Spectral method

The spectrum of the biological activity during exposure shows pronounced short peaks in correspondence to GSM harmonics: 217 Hz, 434 Hz, 651 Hz, etc., as shown in figure 3-20.

Visual comparison between spectra with and without exposure shows that the two share very little in common in terms of frequency content which means that removing the GSM contribution using a spectral filter will not affect much the detected activity. The spectrogram in Figure 3-21 is a colour plot (i.e. 3 dimensional plot) of the spectral power of a given signal plotted against both frequency on abscissa and time on ordinate. This spectrogram shows that the GSM has high and narrow peaks in the harmonic frequencies (vertical dark red lines at 217, 434, 651 Hz, etc.) while biological activity has homogeneous frequency components up to 3 kHz (horizontal red stripe at 1.7-1.8 sec).

This has suggested the application of a band-stop filter to remove GSM interferences without altering the biological signals.

A set of 30 band-stop filters, each one centred on one of the GSM harmonic frequencies (217 Hz, 434 Hz, up to 6510 Hz) was built using the MatLab Signal Processing Toolbox. They are second order Butterworth filters with a bandwidth of 4 Hz.

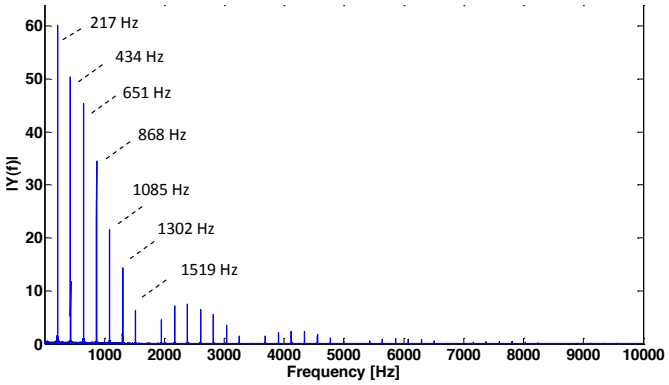

Figure 3-20: spectrum of a single channel recording under GSM exposure. The first 6 harmonics of the GSM signal are indicated.

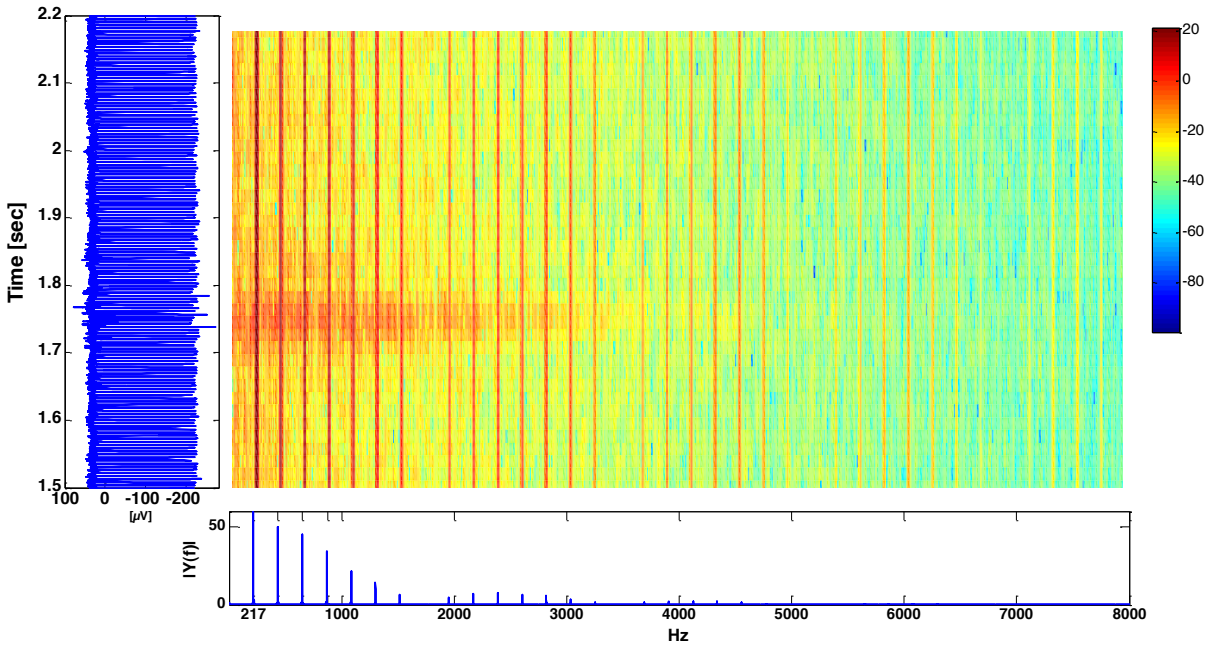

Figure 3-21: On the left vertical: a few hundreds ms of recording under GSM exposure. Few spikes at 1.7-1.8 sec are hidden by the GSM interferences but (in the centre) in the spectral power of the signal are clearly visible by the horizontal red line; At the bottom: the spectrum of the signal.

The filter parameters (cut-off frequencies, order, bandwidth and type) were set in order to have the minimum impact on the signal, and the selection criteria were aimed at attenuating the GSM-interferences amplitude down to the level of the biological noise (± 15 μV) for most of the channels. (for this reason 3 channels, #86, 43, and 61, were discarded *a priori* from all analyses).

Considering that spikes have energy concentrated in the 300 Hz–5 kHz range [Harrison, 08], I have decided to attenuate GSM harmonics up to the 30th rank (6510 Hz).

The time response of the filter causes artefacts in the discontinuity points: at the beginning (fig. 3-22) and at the end of GSM stimulation. In order to privilege the observation of the biological activity response at the beginning of RF exposure I decided to flip the chronological order of the signal before applying the GSM filter to move artefacts before the beginning and after the end of GSM stimulation.

Then the signal was flipped again, to restore the chronological order, and the first 180 seconds of the stimulation were extracted.

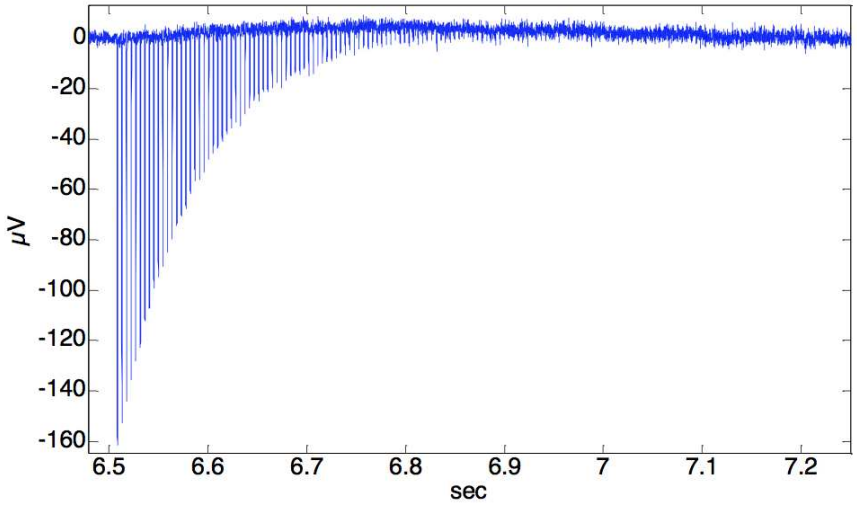

Figure 3-22: signal post GSM filter, at the beginning of the GSM exposure. It is clearly visible the artefact due to the time response of the filter.

To ensure the reliability of this method, I tested the impact of this GSM filter on the number of detected spikes under two conditions: (i) recording of spontaneous activity in the absence of exposure for an electrode of one the recorded activity at 15 DIV (reference signal) and (ii) a composite signal including exposure, obtained as the sum of the reference signal and a pure GSM artefact recording (Fig. 3-23, top). Using the GSM filter on this composite signal allowed us to remove the GSM interference (Fig. 3-23, bottom). The test was carried out using as reference signal the spontaneous activity recorded using each of the 7 most active electrodes and 2 electrodes connected to the masse, that not present activity. This signal processing had a very small effect on spike detection in terms of total number of spikes (Table 3-1). The GSM filter has almost no effect on the spike detection in absence of GSM interferences. However, in the case of the composite signal, most of the relative errors are positive which means that the use of the GSM filter adds extra spikes. This means that the amplitude of the effect of exposure is slightly underestimated. The GSM filter has not been tested in terms of false positive and false negative in the spike detection.

This method has been integrated in SPYCODE as a filter in the Pre-processing section.

The GSM filter was applied systematically to all recordings (with and without GSM exposure).

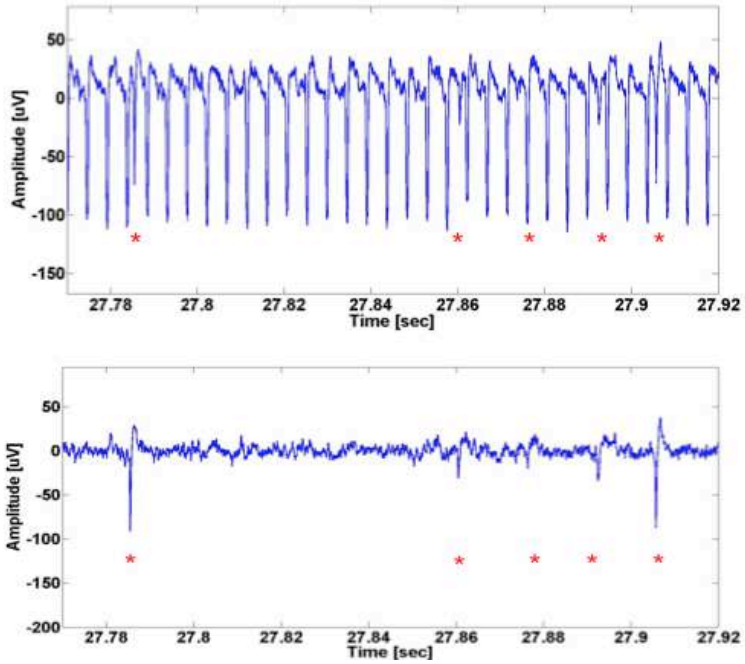

Figure 3-23: composite signal of electrical activity during exposure before (top) and after (bottom).

reference signal		reference signal		composite signal = reference signal + GSM artifact	
no filter		GSM filter		GSM filter	
#channel	# detected spikes	# detected spikes	relative error*	# detected spikes	relative error**
65	1536	1514	–1%	1611	6%
46	1285	1268	–1%	1360	7%
22	953	981	3%	972	-1%
25	894	972	9%	941	-3%
62	851	848	0%	924	9%
34	801	809	1%	845	4%
47	798	796	0%	810	2%

* with respect to reference signal with no filter

** with respect to reference signal with GSM filter

Table 3-1: Impact of the GSM filter on Reference and Composite Signals in terms of number of detected spikes computed for seven channels.

3.10.4 GSM interference: where does it come from?

The amplitude of GSM interference is different for each electrode but it depends on the number of grounded electrodes. However it is the same for all tested MEAs .

The artefact was studied as function of several parameters. For that purpose, a MEA with

neurobasal medium was used. All input pins of the pre-amplifier were grounded and the internal reference electrode (electrode 78) connected to the reference electrode socket. With this configuration no signals should be detected but as shown in figures below, RF pulses were detected by the acquisition system. Various GSM interference amplitudes were obtained in 2 different configurations: pre-amplifier –TEM cell in the standard position (fig. 3-24) and TEM cell rotated of 180° with respect to the initial configuration (fig. 3-25).

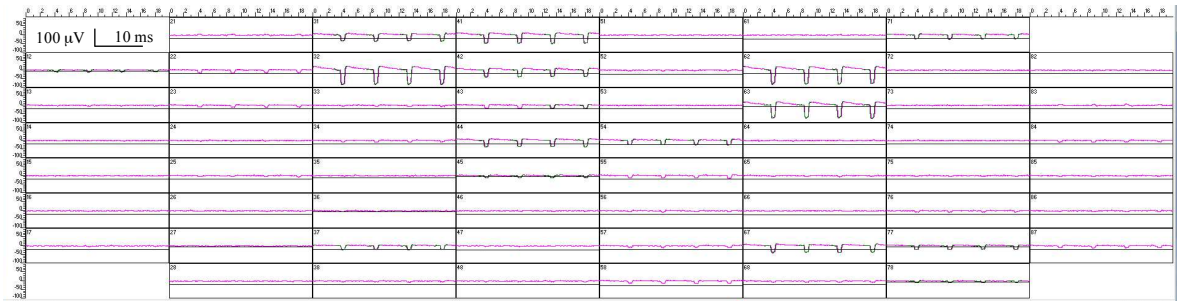

Figure 3-24: standard configuration: pre-amplifier –TEM cell. All input pins of the pre-amplifier were grounded and the internal reference electrode (electrode 78) connected to the reference electrode socket.

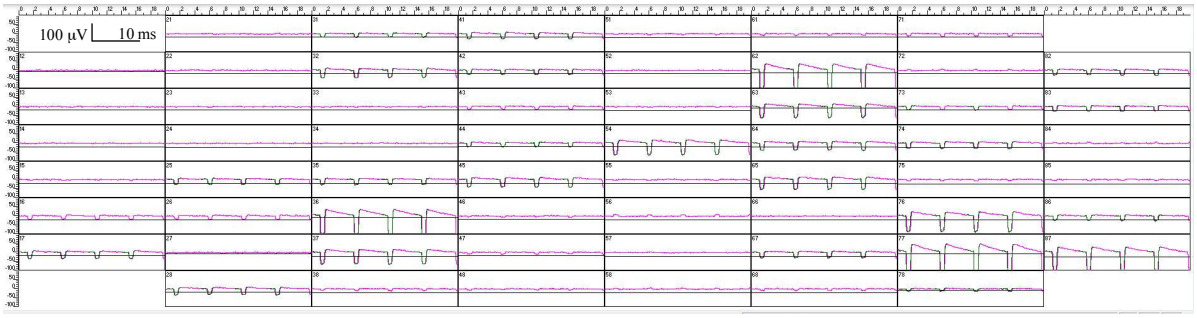

Figure 3-25: configuration: pre-amplifier and TEM cell rotated of 180° with respect to the initial configuration. All input pins of the pre-amplifier were grounded and the internal reference electrode (electrode 78) connected to the reference electrode socket.

The difference between these two examples indicates that the GSM interference is originated from interactions of the pre-amplifier and the RF and not via the interaction electrode-RF.

In fact no interactions appeared among electrode recording area and RF as simulations by Merla et al. have shown.

These observations suggest that the artefact's origin is mainly due to an interference located beyond the electrodes, at the level of the pre-amplifier's pins, under the MEA. For these reasons we shielded the amplifier using RF absorbing material. The contact pins were covered at different level with strip of a silicone rubber material that is electrically non-conductive (ECCOSORB, Emerson&Cuming, USA). This material has a coefficient of absorption (2 dB/cm @ 2GHz) higher than absorbing foam.

The result was a decrease of the artefact amplitude by a factor of 10 leading to a reduction down to the noise level for most of the electrodes. This arrangement will be used in further studies.

3.11 Exposure protocol

In all experiments, after installation of the MEA inside the incubator, we waited for equilibration of the incubator temperature at 37 °C and then waited for 20 min before starting the recordings in order to work in standard cell culture conditions.

Preliminary tests

Preliminary tests were done with several protocols. Spontaneous activity in standard conditions was recorded for long period (from 2h to 24 h) with the sealing membrane.

We adopted a 3-min duration for the exposure or sham phases. Although this duration may seem short as compared to the standard duration of 10-20 min in the literature, it was chosen to (i) limit the temperature elevation in the exposure phases and (ii) observe more easily the expected fast response of the neurons to RF exposure.

Single 3-minute GSM exposure

A 3-min GSM exposure protocol (fig 3-26) has been carried out on few cultures at different ages.

In this case, no sealing membrane was applied on the MEA to prevent evaporation. The appellation 'ZERO' in each exposure protocol indicates the pre-exposure phase, as control phase of the neuronal activity.

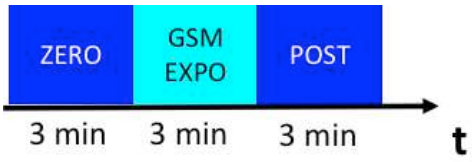

Figure 3-26: Single 3-minute GSM exposure.

Three 3-min GSM exposures

No sealing membrane was applied on the MEA to prevent evaporation.

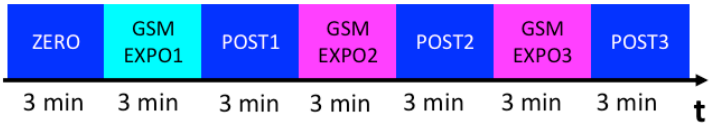

Figure 3-27: Three 3-min GSM exposures.

Single 15 min GSM exposure

A 15 min GSM exposure (fig.3-28) with a sealing membrane was applied on the MEA to prevent evaporation.

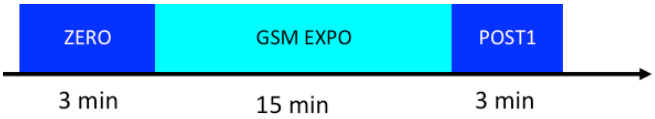

Figure 3-28: **Single 15 min GSM exposure protocol.**

These preliminary studies lead to a improvement of the protocol test: the GSM generator were modulated at 217 Hz, the sealing membrane on the MEA to prevent evaporation was use systematically and sham exposure recording was added.

Main experiment protocol: Three 3-min GSM exposures

The neuronal networks were exposed between 15 days *in vitro* (DIV) and 21 DIV, when neuronal activity is optimal in terms of a balance between random spikes and bursts [Chiappalone et al., 2005, Van Pelt 2005]. All recordings were carried out in three subsequent 3 min periods, i.e., before, during, and after exposure. Sham exposures were also carried out on the day before, using the same exposure protocol but with the generator OFF (Fig. 3-29).

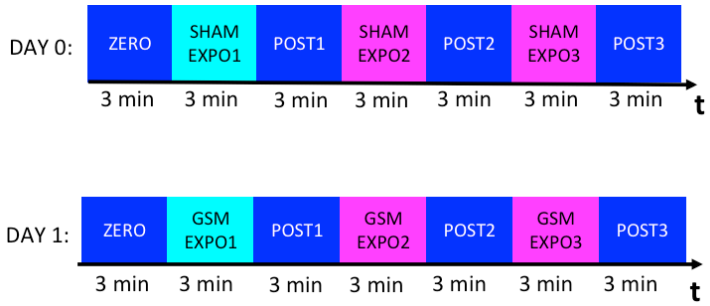

Figure 3-29: Time profile of the test protocols: sham exposure on day 0 and GSM exposure on day 1.

Future protocol: CW and GSM exposures

In future protocol we expose culture from 17 to 21 DIV at a three 3 min CW exposure at a SAR level of 3.2 W/kg, followed by 3 min GSM exposure at a SAR level of 3.2 W/kg and a 3 min GSM exposure at a SAR level of 6.4 W/kg. The schematic representation of the protocol is shown in figure 3-30.

Due to the difficult installation of the membrane, it wasn't used each time. These studies are in progress and no results are available.

PRE 21 min	1° CW 3.2 W/kg	POST1	2° CW 3.2 W/kg	POST2	3° CW 3.2 W/kg	POST3 12 min	GSM 3.2 W/kg	POST4 12 min	GSM 6.4 W/kg	POST5

Figure 3-30: duration of each run is 3 min, differently is specified.

3.12 Choice of metrics

Several metrics based on the spikes and burst were analysed.

3.12.1 Firing Rate

Once spikes have been identified, the easiest and most direct way to characterize the level of activity of a cell is computing its Firing Rate (FR). FR is defined as the total number of spikes collected on all channels during the window time recording, usually 3 min.

Channels were considered as active in term of neuronal electrical activity if they had a spike rate of at least 0.1 Hz.

3.12.2 Mean Firing Rate

The Mean Firing Rate (MFR) of a given culture is defined as the total number of spikes collected during 3 min for the 6 most active channels identified in the pre-exposure period.

3.12.3 Bursting Rate

The Bursting Rate (BR) is defined as the number of bursts detected on all channels during 3 minutes.

3.12.4 Burst Duration

The duration of a burst is defined as the time distance between the first spike of the burst and the last one.

3.12.5 Mean Burst Duration

The Mean Burst Duration is defined as the ratio between the sums of the duration of bursts detected on all channels during an experimental phase and the total number of bursts.

3.12.6 Bursting channels

It is the number of active channel in term of burst during a recording phase. No burst rate threshold was set to consider an active channel as bursting channel.

3.12.7 Network Burst

The number of Network Bursts was computed for each experimental phase, setting at 20% the minimum percentage of channels involved to detect a network burst and at 100 ms the short interval within network bursts

3.12.8 Post Stimulation Time Histogram

The Post Stimulation Time Histogram (PSTH) shows the probability of firing as a function of time after the stimulus onset. This measure is equivalent to a cross-correlation between the train of stimulus presentation and the train of spikes. A peak in the PSTH indicates a higher probability of firing at that particular time after stimulation and can presumably be associated with an excitatory process. Dips in a PSTH indicate a lower time-locked probability of firing and often are associated with inhibitory or refractory processes. The PSTH is used for low stimulation frequencies, at least a post stimulus window of 10 msec. The post stimulus window in the GSM stimulation is 4 ms, it corresponds to the 7 empty slots. Such time window is too short to compute PSTH. Therefore, even if PSTH is this typical metrics of stimulation protocol, it was not computed in our case.

3.12.9 Inter-spike-interval histogram

The ISI histogram (ISIH) serves as an estimator of the actual probability density function. Different shapes of the ISIH give an estimate about the synchronization of the neuronal network, and each shape denotes a set of timing with shared properties. ISIH can be plotted for a single channel or relative to all channels; in this case we talk about Network Averaged ISIH.

3.12.10 Percentage of random spikes

It represents the number of spikes that do not belong to bursts. This parameter is often used correlated to the age of a culture.

3.13 Statistics

As the sample size was small (n = 16 independent cultures) statistical analysis required the use of non-parametric tests. In the analysis of the sham and exposure data, the Shapiro-Wilk test (Anastats software, Rilly sur Vienne, France) was used to process the ratios of FR, BR, Total Burst Duration Mean Burst Duration and Bursting channels to detect a possible effect of GSM exposure on spontaneous activity. This test is used for analysing the normality of a population, but it can also assess the comparison with a fixed value, in a similar way as the student t-test but with fewer numbers of independent samples.

4 RESULTS

In a first part, the most representative preliminary experiments are briefly presented: several studies were carried out with various protocols and analysed as a function of various metrics in order to optimize the experimental protocols. In a second part, the main experiment is described in detail and analysed statistically.

4.1 Preliminary experiments

4.1.1 Spontaneous activity under standard conditions

The spontaneous activity of several cultures was observed for several hours without RF exposure. In Figure 4-1, an example is shown for two cultures at 22 and 25 DIV, respectively.

The FR was computed using the MC_Rack software for all electrodes with a 3 minute time binning. For the spike detection, the hard-threshold was set at 5σ. The sealing membrane was used in these preliminary experiments.

A global reduction of the activity with time was observed with a large variability among cultures in terms of spikes count and rate of the decrease.

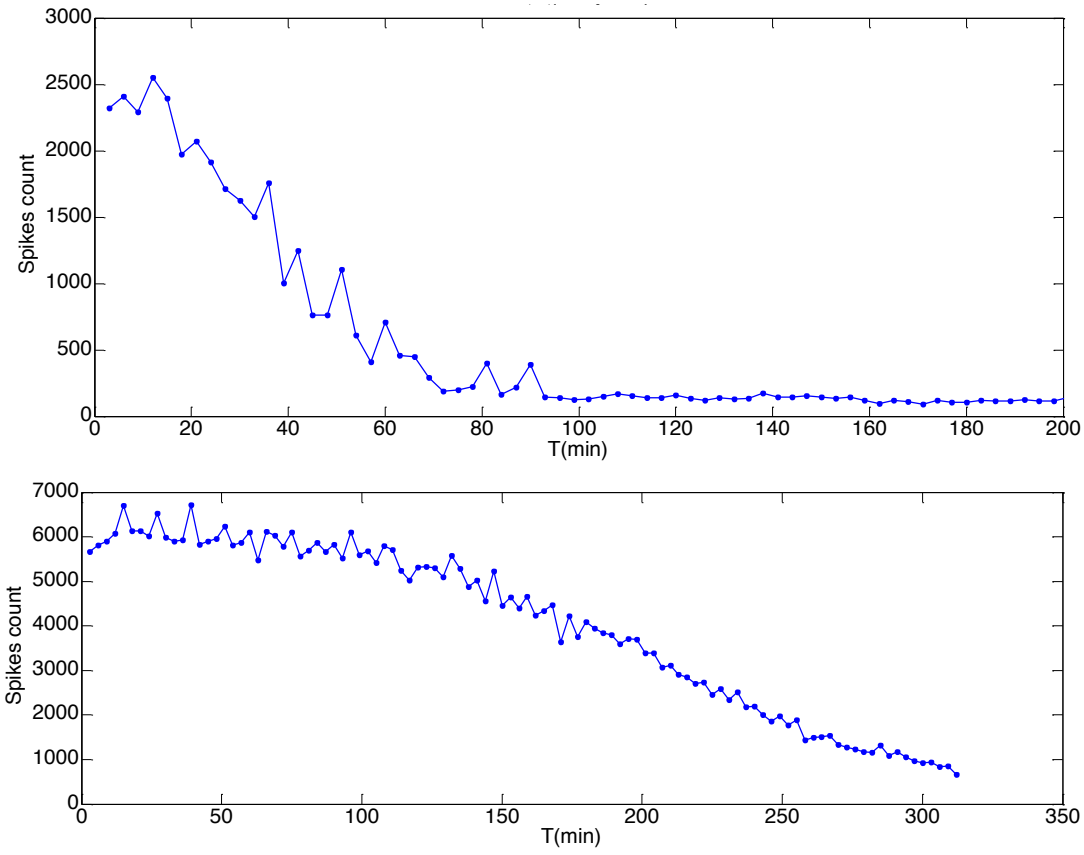

Figure 4-1: FR for 3 minute time bins under standard conditions for several hours. (Top) 22 DIV culture and (bottom) 25 DIV culture.

4.1.2 Analysing pre- and post-exposure phases

At first, we analysed only the pre- and post-exposure phases. The activity was not recorded during the GSM exposure and there were no sham runs. The FR was computed using the MC_Rack software on all electrodes with a 3 minute time binning. For the spike detection, the hard-threshold was set at 5σ. All preliminary data shown below have been analysed qualitatively to show whether there were trends in the variation of the metrics in the presence and absence of GSM exposure.

Single 3 minute GSM exposures

A comparison was made between spontaneous spike activity before and after exposure on 14 cultures exposed at different ages (13 - 40 DIV). A count was done of all spikes detected on the 60 electrodes during the 3 min recordings. As shown in Figure 4-2 there was no change in the number of spikes before and after exposure.

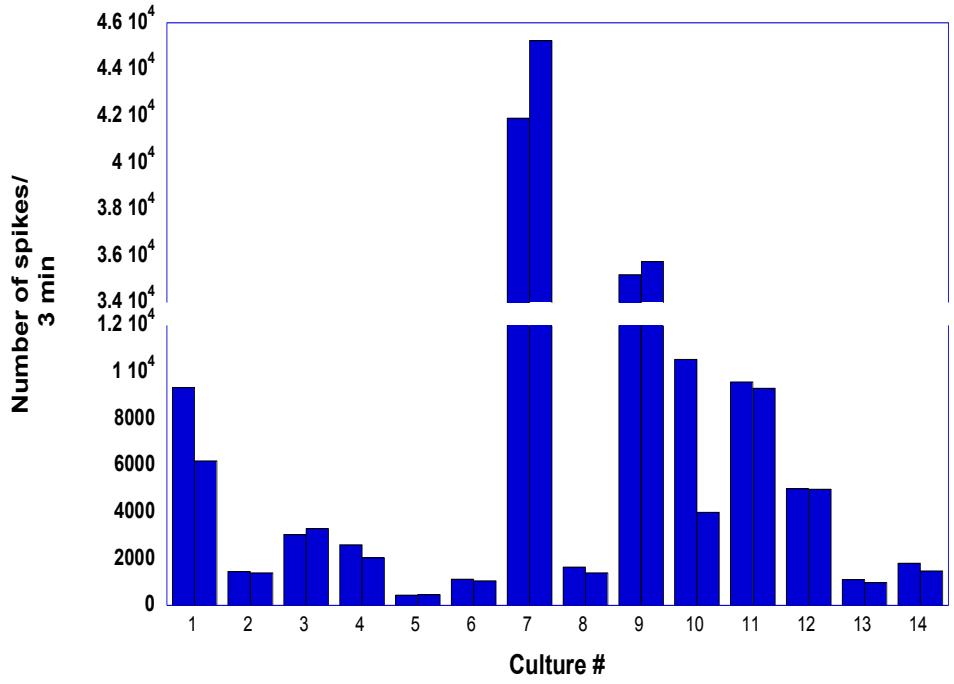

Figure 4-2: fourteen cultures (13 to 43 DIV) were exposed using the three 3 min GSM exposure protocol. The FR of pre- and post-exposure phases is plotted from left to right.

Three 3-minute GSM exposures

The FRs among the four phases (ZERO, POST1, POST2, and POST3) showed no changes compared to the global reduction of activity observed under standard conditions (paragraph 4.1.1).

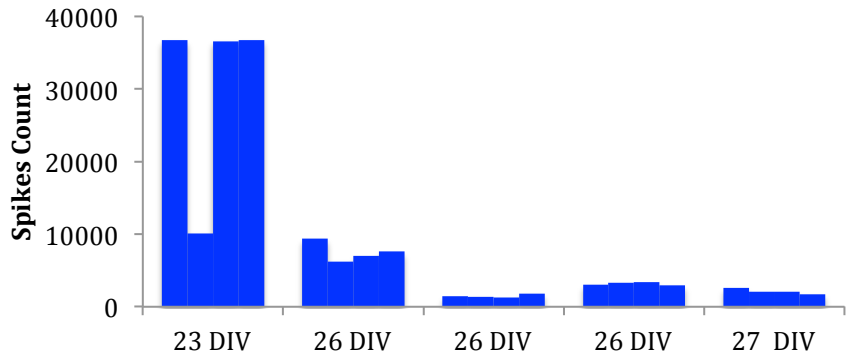

Figure 4-3: Five cultures (23 to 27 DIV) were exposed using the three 3 min GSM exposure protocol. The FR of pre- and post-exposure phases is plotted from left to right as phases ZERO, POST1, POST2, and POST3.

4.1.3 Analysis of exposure phases

In these experiments the sealing membrane was not used and no sham runs were carried out. The data analyses were entirely performed using SpyCode. The GSM-filter was applied to all recordings before computing spike detection using the PTSD method (user default parameters: DT = 8σ, PLP = 2 ms, RP = 1 ms).

Single 3 minute GSM exposures

The activity of two cultures at 13 and 15 DIV was analysed in terms of FR and BR during the three experimental runs: pre-exposure, exposure and post-exposure.

FR seemed to decrease during GSM exposure. When bursts were present, there was also a major decrease in BR during exposure and a recovery in the post-exposure phase (DIV13).

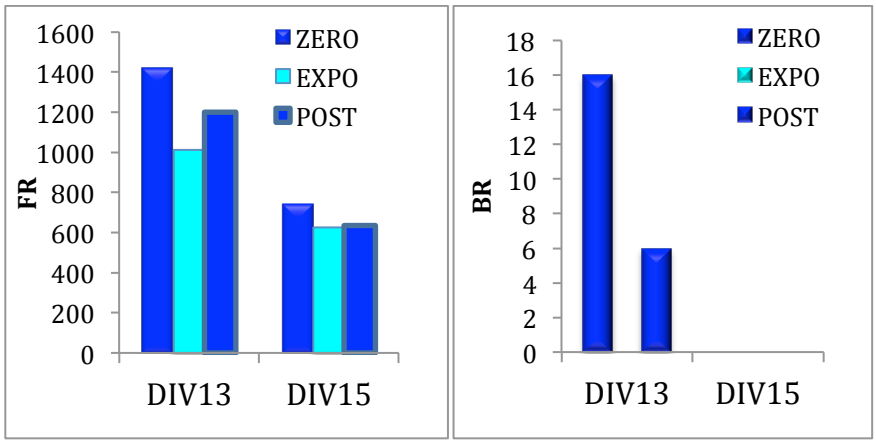

Figure 4-4: FR and BR in 3 min bins relative to two cultures (13 and 15 DIV). In the 15 DIV culture no bursts were detected during exposure.

Three 3 minute GSM exposures

A 23 DIV culture was exposed using the three '3 min GSM exposures' protocol and analysed in terms of FR and BR (fig. 4-5). No effect was observed for such a protocol with a culture 10 days older

than the one presented in Figure 4-4.

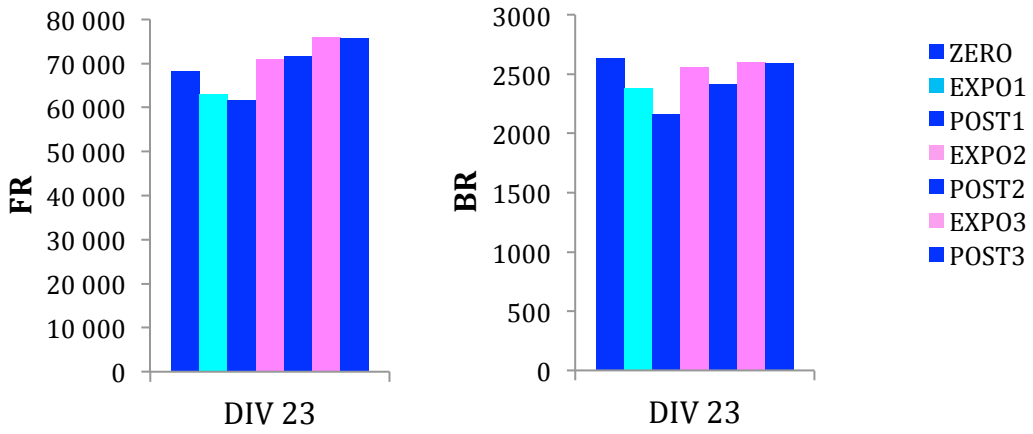

Figure 4-5: FR and BR on 3-minutes bins relative of a 23 DIV culture.

Single 15 minute GSM exposures

The BR and "number of bursting channels" were analysed for two 18 DIV cultures for which the membrane was used.

There was a trend towards a gradual decrease in bursting activity (number of bursts and bursting channels) during the 15-minute exposure and a recovery at the end of the exposure as shown in Figure 4-6.

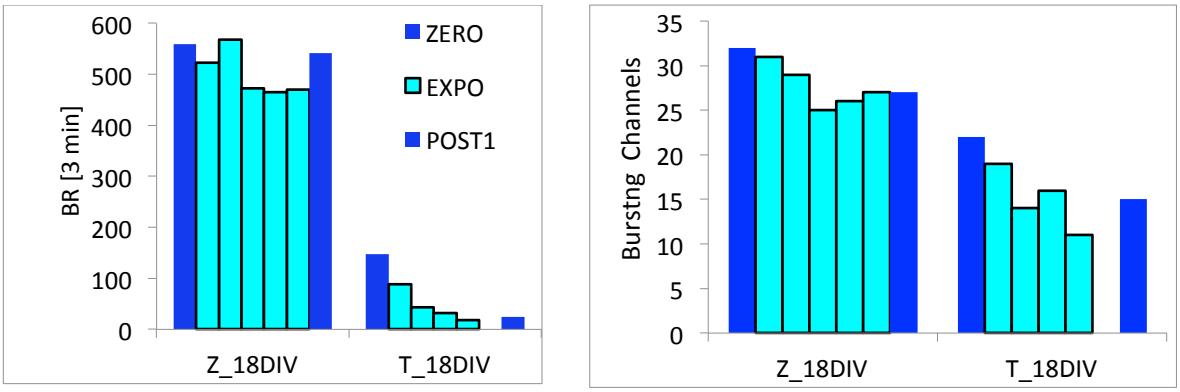

Figure 4-6: The activity of 2 cultures at 18 DIV were analysed in terms of burst (left) and number of bursting channels (right). Each bar corresponds to a 3-minute phase.

4.1.4 Conclusion on preliminary experiments

We have used several protocols described above and tested different metrics.

These preliminary experiments are globally consistent: we observed no differences between the pre and post exposure phases, and, during the exposure phase, there was a decrease in FR and BR in some of the cultures.

We noticed that the effect seemed to occur in the younger cultures. To distinguish between the variations of the spontaneous activity with time and the possible exposure effects we introduced sham

exposures the day before the real GSM exposures in the main experiment. We carried out the three 3 minute protocol with 2-3 week-old cultures.

4.2 Main experiment

Sixteen cultures, with ages ranging from 14 to 21 DIV were sham and GSM-exposed following the 'main experiment' protocol described in Figure 3-21. MFR and BR were used as the most representative metrics (Fig. 4-8 and 4-9). Other metrics relative to burst activity were also considered.

4.2.1 *Pre- versus post*-exposure effects

To distinguish between the variations of the activity due to its baseline fluctuations and possible exposure effects, we introduce sham exposures on the day before the real GSM exposure in the main experiment. In Figure 4-7, the BR mean of each experimental phase was normalized to the ZERO phase value, computed for each experimental phase and plotted with its SEM. During sham exposure and pre- and post-exposure phases of the GSM exposures, the burst activity was globally stable over the 21 min exposure protocol (Shapiro-Wilk test; sham: p=0.63; expo: p=0.31).

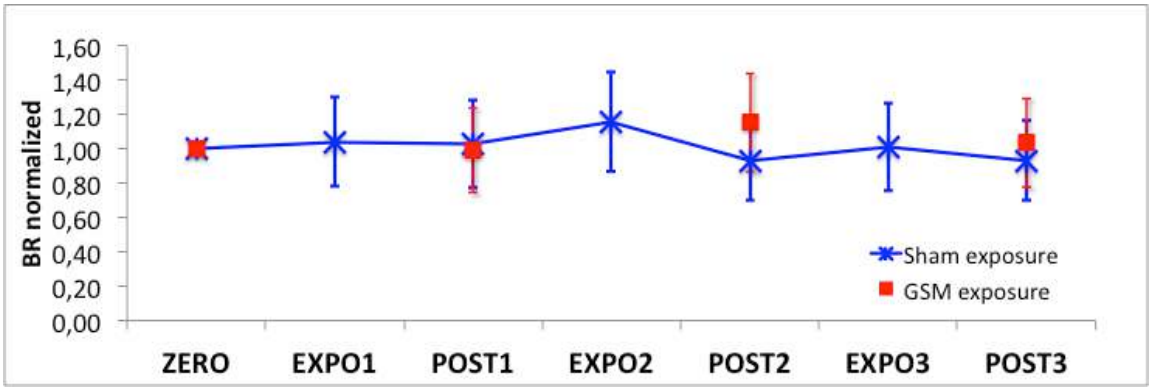

Figure 4-7: mean BR (n=16 cultures), normalized to the ZERO phase ± SEM.

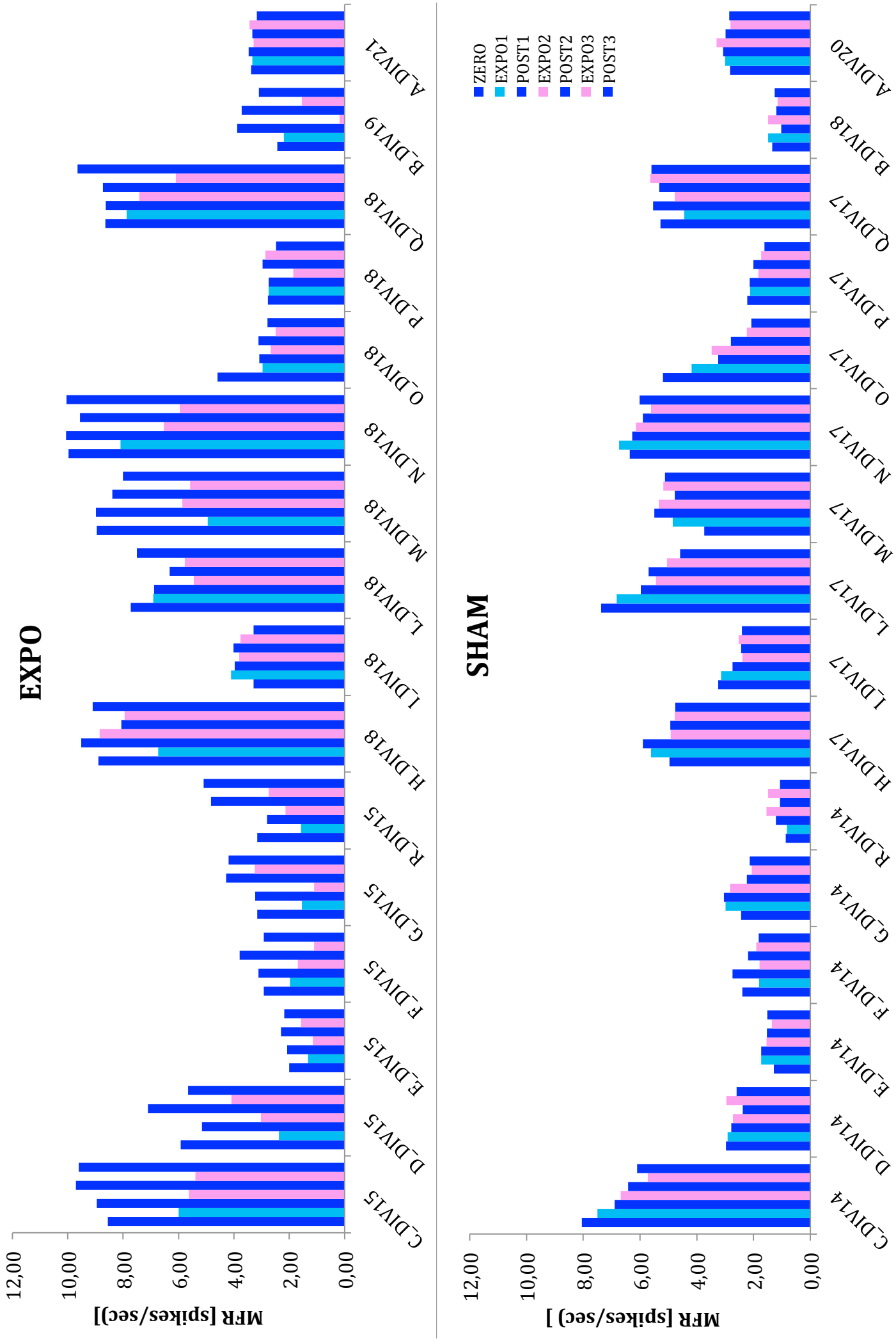

Figure 4-8: MFR for the 6 most active electrodes, during the 7 phases for 16 independent cultures. The age of the culture in DIV (days in vitro) and a letter is given in abscissa to identify each culture.

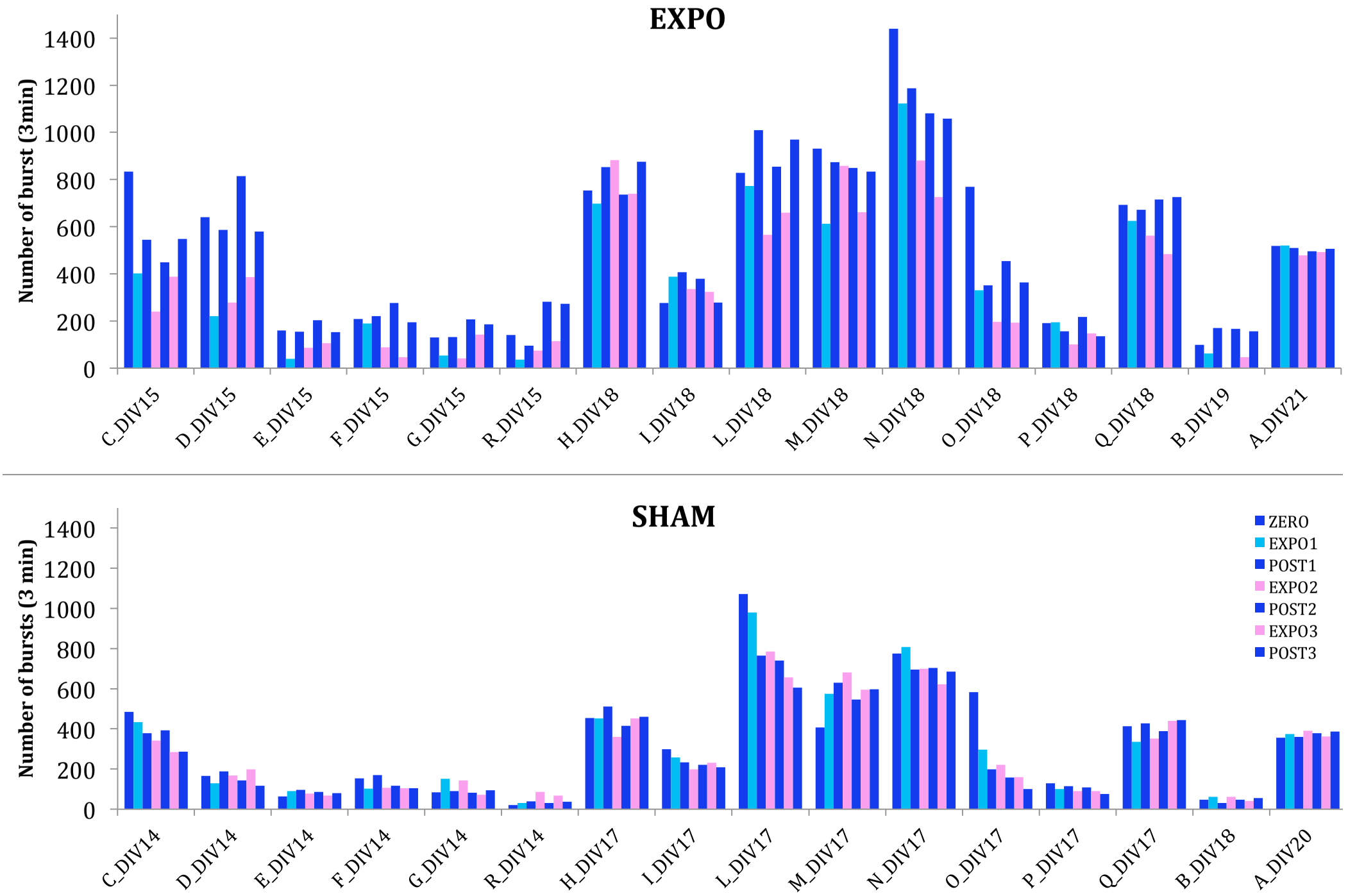

Figure 4-9: Number of burst collected for 3 min recording for the 7 experimental phases. In abscissa there is a letter and the age of the culture in DIV (days in vitro) to identify each culture.

4.2.2 Effects of exposure

Mean Firing Rate and Bursting Rate

The MFR and the BR were computed for each experimental phase for each of the 16 cultures.

In order to analyse the variation of each metric during sham or GSM exposure, the ratio R' was evaluated for parameter X (MFR or BR). R' was defined as $X_{exposure}$/mean(X_{before}; X_{after}), where $X_{exposure}$, X_{before}, and X_{after} are the parameter X value during, before, and after exposure, respectively. An example of R' relative to MFR for three exposures is given in equations (1).

R' was defined to describe the changes observed during sham or GSM exposure with respect to the averaged counts before and after exposure to account for any slope in the activity baseline. Table 4-1 shows that MFR and BR were not altered during sham exposure (as shown in fig. 4-7), but reduced by around 30% during each of the GSM exposures. Moreover, Figures 4-8 and 4-9 suggest that the amplitude of the effect decreased with age from 15 to 21 DIV.

$$R'_{I} = MFR_{EXPO1}/\text{mean}\,(MFR_{ZERO}\,;\,MFR_{POST1})$$
$$R'_{II} = MFR_{EXPO2}/\text{mean}\,(MFR_{POST1}\,;\,MFR_{POST2}) \qquad (1)$$
$$R'_{III} = MFR_{EXPO3}/\text{mean}\,(MFR_{POST2}\,;\,MFR_{POST3})$$

Expo vs mean(pre ; post) (N = 16)		MFR			BR		
		R'_I	R'_{II}	R'_{III}	R'_I	R'_{II}	R'_{III}
GSM EXPOSURE	Observed mean	0.75	0.65	0.73	0.70	0.59	0.66
	p	0.0002	0.0001	0.0002	0.0001	0.00007	0.00003
SHAM EXPOSURE	Observed mean	1.00	1.02	1.01	1.03	1.13	1.06
	p	0.95	0.65	0.87	0.72	0.28	0.45

Table 4-1: values of the ratio R'_I, R'_{II}, and R'_{III} for the MFR and BR, calculated respectively for the GSM and sham experiments. The corresponding p values are based on the Shapiro-Wilk test.

Total Burst Duration, Mean Burst Duration Bursting Channels and Network Bursts

As the amplitude of the effect was higher for the BR, the other metrics were analysed in terms of burst activity. These analyses were done on 12 cultures (A, B, C, D, E, F, G, H, I, L, M, and N) randomly chosen among the 16 cultures.

Total Burst Duration decreased during GSM exposure as shown in Table 4-2 but the Mean Burst Duration was not affected (Table 4-3).

Total Burst Duration (n=12)		Expo vs pre & post		
		R'_I	R'_{II}	R'_{III}
GSM EXPOSURE	Observed mean	0.62	0.53	0.62
	p	0.0004	0.0004	0.0018
SHAM EXPOSURE	Observed mean	1.05	1.10	0.96
	p	0.38	0.48	0.71

Table 4-2: values of the ratio R'_I, R'_{II}, and R'_{III} for the Total Burst Duration calculated respectively for the GSM and sham experiments. The corresponding p values are based on the Shapiro-Wilk test.

Mean Burst Duration (n=12)		Expo vs pre & post		
		R'_I	R'_{II}	R'_{III}
GSM EXPOSURE	Observed mean	0.94	0.81	0.86
	p	0.75	0.04	0.07
SHAM EXPOSURE	Observed mean	1.00	1.02	0.96
	p	0.99	0.76	0.50

Table 4-3: values of the ratio R'_I, R'_{II}, and R'_{III} for the Mean Burst Duration calculated respectively for the GSM and sham experiments. The corresponding p values are based on the Shapiro-Wilk test.

Bursting Channels (n=12)		Expo vs pre & post		
		R'_I	R'_{II}	R'_{III}
GSM EXPOSURE	Observed mean	0.85	0.84	0.89
	p	0.03	0.14	0.07
SHAM EXPOSURE	Observed mean	0.95	0.96	1.01
	p	0.37	0.78	0.93

Table 4-4: values of the ratio R'_I, R'_{II}, and R'_{III} for Bursting Channels calculated respectively for the GSM and sham experiments. The corresponding p values are based on the Shapiro-Wilk test.

These data show that the effect is mainly on the number of bursts since the MBD is not changed by GSM exposure.

The number of Bursting Channels was not affected during GSM exposure (Table 4-4).

To investigate further the mechanism behind the reduction of the number of bursts during GSM exposure, network bursts (NB) were computed for ten cultures. There was a reduction of NB during the exposure phase for some of these cultures as shown in Figure 4-10, but the low number of NB did

not allow for a meaningful statistical analysis.

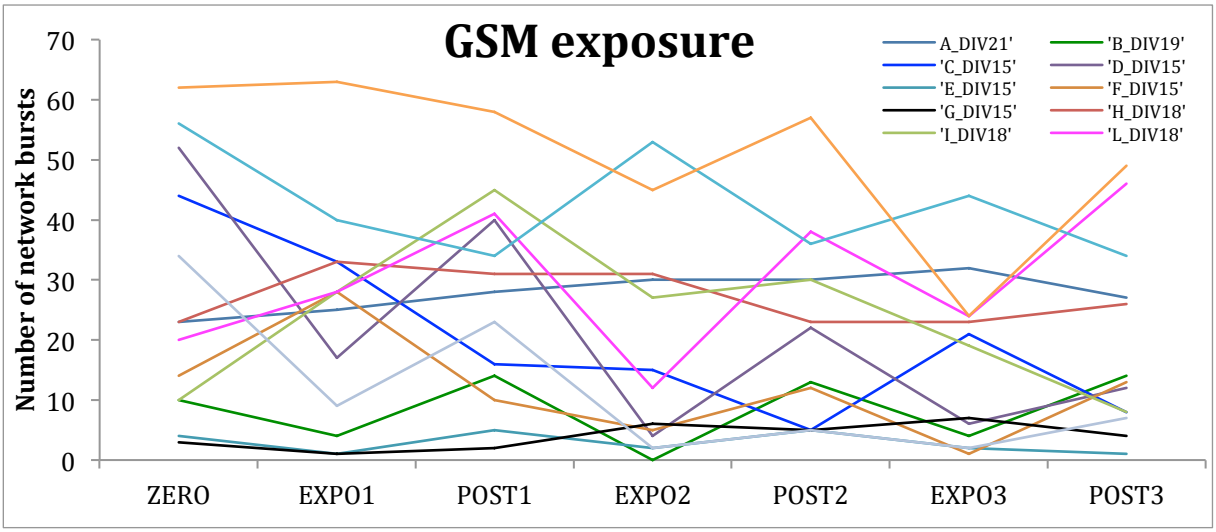

Figure 4-10: Network bursts for the GSM exposure phases for ten cultures (chosen among the 16 initial ones).

It would be interesting to investigate the effects by evaluating the degree of synchronous activity in the network using other metrics such as cross-correlation on burst events. This approach was hindered by the lack of long recordings of the activity, which are needed when working with these metrics.

Inter-Spike-Interval Histogram

A potential specific feature of the effect of GSM was searched for at the 217 Hz modulation frequency (4.6 ms period) by plotting the Network Average ISIH. We therefore analysed six cultures, which showed a large effect on BR.

Figure 4-10 shows the ISIHs for the 7 phases of the GSM exposures protocol for culture C (15 DIV). As there was a reduction in BR, the peak relative to the 'spikes within bursts' at 2-3 ms was, as expected, reduced during exposure. However, there is no alteration of the ISIH at 4.6 ms that would have indicated a specific role for the modulation frequency, such as entrainment of the spikes. These visual observations were extended to the other cultures.

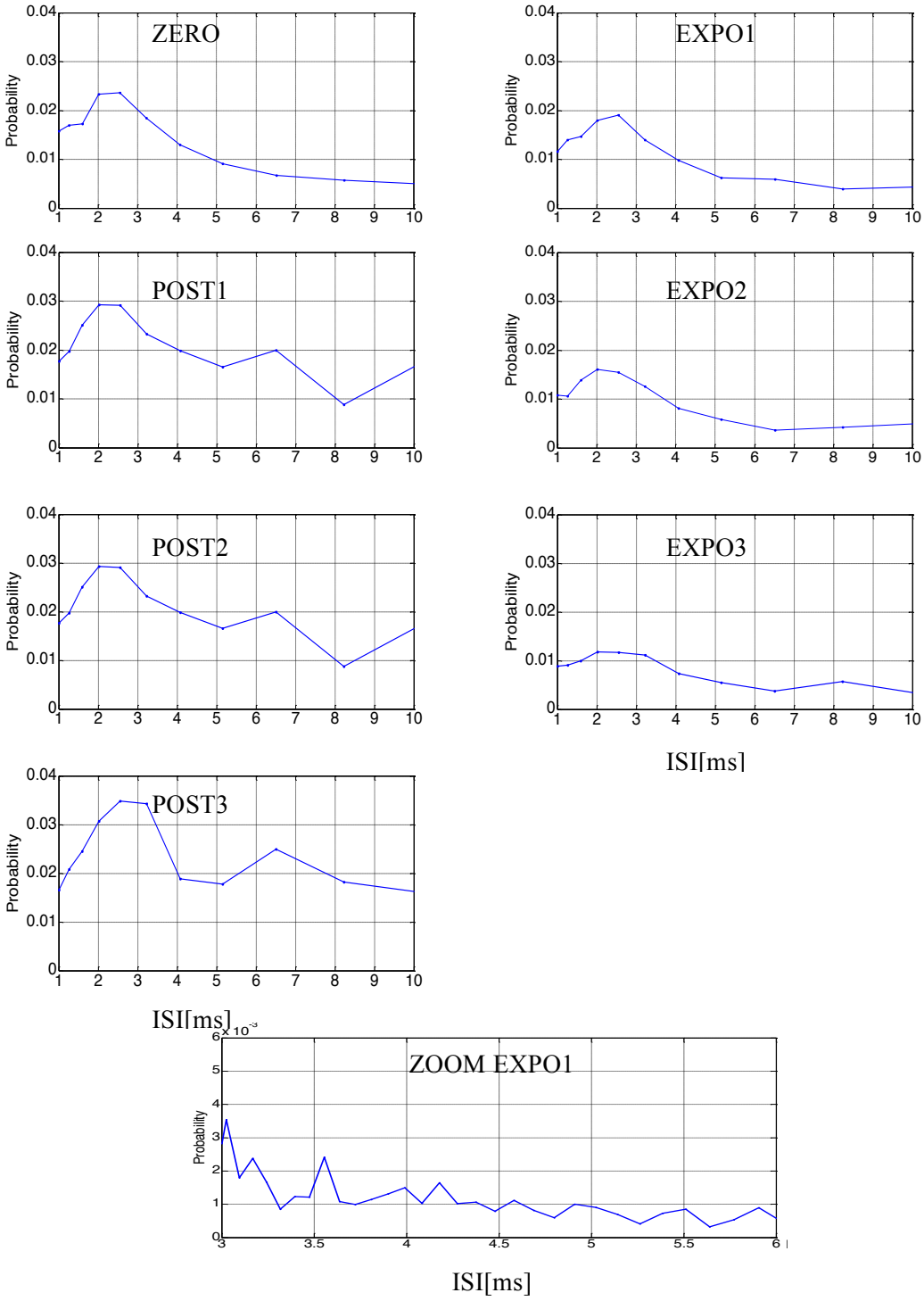

Figure 4-10: Network Average ISIH (1 ms bins) of the 7 runs relative to the GSM exposure, on the left: pre- and post-exposure phases; on the right GSM exposure phases. At bottom a zoom of phase EXPO1 from 3 to 6 ms with 0.1 ms bins showing no alteration at 4.6 ms.

Time profile of the neuronal activity

We studied the time distribution of the activity during the experimental phases using the raster plots calculated using SPYCODE. Figure 4-12 shows, as one of the representative example, the raster plot of culture D (15 DIV) for the ZERO, EXPO1, and POST1 runs of the GSM exposure. Spikes

decrease from approximately the second half of the recording EXPO1 phase to the first part of POST1 phase then the activity rises to reach the same level as in the ZERO phase.

This evolution of the activity with time was also observed in the subsequent GSM exposure phases for the same cultures and for other cultures.

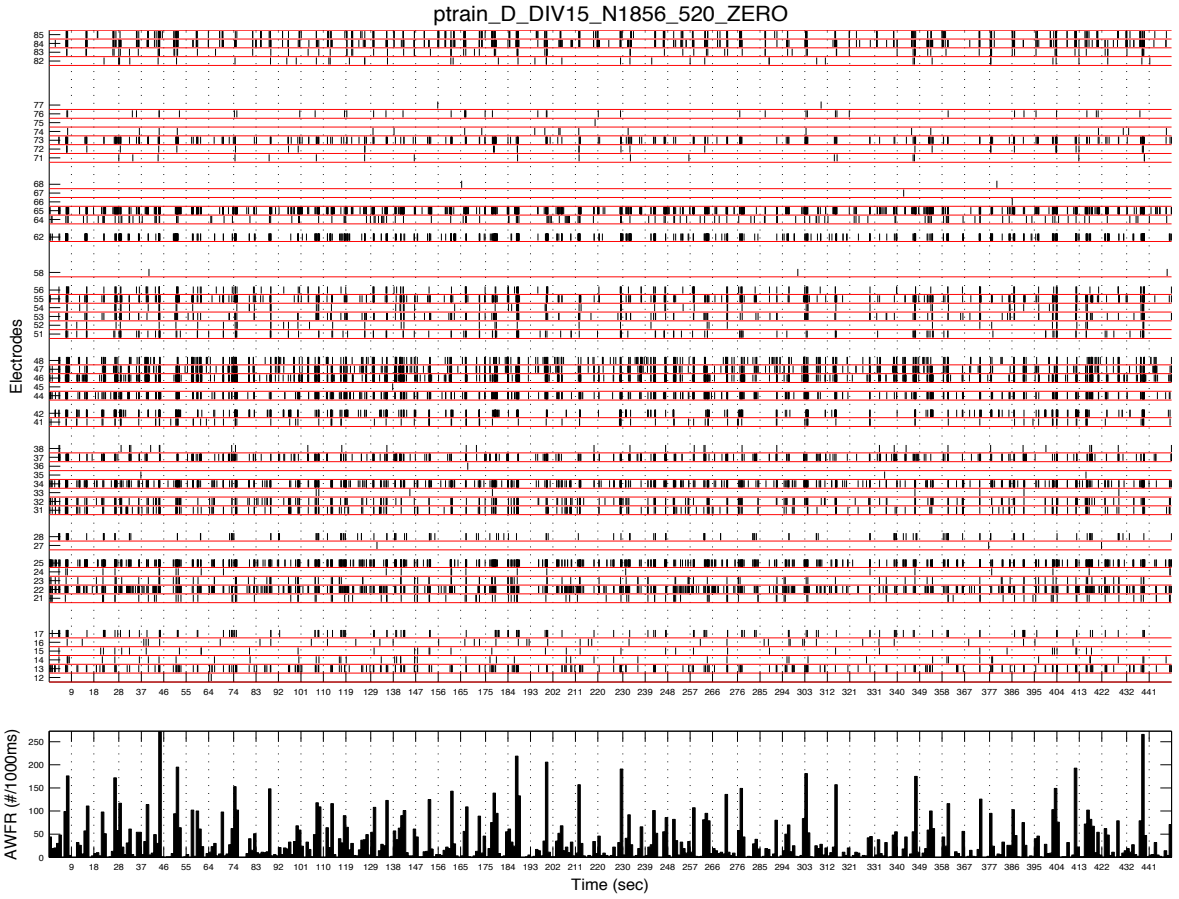

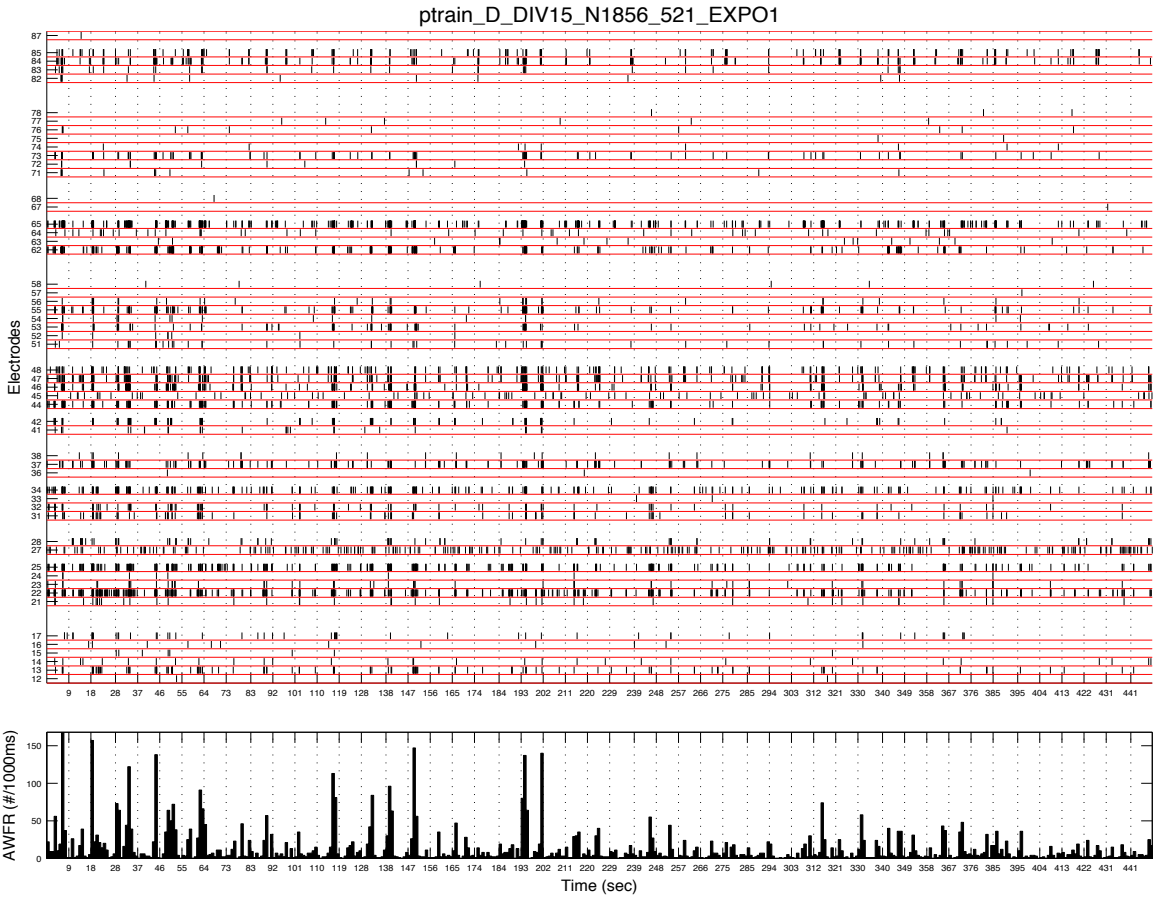

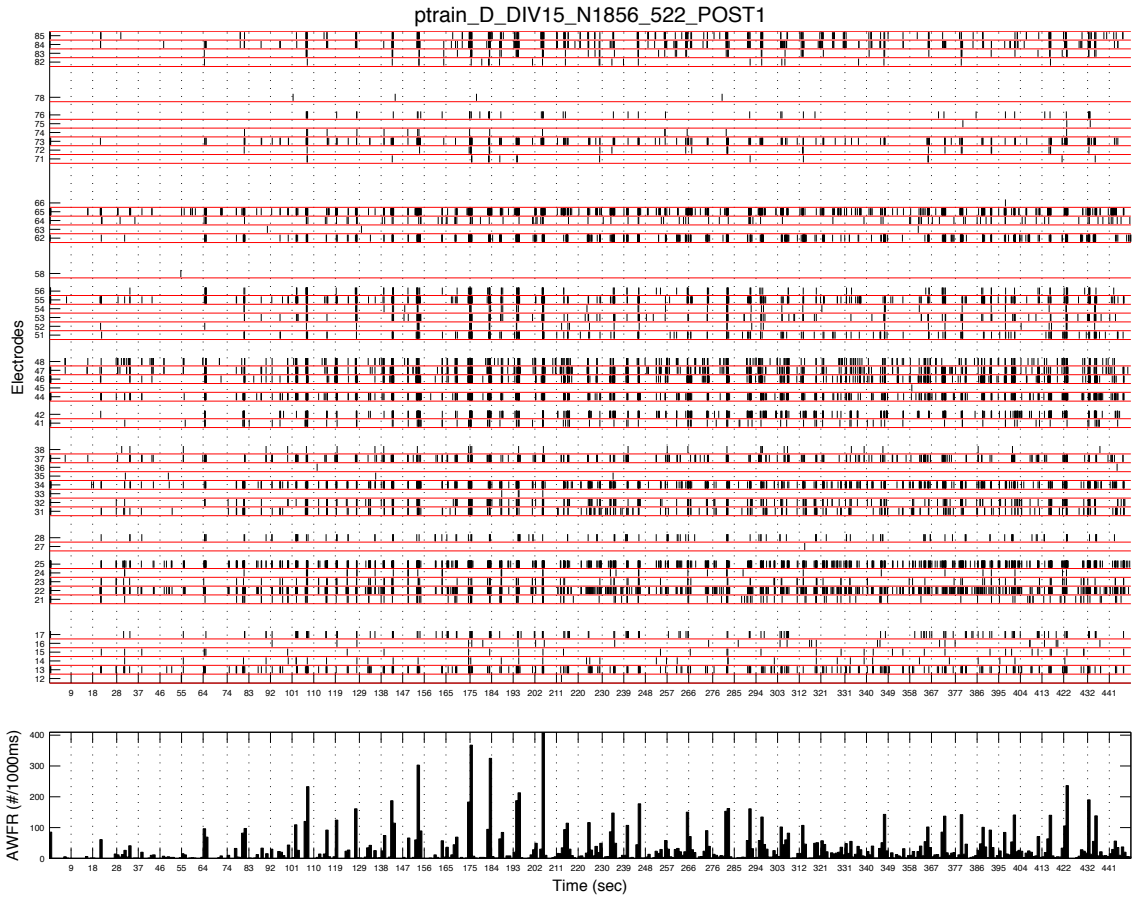

Figure 4-11: Raster plot (i.e. each vertical bar representing a spike). At the bottom of each raster plot the Average Firing Rate (AWFR) was computed for all channels in 1 s time bin.

In conclusion, the 16 cultures showed a significant decrease of MFR and BR during GSM exposures but the duration of the bursts was not affected. The effects of exposure described above are phasic and reversible on that time scale as they end with each exposure phase.

Part of these results (first three phases of the main experiment) have been published recently in a peer-reviewed journal [Moretti et al, 2013] (see appendix D).

5 DISCUSSION & CONCLUSIONS

The main aim of this work was to assess the feasibility of studying the electrical activity of neuronal networks under exposure to mobile-phone RF signals at 1800 MHz. For this purpose, an RF system was built for exposing the biological samples inside MEAs, which had been well characterized in terms of dosimetry [Merla et al., 2011]. In spite of the high quality of this experimental and numerical study, there remains some uncertainty on SAR and temperature at the level of the electrodes, in view of their very small size and the related limitations of the FDTD method for such cases. One can estimate that the SAR level used in this work (3.2 W/kg), at the level of the neurons is known with a 30% uncertainty. As explained below in detail, there is still the possibility that local heating of the electrodes by a few degrees Celsius may affect the activity of the adjacent neurons.

A vast body of knowledge has been gathered in terms of response of the neuronal networks to various physical (mainly electrical stimulation), chemical, and pharmacological agents: the use of MEAs has already been successfully applied to many various types of investigations including modulation of neuronal network activity by viral infection on synaptic transmission [Volmer et al., 2007], magnesium-induced neuronal apoptosis [Dribben et al., 2010], endo-cannabinoids [Piet et al, 2011], and functional toxicological screening [Scelfo et al., 2012].

5.1 Feasibility

As described above, the GSM signal was chosen as it allowed the acquisition of the electrophysiological signal during the seven empty time slots. However, the interference caused by the active timeslot was eliminated using a spectral filter, which allowed us to use the 8 timeslots. We tested the performance of the filter by visual control and in terms of number of spikes and showed that the uncertainty on that number was low. We further demonstrated that the artefact was mainly caused by a direct interference of the amplifier with the GSM RF fields. Even if we cannot totally exclude the possibility of an induction of currents at the electrodes and their leads (see below the discussion on the role of induced currents and temperature elevation), we observed that shielding the amplifier with RF-absorbing material reduced this interference thereby reducing potential induced currents.

The results of preliminary experiments designed at testing the feasibility of the whole experimental setup showed essentially that, over the duration of the exposure protocols, there was little variation of the metrics that were chosen to describe the behaviour of the electrical activity of the neuronal networks. Under GSM exposure, the main findings were that there was a decrease of both the MFR and BR metrics during the 3 min exposure and a full recovery after exposure. However, when the

exposure duration was extended to 15 min, the decrease continued during exposure and the post-exposure recovery was not total. A large experiment was thus designed to increase the statistical power, improve the experimental conditions, and include cultures with different ages. The results obtained with these 16 independent cultures showed no alteration of electrical activity following cessation of the 3 min RF exposures.

However, when the signals were analysed during the time course of the 3 min RF exposures, a significant decrease in spontaneous electrical activity was observed (Fig. 4-8 and 4-9). This can be seen again in Figure 5-1 below, which shows the time courses of the network bursts (NB) for the 7 phases of a run on a 15 DIV culture in the main experiment. In the first exposure phase (blue), the decrease of the number of NB as a function of duration of exposure is obvious as well as the "recovery" during the sham exposure phases (uncoloured). This is consistent with the observation of a continuous decrease of burst number during the 15 min exposure (Fig. 4-6).

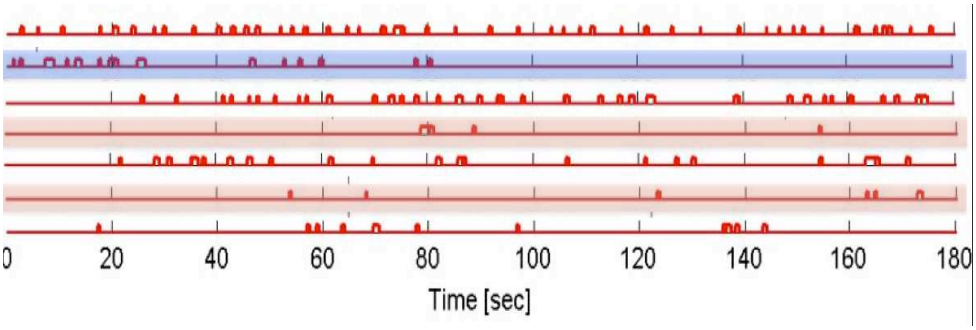

Figure 5-1: Raster plot for network bursts (red rectangles) in culture D of the main experiment. From top to bottom: Phases Zero, Expo1, Post1, Expo2, Post2, Expo3, and Post3.

The feasibility of our project was thus well demonstrated as the whole process of culture of neuronal networks, exposure of these cells to RF, acquisition of the electrical activity, filtering and analysis was performed with success.

5.2 Sensitivity analysis

A sensitivity analysis was performed to determine the dependence of the effect on several conditions. Two examples are given in the figures below. The first focuses on the age of the culture. It was mentioned in the results section that there was a trend towards the disappearance of the effect with age. Figure 5-2 shows that indeed the BR reduction decreases from ca. 55% at 15 DIV to 0% at 20 DIV. The most straightforward interpretation of this observation is that this phenomenon is related to the shift from spike to burst activity that occurs with age over the first three weeks of culture during the development of the culture.

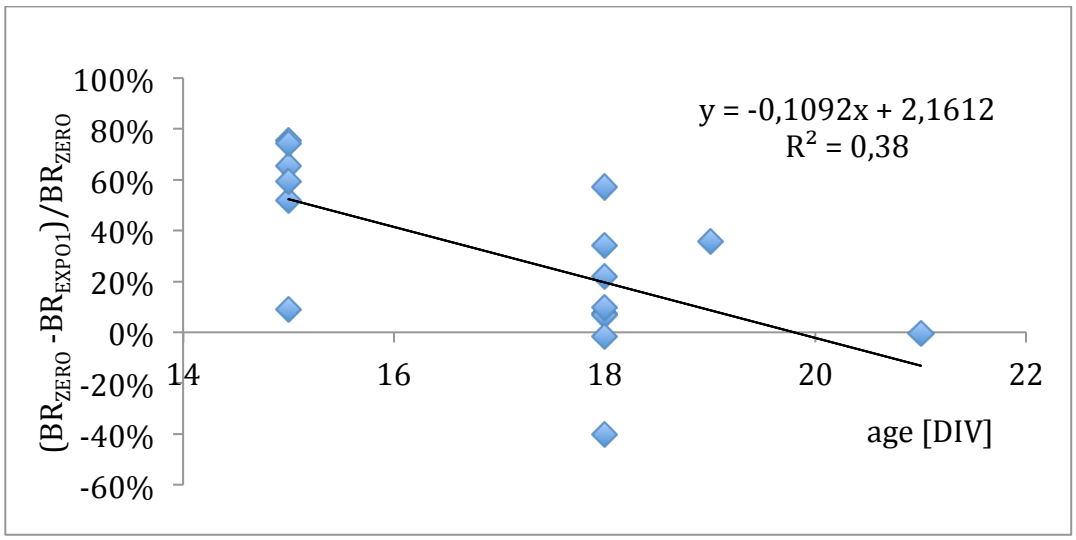

Figure 5-2: Sensitivity analysis. Amplitude of the effect on BR as function of the age of the cultures.

As a consequence one can notice that the amplitude of the effect is more salient for younger cultures (e.g., ca. 50% at 15 DIV) as shown in the table 5-1:

	R'I	R'II	R'III
DIV15	0,58	0,48	0,78
	0,36	0,40	0,55
	0,25	0,48	0,59
	0,88	0,36	0,20
	0,40	0,24	0,73
	0,31	0,40	0,42
Observed mean	**0,46**	**0,39**	**0,54**
p	0,00253	0,00001	0,00331

	R'I	R'II	R'III
DIV18	0,87	1,11	0,92
	1,13	0,85	0,98
	0,84	0,61	0,72
	0,68	1,00	0,79
	0,85	0,78	0,68
	0,59	0,49	0,47
	1,11	0,53	0,83
	0,92	0,81	0,67
Observed mean	**0,87**	**0,77**	**0,76**
p	0,101	0,220	0,004

Table 5-1: Statistical analysis of the RF effect for 15 DIV (n=6) and 18 DIV cultures (n=8).

Within the scope of this sensitivity analysis, we looked for a "predictor" of the effect by plotting the amplitude of the effect as a function of the various metrics measured during phase ZERO, that is before exposure. An example is given in Figure 5-3 below in which the increase in the amplitude of the effect with the percentage of random spikes in zero phases is shown for 12 cultures. For cultures having a proportion of random spikes of at least 40% during phase ZERO, the probability of having a large amplitude of the effect is thus much larger than those with a small proportion of random spikes.

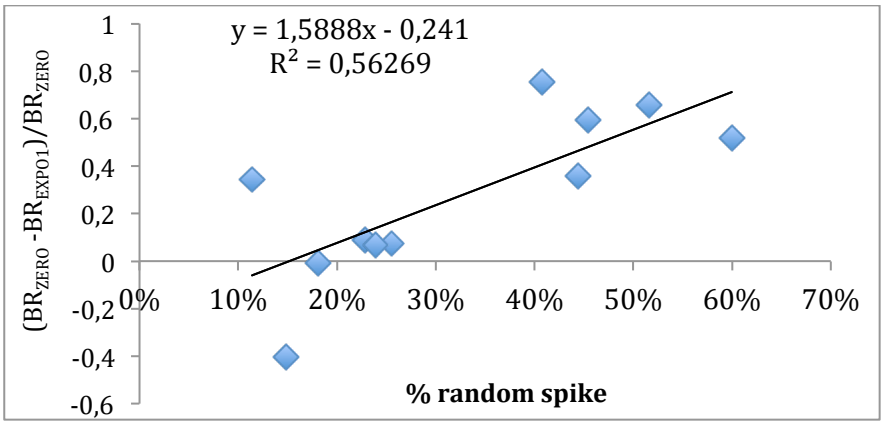

Figure 5-3: Amplitude of the effect as a function of the percentage of random spikes in the ZERO phase.

5.3 Mechanistic hypotheses

Regarding the nature of the mechanism behind the observed effect, one can first learn from the literature: there are several stimuli that are known to elicit inhibitory effects on neuronal networks, such as pharmacological agents [McCabe et al., 2007; Piet et al., 2011], toxic agents such as the Ni ion [Gavazzo et al., 2011] or a decrease in temperature leading to a decrease in bursting behaviour [Rubinsky et al., 2007]. However, none of those operate in a reversible manner as rapidly as observed in our work. The inhibitory effect of GSM exposure seems therefore to be specific, at least for short exposure durations. The rapid onset of the effect and its reversibility are both in favour of a mechanism occurring at the neuronal membrane where fast bioelectric phenomena can be generated with relatively little inertia.

5.3.1 Role of temperature elevation

The role of temperature elevation in the elicitation of the observed effect of GSM exposure must be discussed in terms of potential "nonthermal effects", i.e., biological effects that are not caused by temperature elevation in the tissues. To date, these nonthermal effects have not been well documented [AGNIR 2012; SSM 2013].

In the investigations of the Gimsa group, performed using continuous wave (CW) and Universal Mobile Telecommunications System (UMTS) signals at up to 2.6 W/kg, there was a rise in temperature of up to 0.24 °C. Around 33 % of the evaluable neurons showed an increase in activity, which correlated with the power of the UMTS signal. No influence of the power control of the UMTS signal was found at 10 or 740 Hz. The conclusion of the authors was that the mechanism behind the increase in activity was of a thermal nature [Sakowski and Gimsa, 2008].

In our experimental system, the temperature elevation of the neurons had a time constant of 13 min and reached 0.3 °C at steady state for a SAR of 3.2 W/kg [Merla et al., 2011]. Under our exposure conditions, the temperature elevation at the end of the 3 min exposure was thus around 0.06 °C. This elevation is very small compared to the 0.24 °C temperature elevation measured in the experimental

work of the Gimsa group described above, and is very unlikely to be sufficient to cause a reversible effect in a cellular system.

However, when using the GSM signal, the energy is not deposited in a continuous manner since during the ON timeslot, the power is 8 times the average power. A rough calculation based on the formula for heat diffusion from a heated sphere in water gives an estimate of the temperature elevation in the 40 µm voxel just above one of the electrodes, based on the SAR determination of Merla et al. (i.e., SAR of 10 W/kg in those voxels for an incident power of 1 W). The thermal response time of the sphere is $\tau = a^2/2\alpha$ where a is the radius of the sphere, α the thermal diffusivity of the sphere. Temperature elevation at time τ is given as $\Delta T = q\tau/\rho c_p$ where q is the volumetric heating (equivalent to SAR), ρ is the solution density, and c_p is the specific heat of the solution. For a sphere with 40 µm diameter, with $\alpha = 1.43 \times 10^{-7}$ m^2/s, $\rho = 1000$ kg/m^3, and $c_p = 4 \times 10^{-3}$ J/kg K, we find $\tau = 1.4$ ms. Thus, ΔT is ca. 2.8 °C for the considered voxel. On the basis of the outcome of this crude calculation, we cannot exclude a localised thermal effect on a neuron in contact with the electrode.

However, there is very little information in the literature about the effect of temperature changes around 37 °C on MFR and BR. Such a study should be performed from 35 to 39 °C by adjusting the set point of the incubator to determine whether a putative temperature elevation caused by RF exposure causes a reduction in bursting. An experiment was done by Kang & Nam [2008] using a near-infrared laser (785 nm, 1.9×10^3 J/cm^2) as a source for heating an hippocampal neuronal network that showed that the spontaneous spike rate was significantly decreased in 72.1 % of the channels during the 10 min exposure but returned to their initial values when exposure ended. The authors were able to reproduce these effects by raising the culture plate temperature by 4 °C, which strongly suggests that the thermal energy of NIR laser was dominant in their experiment. However, NIR laser stimulation was reversible and seemed not to affect the viability of the neuronal network. This type of heating effect thus occurs in the same direction as the one we observed.

The only way to ascertain the role of this "pulsed" TDMA amplitude modulation will be to perform exposures at the same SAR level (3.2 W/kg) using continuous wave RF (CW). The elicitation of the effect should also be further studied systematically as a function of SAR, modulation pattern (modulation frequency in particular), and duration of exposure.

5.3.2 Other mechanisms

With regards to other types of mechanisms, related to electrical stimulation, the studies by the Potter group in the USA and [Wagenaar et al, 2005] in particular offer several observations and hypotheses that are worth considering. Using culture and acquisition protocols similar to ours, these authors observed that electric stimulation with 50 stim/sec distributed across 25 electrodes, completely suppressed bursting in all cultures tested. They noticed that, in contrast to burst suppression by partial blocking of excitatory synaptic transmission (e.g., Mg^{2+}), such distributed

stimulation did not reduce the ability of the culture to respond to additional stimuli. Such behaviour is usually rationalized by invoking a lack of input signals to the neurons (in contrast to the in vivo situation). The electrical stimulation may be providing these inputs, which, in our work, would be related to the GSM RF field.

One of the questions raised by the authors, besides the therapeutic use of this approach in epilepsy was whether such persistent stimulation *in vitro* might influence network topology, that is induce plasticity (see below in the perspectives section).

The estimation given above of the peak electric field at the level of the neurons under RF exposure gave 112 V/m which is much lower than that the field commonly applied during stimulation via the MEA electrodes (ca. 1000 V/m). However, several authors have reported that sub-threshold repetitive electrical stimulation, in addition to noise, alters the electrophysiology of neuronal networks. An example is given in the work of Köndgen et al., [2008] who injecting a superposition of a small-amplitude sinusoidal signals and a background noise onto a cortical neuronal network. They characterized the evoked firing probability in the frequency range 1-1000 Hz, while quantifying the response amplitude and phase-shift. They found that neurons unexpectedly tracked fast transients, as their response amplitude had no attenuation up to 200 Hz. This most interesting finding suggests that our experimental model might respond in a different way to a signal with a fundamental frequency below 200 Hz.

Further consideration of potential mechanisms can be drawn from the literature on the response of neuronal networks to rapid low-level stimulation. Using patch-clamp techniques, German and Russian research groups [Tchumatchenko et al, 2011] showed that (i) populations of visual cortex neurons (slices of rat cortex) respond immediately to subtle 20 pA change of mean input current in the soma, (ii) populations of cortical neurons *in vivo* can encode fast varying signals up to 200–300 Hz in their firing, and (iii) populations consisting of a few thousand neurons can reliably detect small changes of mean input current within the first few milliseconds after stimulus onset. It is remarkable that, in that work performed using a protocol in some ways similar to ours (rapid stimulation below action potential threshold), neuronal networks responded by encoding signals with modulation at up to 300 Hz.

In an earlier report by the American physicist RK Adair [Adair, 2001], a mechanism was proposed showing that sensory systems exposed to signals that are generally smaller than the noise levels of individual primary detectors, are manifest in very small increases in the firing rates of sets of afferent neurons. For such systems, this kind of network can act to generate relatively large changes in the firing rate of secondary ‘‘coincidence’’ neurons and generate ‘‘yes–no’’ spike signals that can direct behavioural responses.

In the research area of mechanisms of low-level EMF bioeffects the concept of stochastic resonance has often been mentioned as contributing to the occurrence of the effects. Stochastic

resonance is a phenomenon that involves coupling between deterministic and random dynamics in non-linear systems leading to improved detection of low-level input signals when the noise level in the non-linear system increases. As a consequence, the detection of a sub-threshold input signal is improved when a certain level of noise is added. This is postulated to be true for effects on neuronal networks [Mino et Durand DM, 2010].

The consequences in terms of interpretation of the human EEG data that were obtained using GSM signals and not CW [e.g., Croft et al., 2010] are obviously difficult to assess at this time.

Experimental demonstration of the feasibility was thus achieved in this work, which opens new perspectives regarding the study of the effects of exposure to RF signals on neuronal tissue functioning.

6 PERSPECTIVES

Assuming that the found effect of GSM exposure on the activity of neuronal networks is further independently validated, one will need to experiment with animal models in order to bridge the gap between these *in-vitro* data and the human ones. RF exposure of mice using a loop antenna with simultaneous recording of EEG using intracranial electrodes is technically feasible [Lévêque et al, 2004] and would be highly informative.

Further research that should be considered is outlined below, starting with those experiments that can be done using the equipment already available and continuing with projects that will necessitate extensive development of the equipment and methods.

6.1.1 Short-term perspectives

- *CW exposure*: Following our finding of an effect of GSM exposure on the bursting rate of young neuronal networks, the next step in the elucidation of the mechanism is to test the controversial hypothesis that modulated RF might be more effective in eliciting biological effects than CW. This hypothesis is based on the fact that in the GSM signal, as an example, the peak emitted power and therefore the SAR in the exposed target is 8 times greater than the average power (i.e., CW). If such a peak power is above the threshold for eliciting the effect, only the GSM exposure will trigger the events linked with the effect. Such a strategy has been designed and implemented in several studies in the last years [see review by Juutilainen et al, 2011]. The conclusion of the authors was that, while the majority of recent studies have reported no modulation-specific effects, there are a few exceptions indicating that there may be specific effects from amplitude-modulated RF fields on the human central nervous system. A series of exposure is thus planned, under conditions similar to that of the main experiment described above with both GSM and CW exposures done at the same averaged SAR of 3.2 W/kg. Following this set of runs, more exposures will be performed with the GSM signal at 6.4 W/kg, i.e., at twice the initial level to assess the dose-response behaviour of the effect. At the end of this study with various exposure parameter levels, we will have gathered more information on the putative thermal nature of the effect.

- *Pharmacological study of the plasticity under RF exposure*. One of the key questions related to the observation of effects of exposure to an agent on the electrical activity of neuronal cultures is whether there is associated plasticity. Such induced long-term plasticity has been described in several cases and in particular when using the molecule bicuculline [Arnold et al., 2005]. In that experiment, a 15 min exposure of the networks to this $GABA_A$ receptor antagonist induced an increase in synaptic efficacy at excitatory synapses that was associated with an increase in the frequency of miniature AMPA receptor-mediated excitatory

postsynaptic currents (EPSCs) and a change in network activity from uncoordinated firing of neurones to a highly organized, periodic and synchronous burst pattern.

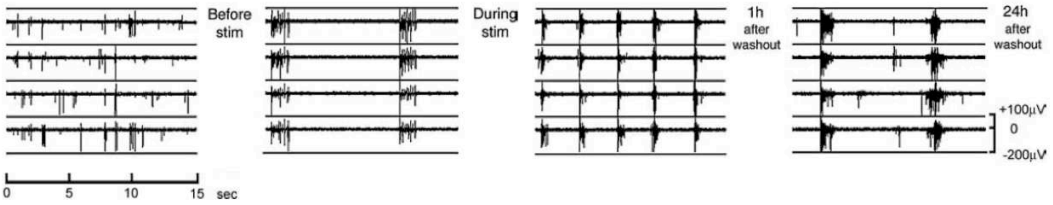

The hypothesis that we want to test is that GSM exposure affects bicuculline –induced synaptic plasticity. The experimental protocol will therefore be to record the spontaneous activity, then expose the neurons to bicuculline in the presence and absence of GSM for 15 min, then reassess the activity and wash away the bicuculline by changing the medium three times and finally analyse the spike and burst activity after one and two hours as a function of the presence of GSM exposure.

- *Temperature measurement at the microscopic level*. In order to assess the role that temperature elevation of the electrodes might play in altering the activity of the neurons, it is planned to measure the steady-state temperature around the electrode using chemicals (e.g., Rhodamine B) or an IR camera (e.g., OptoTherm InfraSight MI 320 IR camera).

6.1.2 Longer-term perspectives

- *Stimulation using ELF fields*. With the aim to monitor directly the effects of the amplitude modulation without the need for the 1800 MHz carrier, exposure of the networks using direct electrical stimulation at 217 Hz at low voltage (hundreds of μV) using the MEA electrodes can be tested. Applying ELF magnetic fields to the culture at 217 Hz would also produce electric fields and currents at the level of the neurons, but with a field configuration different than by using the electrodes for usual electrical stimulation.

- *Optical stimulation*, that is delivery of energy to the cells in culture using light, could be done without the need for metallic electrodes by using NIR LEDs or lasers to trigger electrical activity via a different type of interaction of the electromagnetic fields with the neurons. As an example, fast heating of the neuronal network could be achieved using an NIR laser at (1.472 μm, 150 mW Anritsu, Japan) [Slyadnev et al., 2001].

Another more involved approach would be to use pulsed laser stimulation using in the IR at 1.5 μm which is known to directly stimulate neurons without any genetic or chemical pre-treatment [Shapiro et al., 2012]. These authors have shown that pulsed IR excites cells through a novel, electrostatic mechanism: IR pulses are absorbed by water, producing a rapid local increase in

temperature. This heating reversibly alters the electrical capacitance of the plasma membrane, thereby depolarizing the target cell. This mechanism is fully reversible and requires only the most basic properties of cell membranes.

7 Bibliography

Adair RK . Simple neural networks for the amplification and utilization of small changes in neuron firing rates. *Proc Natl Acad Sci USA. 2001* **98:** 7253-7258

AGNIR (Advisory Group on Non-ionising Radiation) (2012). Health Effects from Radiofrequency Electromagnetic Fields. RCE 20 document of the British Health Protection Agency; Radiation, chemical and environmental hazards.

Arnold FJL, Hofmann F, Bengtson CP, Wittmann M, Vanhoutte P, Bading H. Microelectrode array recordings of cultured hippocampal networks reveal a simple model for transcriptionand protein synthesis-dependent plasticity. (2005) J Physiol 564.1 3–19.

Baliatsas C, Van Kamp I, Lebret E, Rubin GJ. (2012) Idiopathic environmental intolerance attributed to electromagnetic fields (IEI-EMF): a systematic review of identifying criteria. BMC Public Health 12: 643

Beason RC, Semm P. (2002) Responses of neurons to an amplitude modulated microwave stimulus. Neurosci Lett 333: 175-178

Bologna LL, Pasquale V, Garofalo M, Gandolfo M, Baljon PL, Maccione A, et al. (2010) Investigating neuronal activity by SPYCODE multi-channel data analyzer. Neural Netw 23(6):685-697.

Borghi T, Gusmeroli R, Spinelli AS, Baranauskas G. (2007) A simple method for efficient spike detection in multiunit recordings. J Neurosci Meth;163:176–80.

Chiappalone M, Bove M, Vato A, Tedesco M, Martinoia S. 2006. Dissociated cortical networks show spontaneously correlated activity patterns during in vitro development. Brain Res 1093(1):41-53.

Chiappalone M, Novellino A, Vajda I, Vato A, Martinoia S, Van Pelt J. (2005) Burst detection algorithms for the analysis of spatio-temporal patterns in cortical networks of neurons. Neurocomputing 65:653-662.

Chiappalone M, Vato A, Berdondini L, Koudelka-Hep M, Martinoia S.(2007) Network dynamics and synchronous activity in cultured cortical neurons. Int J Neural Syst 17(2):87-103.

Chiappalone M, Vato A, Tedesco MB, Marcoli M, Davide F, Martinoia S. (2003) Networks of neurons coupled to microelectrode arrays: A neuronal sensory system for pharmacological applications. Biosens Bioelectron 18(5-6):627-634.

Chizhenkova RA. (2004) Pulse activity of populations of cortical neurons under microwave exposures of different intensity. Bioelectrochemistry 63: 343-346.

Chou CK and Guy AW (1978) Effects of EMF on isolated nerve and muscle preparations. IEEE MTT 26: 141-147.

Cocatre-Zilgien, J. H., & Delcomyn, F. (1992) Identification of bursts in spike trains. Journal of Neuroscience Methods, 41, 19–30.

Courtney KR, Lin JC, Guy AW, Chou CK (1975) Microwave effect on rabbit superior cervical ganglion. IEEE MTT 23: 809-813.

Croft RJ, Leung S, McKenzie RJ, Loughran SP, Iskra S, Hamblin DL, Cooper NR. (2010) Effects of 2G and 3G mobile phones on human alpha rhythms: Resting EEG in adolescents, young adults, and the elderly. Bioelectromagnetics 31: 434-444

Crouzier D, Debouzy, Bourbon, Collin, Perrin, Testylier G. (2007). Neurophysiologic effects at low level 1.8 GHz radiofrequency field exposure: a multiparametric approach on freely moving rats. Pathologie Biologie 55: 134–142.

Curcio G, Ferrara M, Moroni F, D'Inzeo G, Bertini M, De Gennaro L. (2005) Is the brain influenced by a phone call? An EEG study of resting wakefulness. Neurosci Res 53: 265-270

Daus AW, Goldhammer M, Layer PG, Thielemann C. (2011) Electromagnetic exposure of scaffold-free three-dimensional cell culture systems. Bioelectromagnetics 32: 351-359.

Dribben WH, Eisenman LN, Mennerick S (2010). Magnesium induces neuronal apoptosis by suppressing excitability. Cell Death and Disease. 1: e63: 1-9.

Eytan D, Marom S. 2006. Dynamics and effective topology underlying synchronization in networks of cortical neurons. J Neurosci 26(33):8465-8476.

Fox MD, Raichle ME (2007) Spontaneous fluctuations in brain activity observed with functional magnetic resonance imaging. Nat. Rev. Neurosci. 8, 700-711.

Gavazzo P, Tedesco M, Chiappalone M, Zanardi I, Marchetti C. (2011). Nickel modulates the electrical activity of cultured cortical neurons through a specific effect on N-methyl-D-aspartate receptor channels. Neuroscience 177: 43-55.

Green AC, Scott IR, Gwyther RJ, Peyman A, Chadwick P, Chen X, Alfadhl Y, Tattersall JE. (2005) An investigation of the effects of TETRA RF fields on intracellular calcium in neurones and cardiac myocytes. Int J Radiat Biol 81: 869-885

Haarala C, Ek M, Björnberg L, Laine M, Revonsuo A, Koivisto M, Hämäläinen H. (2004) 902 MHz mobile phone does not affect short term memory in humans. Bioelectromagnetics 25: 452-456

Haarala C, Takio F, Rintee T, Laine M, Koivisto M, Revonsuo A, Hämäläinen H. (2007) Pulsed and continuous wave mobile phone exposure over left versus right hemisphere: Effects on human cognitive function. Bioelectromagnetics 28: 289-295

Harrison, R. R. (2008). The design of integrated circuits to observe brain activity. Proceedings of the IEEE, 96, 1203—1216.

Hebb, D.O. (1961). "Distinctive features of learning in the higher animal". In J. F. Delafresnaye

(Ed.). Brain Mechanisms and Learning. London: Oxford University Press.

Hodgkin and Huxley (1952). A quantitative description of membrane current and its application to conduction and excitation in nerve, Journal of Physiology, vol. 117, pp 500-544.

ICNIRP (International Commission on Non-Ionizing Radiation Protection) Guidelines for limiting exposure to time-varying electric, magnetic, and electromagnetic fields (up to 300 GHz) Health Physics 1998, 74:494-522

ICNIRP 2009, Exposure to high frequency electromagnetic fields, biological effects and health consequences (100 kHz-300 GHz). Vecchia P, Matthes R, Ziegelberger G, Lin J, Saunders R, Swerdlow A. ISBN 983-3-934994-10-2

Jimbo Y, Robinson HP, Kawana A. 1998. Strengthening of synchronized activity by tetanic stimulation in cortical cultures: Application of planar electrode arrays. IEEE Trans Biomed Eng 45(11):1297-1304.

Jimbo Y, Tateno T, Robinson HP. (1999) Simultaneous induction of pathway-specific potentiation and depression in networks of cortical neurons. Biophys J 76(2):670-678.

Juutilainen J, Höytö A, Kumlin T, Naarala J. (2011) Review of possible modulation-dependent biological effects of radiofrequency fields. Bioelectromagnetics 32: 511-534

Kang G, Nam Y. In vitro neuronal activity change induced by thermal effects of near-infrared laser stimulation. 6th Int. Meeting on Substrate-Integrated Microelectrodes, 2008. ISBN 3-938345-05-5

Karniel A, Kositsky M, Fleming KM, Chiappalone M, Sanguineti V, Alford ST, Mussa-Ivaldi FA. 2005. Computational analysis in vitro: Dynamics and plasticity of a neuro-robotic system. J Neural Eng 2(3):S250-S265.

Koester P, Sakowski J, Baumann W, Glock HW, Gimsa J. 2007. A new exposure system for the in vitro detection of ghz field effects on neuronal networks. Bioelectrochemistry 70(1):104-114.

Köndgen H, Geisler C, Fusi S, Wang XJ, Lüscher HR, Giugliano M. (2008) The dynamical response properties of neocortical neurons to temporally modulated noisy inputs in vitro. Cereb Cortex 18: 2086-2097

Kwon MS, Hämäläinen H. (2011) Effects of mobile phone electromagnetic fields: critical evaluation of behavioral and neurophysiological studies. Bioelectromagnetics 32: 253-272.

Legendy C.R. and Salcman M. (1985): Bursts and recurrences of bursts in the spike trains of spontaneously active striate cortex neurons. J. Neurophysiology, 53(4) : 926-939).

Lévêque P, Dale C, Veyret B, Wiart J. (2004) Dosimetric analysis of a local exposure system for rat operating at 900 MHz. IEEE MTT, 52: 2067-2075.

Liberti, M. Apollonio, F. ; Paffi, A. ; Pellegrino, M. ; d'Inzeo, G. (2004) A coplanar-waveguide system for cells exposure during electrophysiological recordings Microwave Theory and

Techniques, IEEE Transactions on 52 , 11 : 1429-1432

López-Martín E, Bregains J, Relova-Quinteiro JL, Cadarso-Suárez C, Jorge-Barreiro FJ, Ares-Pena FJ. (2009) The action of pulse-modulated GSM radiation increases regional changes in brain activity and c-Fos expression in cortical and subcortical areas in a rat model of picrotoxin-induced seizure proneness. J Neurosci Res 87: 1484-1499.

Loughran SP, Benz DC, Schmid MR, Murbach M, Kuster N, Achermann P. (2013) No increased sensitivity in brain activity of adolescents exposed to mobile phone-like emissions. Clin Neurophysiol (in press).

Loughran SP, McKenzie RJ, Jackson ML, Howard ME, Croft RJ. (2012) Individual differences in the effects of mobile phone exposure on human sleep: rethinking the problem. Bioelectromagnetics 33: 86-93

Lustenberger C, Murbach M, Dürr R, Schmid MR, Kuster N, Achermann P, Huber R. (2013) Stimulation of the brain with radiofrequency electromagnetic field pulses affects sleep-dependent performance improvement. Brain Stimul (in press).

Maby E, Le Bouquin Jeannès R, Faucon G, Liégeois-Chauvel C, De Seze R. (2005) Effects of GSM signals on auditory evoked responses. Bioelectromagnetics 26: 341-350

Maccione A, Gandolfo M, Massobrio P, Novellino A, Martinoia S, Chiappalone M. 2009. A novel algorithm for precise identification of spikes in extracellularly recorded neuronal signals. J Neurosci Methods 177: 241-249.

Madhavan R, Chao ZC, Potter SM. 2007. Plasticity of recurring spatiotemporal activity patterns in cortical networks. Phys Biol 4(3):181-193.

Marchionni I, Paffi A, Pellegrino M, Liberti M, Apollonio F, Abeti R, Fontana F, D'Inzeo G, Mazzanti M. (2006) Comparison between low-level 50 Hz and 900 MHz electromagnetic stimulation on single channel ionic currents and on firing frequency in dorsal root ganglion isolated neurons. Biochim Biophys Acta 1758: 597-605.

Marom S, Shahaf G. 2002. Development, learning and memory in large random networks of cortical neurons: Lessons beyond anatomy. Q Rev Biophys 35(1):63-87.

Martinoia S, Bonzano L, Chiappalone M, Tedesco M, Marcoli M, Maura G. 2005. In vitro cortical neuronal networks as a new high-sensitive system for biosensing applications. Biosens Bioelectron 20(10):2071-2078.

Massobrio P, Massobrio G, Martinoia S (2007) Multi-program approach for simulating recorded extracellular signals generated by neurons coupled to microelectrode arrays. Neurocomputing 70 2467–2476

McCabe AK, Easton CR, Lischalk JW, Moody WJ. 2007. Roles of glutamate and GABA receptors in setting the developmental timing of spontaneous synchronized activity in the developing mouse cortex. Dev Neurobiol 67: 1574-1588.

McRee and Wachtel (1982) Pulse microwave effects on nerve vitality. Radiat Res. 91: 212-218.

McRee DI and Wachtel H (1980) The effects of microwave radiation on the vitality of isolated frog sciatic nerves. Radiat Res. 82: 536-546.

Merla C, Ticaud N, Arnaud-Cormos D, Veyret B, Leveque P. (2011). Real-time RF exposure setup based on a multiple electrode array (MEA) for electrophysiological recording of neuronal networks. Microwave Theory and Techniques, IEEE Transactions on 59(3):755-762.

Metzner, W., Koch, C., Wessel, R., & Gabbiani, F. (1998). Feature extraction by burst-like patterns in multiple sensory maps. The Journal of Neuroscience, 18(6), 2283–2300.

Mino H, Durand DM. (2010) Enhancement of information transmission of sub-threshold signals applied to distal positions of dendritic trees in hippocampal CA1 neuron models with stochastic resonance. Biol Cybern 103: 227-236

Mok SY, Lim YM, Goh SY (2009) A device to facilitate preparation of high-density neural cell cultures in meas. J Neurosci Methods 179(2):284-291.

Moretti D, Garenne A, Haro E, Poulletier de Gannes F, Lagroye I, Veyret B, Lewis N (2013). In-vitro exposure of neuronal networks to the GSM-1800 signal. Bioelectromagnetics [in press].

OMS (2010) RF research recommendations www.who.int/peh-emf/research/agenda /en/index.html

Paffi A, Apollonio F, d'Inzeo G, Liberti M. (2013) Stochastic resonance induced by exogenous noise in a model of a neuronal network. Network

Paffi A, Gianni M, Maggio F, Liberti M, Apollonio F, D'Inzeo G. (2007) Effects of an exogenous noise on a realistic network model: encoding of an EM signal. Conf Proc IEEE Eng Med Biol Soc 2007: 2404-2407

Pasquale V, Martinoia S, Chiappalone M. 2010. A self-adapting approach for the detection of bursts and network bursts in neuronal cultures. J Comput Neurosci 29(1-2):213-229.

Perentos N, Croft R, McKenzie R, Cosic I. (2013) The alpha band of the resting EEG under pulsed and continuous RF exposures. IEEE Trans Biomed Eng (in press).

Perkel DH, Gerstein GL, Moore GP. (1967). Neuronal spike trains and stochastic point processes. I. The single spike train. Biophys J.;7(4):391–418.

Piet R, Garenne A, Farrugia F, Le Masson G, Marsicano G, Chavis P, Manzoni OJ.(2011). State-dependent, bidirectional modulation of neuronal network activity by endocannabinoids. J Neurosci 31: 16591-16596.

Platano D, Mesirca P, Paffi A, Pellegrino M, Liberti M, Apollonio F, Bersani F, Aicardi G. (2007) Acute exposure to low-level CW and GSM-modulated 900 MHz radiofrequency does not affect Ba(2+) currents through voltage-gated calcium channels in rat cortical

neurons. Bioelectromagnetics 28: 599-607.

Regel SJ, Achermann P. (2011) Cognitive performance measures in bioelectromagnetic research--critical evaluation and recommendations. Environ Health 10: 10

Regel SJ, Gottselig JM, Schuderer J, Tinguely G, Rétey JV, Kuster N, Landolt HP, Achermann P. (2007) Pulsed radio frequency radiation affects cognitive performance and the waking electroencephalogram. Neuroreport 18: 803-807

Rubin GJ, Hillert L, Nieto-Hernandez R, van Rongen E, Oftedal G. (2011) Do people with idiopathic environmental intolerance attributed to electromagnetic fields display physiological effects when exposed to electromagnetic fields? A systematic review of provocation studies. Bioelectromagnetics 32: 593-609

Rubinsky L, Raichman N, Baruchi I, Shein M, Lavee J, Frenk H, Ben-Jacob E. 2007. Study of hypothermia on cultured neuronal networks using multi-electrode arrays. J Neurosci Methods 160: 288-293.

S. M. Potter, "How should we think about bursts?," in Proc. MEA. Meeting 2008, Reutlingen, Germany, July 2008, pp. 22–25.

Sakowski J, Gimsa J. 2008. Exposure of neuronal networks on MEA using UMTS generic signals. DMF (Deutsches Mobilfunk-Forschungsprogramm) programme report. www.emf-forschungsprogramm.de/forschung/biologie/biologie_abges/bio_010_AB_Anhang_2.pdf. (last accessed February 2012).

Sauter C, Dorn H, Bahr A, Hansen ML, Peter A, Bajbouj M, Danker-Hopfe H. (2011) Effects of exposure to electromagnetic fields emitted by GSM 900 and WCDMA mobile phones on cognitive function in young male subjects. Bioelectromagnetics 32: 179-190

Scelfo B, Politi M, Reniero F, Palosaari T, Whelan M, Zaldivar JM. 2012. Application of multielectrode array (MEA) chips for the evaluation of mixtures neurotoxicity. Toxicol 299: 172–183.

Schmid MR, Loughran SP, Regel SJ, Murbach M, Bratic Grunauer A, Rusterholz T, Bersagliere A, Kuster N, Achermann P. (2012) Sleep EEG alterations: effects of different pulse-modulated radio frequency electromagnetic fields. J Sleep Res 21: 50-58.

Shahaf G, Marom S. 2001. Learning in networks of cortical neurons. J Neurosci 21(22):8782-8788.

Shapiro MG, Homma K, Villarreal S, Richter CP, Bezanilla F. (2012) Infrared light excites cells by changing their electrical capacitance. Nat Commun 3: 736

Slyadnev MN, Tanaka Y, Tokeshi M, Kitamori T. (2001). Photothermal Temperature Control of a Chemical Reaction on a Microchip Using an Infrared Diode Laser. Anal. Chem., 73, 4037-4044

SSM (2013) Rapport de l'Agence de Radioprotection suédoise

http://www.stralsakerhetsmyndigheten.se/Publikationer/Rapport/Stralskydd/2013/201319/

Stefanics G, Thuróczy G, Kellényi L, Hernádi I. (2008) Effects of twenty-minute 3G mobile phone irradiation on event related potential components and early gamma synchronization in auditory oddball paradigm. Neuroscience 157: 453-462

Suhhova A, Bachmann M, Karai D, Lass J, Hinrikus H. (2013) Effect of microwave radiation on human EEG at two different levels of exposure. Bioelectromagnetics 34: 264-274

Tam, D. C. (2002) An alternate burst analysis for detecting intra-burst firings based on inter-burst periods. Neurocomputing, 44–46, 1155–1159.

Tateno T, Kawana A, Jimbo Y. 2002. Analytical characterization of spontaneous firing in networks of developing rat cultured cortical neurons. Phys Rev E Stat Nonlin Soft Matter Phys 65(5 Pt 1):051924.

Tattersall JE, Scott IR, Wood SJ, Nettell JJ, Bevir MK, Wang Z, Somasiri NP, Chen X. (2001) Effects of low intensity radiofrequency electromagnetic fields on electrical activity in rat hippocampal slices. Brain Res 904: 43-53.

Tchumatchenko T, Malyshev A, Wolf F, Volgushev M. Ultrafast Population Encoding by Cortical Neurons. 2011 The Journal of Neuroscience, , 31:12171–12179.

Thuróczy G, Kubinyi G, Bodó M, Bakos J, Szabó LD. (1994) Simultaneous response of brain electrical activity (EEG) and cerebral circulation (REG) to microwave exposure in rats. Rev Environ Health 10: 135-148.

Trunk A, Stefanics G, Zentai N, Kovács-Bálint Z, Thuróczy G, Hernádi I. (2013) No effects of a single 3G UMTS mobile phone exposure on spontaneous EEG activity, ERP correlates, and automatic deviance detection. Bioelectromagnetics 34: 31-42

Van Pelt J, Corner MA, Wolters PS, Rutten WL, Ramakers GJ. 2004. Longterm stability and developmental changes in spontaneous network burst firing patterns in dissociated rat cerebral cortex cell cultures on multielectrode arrays. Neurosci Lett 361(1-3):86-89.

van Pelt J, Vajda I, Wolters PS, Corner MA, Ramakers GJ. 2005. Dynamics and plasticity in developing neuronal networks in vitro. Prog Brain Res 147:173-188.

van Pelt J, Wolters PS, Corner MA, Rutten WL, Ramakers GJ. 2004. Long-term characterization of firing dynamics of spontaneous bursts in cultured neural networks. IEEE Trans Biomed Eng 51(11):2051-2062.

Van Rongen E, Croft R, Juutilainen J, Lagroye I, Miyakoshi J, Saunders R, de Seze R, Tenforde T, Verschaeve L, Veyret B, Xu Z. 2009. Effects of radiofrequency electromagnetic fields on the human nervous system. J Toxicol Environ Health B Crit Rev 12: 572-597.

Vato A, Bonzano L, Chiappalone M, Cicero S, Morabito F, Novellino A, Stillo G. (2004) Spike manager: A new tool for spontaneous and evoked neuronal networks activity characterization. Neurocomputing 58:1153-1161.

Vecchio F, Babiloni C, Ferreri F, Buffo P, Cibelli G, Curcio G, van Dijkman S, Melgari JM, Giambattistelli F, Rossini PM. (2010) Mobile phone emission modulates inter-hemispheric functional coupling of EEG alpha rhythms in elderly compared to young subjects. Clin Neurophysiol 121: 163-171

Volmer R, Prat CM, Le Masson G, Garenne A, Gonzalez-Dunia D.(2007). Borna disease virus infection impairs synaptic plasticity J Virol 81: 8833-8837.

Vorobyov V, Pesić V, Janać B, Prolić Z. (2011) Repeated exposure to low-level extremely low frequency-modulated microwaves affects baseline and scopolamine-modified electroencephalograms in freely moving rats. Int J Radiat Biol 80: 691-698.

Vorobyov VV, Galchenko AA, Kukushkin NI, Akoev IG. (1997) Effects of weak microwave fields amplitude modulated at ELF on EEG of symmetric brain areas in rats. Bioelectromagnetics 18: 293-298

Wachtel H, Seaman R, Joines W (1975) Effects of low-intensity microwaves on isolated neurons. Ann N Y Acad Sci. 247: 46-62.

Wagenaar DA, Madhavan R, Pine J, Potter SM. (2005). Controlling bursting in cortical cultures with closed-loop multi-electrode stimulation. J Neurosci 25: 680-688.

www.hpa.org.uk./Publications/Radiation/HPAResponseStatementsOnRadiationTopics/radresp_AGNIR2012/ (Didcot, UK, last accessed May 2013).

Xu S, Ning W, Xu Z, Zhou S, Chiang H, Luo J. (2006) Chronic exposure to GSM 1800-MHz microwaves reduces excitatory synaptic activity in cultured hippocampal neurons. Neurosci Lett 398: 253-257.

8 APPENDICES

8.1 Appendix A: Primary neurons protocols (standard)

Primary neuronal cultures on MEA QWANE MEA60 200/40Pt (June 2012)

Classical protocol

8.1.1 Preparation of the coating on the day before the culture

Chemicals**:**

- Ethanol 70 ° (EtOH); sterile pyrogen-free water (PPI) (Gibco ™ 15230, 100ml)
- Poly (ethyleneimine) solution (PEI) (Sigma-Aldrich, Inc. P3143)
- Boric acid, crystalline (Fisher Scientific, A73-500)
- Borax (sodium tetraborate) (Sigma-Aldrich, Inc., B0127); 1 N HCl
- Laminin, 1mg/ml (Sigma-Aldrich, Inc., L2020); Borate buffer; 3.10 g boric acid; 4.75 g borax (sodium tetraborate)

Dissolve in 1 litre of deionized water. Adjust the pH to 8.4 using 1N HCl.

Stock PEI solution: 0.05-0.1% PEI dissolved in borate buffer or 1 ml of PEI in 1L of borate buffer at pH 8.4

Laminin solution: 50 g / ml laminin in the culture medium (or 1 mg in 20 ml of laminin NBM medium)

Small equipment:

• MEA (Multi Electrode Arrays; MultiChannel Systems)

• Petri dishes (100 mm Nunclon ™); Micropipette Gilson® P200 (200 µl) + cones

• Aluminium foil; tape; autoclave indicator strip.

Sterilize the MEA by rinsing with 85% ethanol (2 min), drying and then placing the MEA, wrapped in foil, at 56 °C for 8 hours. Place the MEA in 100 mm diameter Petri dishes. Place 500 µl of PEI on MEA: incubate at 4 °C overnight in 100 mm packing boxes in foil.

Thaw laminin overnight at 4 °C. The next day, rinse three times with distilled water. Place 200 µl of laminin (50 mg / ml solution) on the MEA. Place the MEA in the incubator for at least 2 hours. Discard Laminin solution without rinsing. Let it dry 2-3 min. Install the cells.

8.1.2 Dissection

Before sacrifice:

Prepare five 100 mm diameter petri dishes with 10 ml of HBSS or PBS w/o Ca-Mg + 1% Penicillin-Streptomycin and five 35 mm diameter Petri dishes containing 5 ml of DMEM + 1% Penicillin-Streptomycin.

Prepare sterile instruments.

1) Kill a pregnant rate (17 to 18 days) by elongation after isoflurane anaesthesia.

2) Sterilize the abdomen of the animal with 70% ethanol. Lift the skin of the abdomen with a

forceps and make an incision from the pelvis to the thorax (without cutting the peritoneum). Separate the skin from the muscle tissue as much as possible. Sterilize again scissors and abdomen in 70% alcohol. Then incise the abdomen to find the uterus and embryos. Using a wide clamp, grasp the uterus containing the embryos and to take out all the embryos and then detach with scissors to recover embryos in Petri dishes filled with HBSS.

3) Slightly incise the placenta (at the ball level) of each embryo and use the two clamps on the membranes to remove the embryo. Cut the umbilical cord using two clamps and place the embryos into a new Petri dish with HBSS.

4) Decapitate the embryos and transfer the heads in the small Petri dishes.

5) With a conventional clamp, stabilizing the head with fine clamp against a wall of the box and put the clamps with curved tips into the eye sockets. Raise the head and cut the skull from the base of the neck towards the nose. Then squeeze the walls of the skull to get the brain out. Place the brain in one of the small Petri dishes containing DMEM.

6) Separate the two hemispheres. Turn over each cerebral hemisphere to see the inside. First remove a soft mass than the meninges (vascularized membrane). Take the cortex with fine scissors and place it in a small Petri dish containing 5 ml DMEM-Glutamax™ I + 1% penicillin-streptomycin.

8.1.3 Dissociation and development of culture cells

Material:

• Sterile cotton-plugged Pasteur pipettes.

• Pipettes Gilson® P1000 (1000 µl), P 200 (200µl) + cones; Racks;

• Various sterile tubes (15 ml, 50 ml); Microscope; Automatic Countess cell counter;

• 2 tweezers.

Chemicals:

• DMEM Glutamax ™ I: Dulbecco's Modified Eagle's Medium (Gibco ™ 31966 1X, High Glucose, 500 ml)

• NBM: Neurobasal ™ Medium (Gibco ™ 21103 • 049, 1X, liquid, 500 ml)

• B27 Serum Free supplement (Gibco ™ 17504 • 044, 50X, liquid, 10 ml)

• GlutaMAX ™ • I Supplement (Gibco ™ 35050 • 038, 200 mM, 100 ml)

• P / S: Penicillin / Streptomycin: Antibiotics (Gibco ™ 15140 • 122)

Preparing the NBM medium

• 2% B27; 1% GlutaMaxI; 1% P / S; Trypsin (1X) (Gibco ™ 25050 • 014, Liquid, 100ml); DNase (Sigma ® D5025); STI: Soybean Trypsin Inhibitor (Gibco ™ 17075); Trypan Blue (Sigma® T8154).

Protocol:

Work under the hood.

- Remove excess DMEM-P-Glutamax™ I and finely chop the cortex with the side edge of a clamp

- In a 15 ml tube, suspend the pieces in 5 ml of DMEM-P-Glutamax ™ I.

- Allow to settle, remove excess DMEM Glutamax ™-P-I and to 1.5 ml trypsin solution and place the tube in the incubator for 25 min leaving the cap slightly open.

- Remove excess trypsin, add 10 ml of DMEM-P-Glutamax ™ I.

- Centrifuge at 1000 rpm 4 °C briefly, remove the supernatant, then put 3 ml DMEM-P-Glutamax ™ I; Add 100 µl of STI; with a Pasteur pipette, perform a mechanical dissociation vigorously 15 times, then 5 times by bringing the tip of the pipette in contact with the bottom of the tube for finer dissociation. Check the absence of clusters in the Pasteur pipette;

- Make up to 10 ml and centrifuge again briefly;

- Place the supernatant in a new 15 ml tube; Centrifuge at 1000 rpm for 5 min; Discard the supernatant;

- In the base of the tube, there is a mixture of dead and living cells, so add 500 µl trypsin + 500 µl DMEM-P-Glutamax ™ I;

- Leave in for 1 minute, then add 100 µl STI, wait 1 minute and add 50 µl DNase;

- Leave for 2-3 min at ambient temperature and made up to 10 ml with DMEM-PGlutamax ™ I;

- Centrifuge again at 1000 rpm for 5 min (the base should have decreased);

- Remove the supernatant and resuspend in 2 ml of NBM with added supplements;

- Count the cells with 10 µl trypan blue and 10µl of cell suspension; place 10 µl of the mixture on the slide cell counter and count using the automatic cell counter. Count twice; dilute the cell suspension to give 2 x 10^6 cells / ml.

- Discard laminin.

- At the centre of the MEA place 50 µl of this cell suspension and place the boxes in the incubator for at least 2 hours.

- After the 2 hours, add 900 µl of NBM medium in each MEA. Place the tip of the P1000 in a corner of the MEA and gently pour the NBM medium.

8.1.4 Maintenance of cells in culture

Material:

- Pipettes Gilson® P1000 (100µl) + cones

Chemicals:

- NBM medium (Neurobasal ™ Medium), with supplements

Protocol:

Under the hood: It is imperative to work in aseptic conditions;

- First take the medium out of the fridge so that it is not be too cold for the cells;

- Change the medium 2 times per week: remove 500 µl and place 1000 µl of medium.

8.2 Appendix B: Primary neurons protocol, Papain Dissociation system protocol

Papain Dissociation System Protocol Summary

Sterile procedures should be used throughout:

1. Add 32ml of EBSS (Vial 1) to the albumin-ovomucoid inhibitor mixture (Vial 4) and allow the contents to dissolve while preparing the other components. Mix before using and equilibrate with O_2:CO_2 . Reconstitute for the first use, then store at 2-8°C and reuse.

2. Add 5ml of EBSS (Vial 1) to papain vial (Vial 2). Place Vial 2 in 37°C water bath for ~10 minutes or until the papain is completely dissolved and the solution appears clear. If solution appears alkaline (red or purple) equilibrate the solution with 95%O_2:5%CO_2 . The solution should be used promptly but can be held at room temperature during the dissection. A separate papain vial is provided for each dissociation. (If desired the papain can be transferred to a centrifuge tube or other container before proceeding.)

3. Add 500ul of EBSS to a DNase vial (Vial 3). Mix gently—DNase is sensitive to shear denaturation. Add 250ul of this solution to the vial containing the papain. This preparation contains a final concentration of approximately 20 units/ml papain and 0.005% DNase. Save the balance of the DNase vial to use in Step #7. A separate DNase vial is provided for each dissociation.

4. Place tissue in the papain solution. Tissue should be slightly minced or cut into small pieces (this can be done separately or on the side of the tube containing the papain.) Displace the air in vial with sterile O_2:CO_2. Do not bubble gas through the solution. Immediately cap the vial.

5. Incubate the vial containing the tissue at 37°C with constant agitation (a rocker platform is ideal) for 30 min to 1 ½ hrs. The amount of time must be determined empirically; however, embryonic tissue generally requires less time than postnatal tissue.

6. Triturate the mixture with 10ml pipette. Allow any pieces of undissociated tissue remaining after trituration to settle to the bottom of the tube. Vigorous trituation of neuronal tissue results in a high yield of cells, most of which are spherical and devoid of proximal processes. Gentle trituration results in more undissociated tissue fragments and a lower yield of cells although many of these now retain their proximal processes.

7. Carefully remove the cloudy cell suspension, place in sterile screw capped tube and centrifuge at 300 x g for 5 minutes at room temperature. Be careful to avoid including any pieces of undissociated tissue. During this time prepare medium to resuspend the pelleted cells. Mix 2.7ml EBSS (Vial 1) with 300ul reconstituted albumin-ovomucoid inhibitor solution (Vial 4) in a sterile tube. Add 150ul of DNase solution (Vial 3) saved at Step #3.

8. Discard the supernatant and immediately resuspend the cell pellet in the diluted DNase/albumin-inhibitor solution prepared in Step #7.

9. Prepare discontinuous density gradient: Add 5ml of albumin-inhibitor solution (Vial 4) to a centrifuge tube, carefully layer the cell suspension on top, then centrifuge at 70 x g for 6 minutes at room temperature. The interface between the two layers of the gradient should be clearly visible although minimal mixing at this boundary does not affect the result. Dissociated cells pellet at the bottom of the tube, membrane fragments remain at the interface.

10. Discard the supernatant and immediately resuspend the pelleted cells in medium for cell culture or for flow cytometric analysis.

r07.11

Worthington Biochemical Corporation • Lakewood, New Jersey 08701
800-445-9603 • 732-942-7660 • Fax: 800-368-3108 • 732-942-9270 • www.worthington-biochem.com

8.3 Appendix C: Ayanda MEA

MEA60 200 Pt GND

Product type

Multi-electrode array biochip compatible with the MEA60 data acquisition system from Multi Channel Systems MCS GmbH, Reutlingen, germany.

Characteristics

Substrate dimension:	15 mm x 15 mm x 0.7 mm
Substrate material:	float glass
Insulation material:	SU-8 epoxy, thickness 5 μm
Number of electrodes:	60 (59 recording electrodes and 1 large GND electrode)
Electrode material:	platinum
Electrode geometry:	planar
Electrode layout:	8 x 8 matrix without corner electrodes
Electrodes dimension:	ø 40 μm circular electrodes
Electrode spacing:	200 μm centre to centre
Impedance @ 1 kHz:	500-650 kΩ
Noise level:	20-25 μV, GND < 2 kΩ
Re-use: type	several times depending on and duration of cultures.
Required accessories:	MEA60 Spa-Y1 or MEA60 Spa-Y2

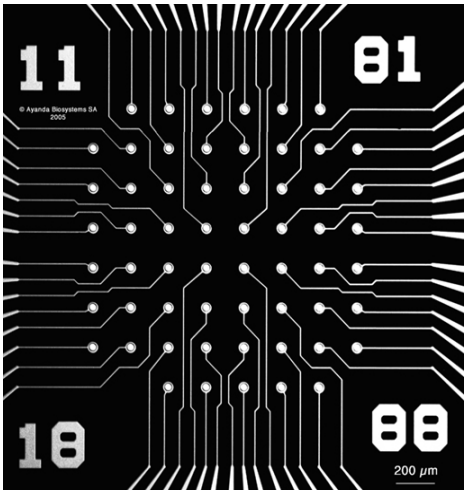

Applications

Organotypic slice cultures and dissociated cell cultures (brain tissue, spinal cord, retina, heart muscle cells, etc.)

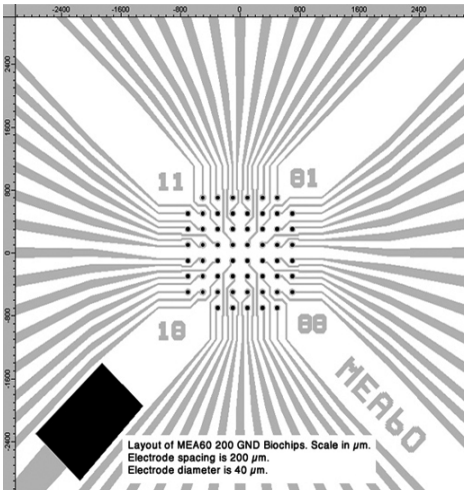

8.4 Appendix D: Moretti et al, 2013

Bioelectromagnetics 34:571–578 (2013)

In Vitro Exposure of Neuronal Networks to a GSM-1800 Signal

Daniela Moretti,[1,2] André Garenne,[3,4] Emmanuelle Haro,[1,2] Florence Poulletier de Gannes,[1,2] Isabelle Lagroye,[1,2,5] Philippe Lévêque,[6,7] Bernard Veyret,[1,2,5] and Noëlle Lewis[1,2]

[1]*University of Bordeaux, IMS Laboratory (Intégration du Matériau au Sysźme),Talence, France*
[2]*CNRS (Centre National de la Recherche Scientifique), IMS, UMR 5218,Talence, France*
[3]*University of Bordeaux, IMN Laboratory (Institut des Maladies Neurodégénératives), Bordeaux, France*
[4]*CNRS, IMN, UMR 5293, Bordeaux, France*
[5]*EPHE (École Pratique des Hautes Études), Bioelectromagnetics Laboratory,Talence, France*
[6]*University of Limoges, XLIM Research Institute, CNRS, Limoges, France*
[7]*CNRS, XLIM, UMR 7252, Limoges, France*

The central nervous system is the most likely target of mobile telephony radiofrequency (RF) field exposure in terms of biological effects. Several electroencephalography (EEG) studies have reported variations in the alpha-band power spectrum during and/or after RF exposure, in resting EEG and during sleep. In this context, the observation of the spontaneous electrical activity of neuronal networks under RF exposure can be an efficient tool to detect the occurrence of low-level RF effects on the nervous system. Our research group has developed a dedicated experimental setup in the GHz range for the simultaneous exposure of neuronal networks and monitoring of electrical activity. A transverse electromagnetic (TEM) cell was used to expose the neuronal networks to GSM-1800 signals at a SAR level of 3.2 W/kg. Recording of the neuronal electrical activity and detection of the extracellular spikes and bursts under exposure were performed using microelectrode arrays (MEAs). This work provides the proof of feasibility and preliminary results of the integrated investigation regarding exposure setup, culture of the neuronal network, recording of the electrical activity, and analysis of the signals obtained under RF exposure. In this pilot study on 16 cultures, there was a 30% reversible decrease in firing rate (FR) and bursting rate (BR) during a 3 min exposure to RF. Additional experiments are needed to further characterize this effect. Bioelectromagnetics 34:571–578, 2013. © 2013 Wiley Periodicals, Inc.

Key words: feasibility study; GSM-1800 signal; neuronal networks; electrical activity; in vitro

INTRODUCTION

Evaluation of many potential mechanisms suggests that dielectric heating leading to temperature elevation in tissues is the dominant and possibly only mechanism for biological effects of the radiofrequency (RF) fields relevant to wireless communications [AGNIR, 2012]. Under typical exposure conditions of mobile telephony, the central nervous system is the most likely target of RF exposure in terms of biological effects, and several electroencephalography (EEG) studies have reported variations in the EEG power spectrum during and/or after RF exposure, in resting EEG and during sleep [Van Rongen et al., 2009; Croft et al., 2010; Schmid et al., 2012]. The most recent of these studies provides some evidence that RF exposure may directly influence brain functions. Therefore, it is crucial to clarify the mechanisms underlying these potential RF effects on the brain, both at cellular and network levels. In this context, the extracellular observation of the spontaneous electrical activity of neuronal networks under RF exposure can be an efficient tool to detect the occurrence of low-level RF effects on the nervous system.

Grant sponsors: French Ministry of Research; University of Bordeaux 1; CNRS; Bouygues Telecom.

*Correspondence to: Daniela Moretti, IMS Laboratory, 351, Cours de la Liberation, 33405 Talence Cedex, France.
E-mail: daniela.moretti@ims-bordeaux.fr

Received for review 19 December 2012; Accepted 11 June 2013

DOI: 10.1002/bem.21805
Published online 1 August 2013 in Wiley Online Library (wileyonlinelibrary.com).

Our research group has developed a dedicated experimental setup in the GHz range for the simultaneous RF exposure of neuronal networks [Merla et al., 2011] and monitoring of electrical activity. A similar setup had been previously built for the same purpose, based on a rectangular waveguide [Koester et al., 2007]. Preliminary electrophysiological data were not included in the initial publication but in subsequent reports a correlation between the electrical activity and specific absorption rate (SAR) was reported [Gimsa, 2007; Sakowski and Gimsa, 2008]. In our work, a transverse electromagnetic (TEM) cell was used to expose the neuronal networks to Global System for Mobile Communications at 1800 MHz (GSM-1800) signals at an SAR level of 3.2 W/kg. The GSM signal was selected among the many wireless communications signals as it provides seven empty timeslots out of eight, which is favorable for recording the neuronal signals in the absence of RF fields. This work provides the proof of feasibility and preliminary results of the entire investigation regarding dosimetry of the exposure system, culture of the neuronal network, recording of the electrical activity, and analysis of the signals obtained under RF exposure.

MATERIALS AND METHODS

Acquisition System

The electrophysiological interface that we used was commercial microelectrode arrays (MEAs) from Qwane Biosciences (Qwane, Lausanne, Switzerland). These biochips are built on 15 mm × 15 mm glass substrates mounted on printed circuit boards (PCB; 50 mm × 50 mm) using standard microfabrication technologies. They provide 60 platinum electrodes (200 μm spaced with 40 μm diameter tips) and a 6 mm-high glass cylinder was used as the culture chamber and sealed with biocompatible silicone. For our application, the pre-amplifier (MEA1060-Inv, Multi Channel Systems (MCS), Reutlingen, Germany) had to be placed underneath the MEA to allow the insertion of the culture chamber inside the exposure system; we thus had custom MEAs built by Qwane Biosciences, in which the contact pads were placed on the lower side of the PCB (Figs. 1 and 2).

Exposure Setup

The MEA, hosting the neuronal network, was placed via a hole in the ground plane inside a TEM

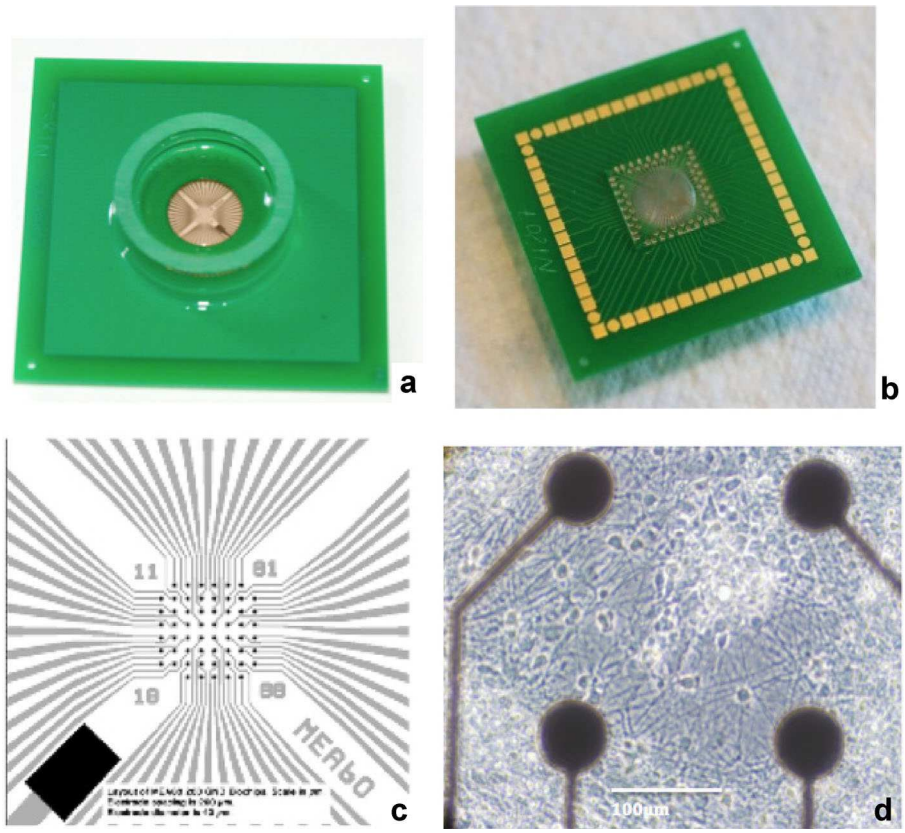

Fig.1. MEA views. **a**: Upper side of MEA with the culture chamber, and (**b**) lower side; (**c**) electrode layout grid; (**d**) zoom on electrode tips and neurons in culture.

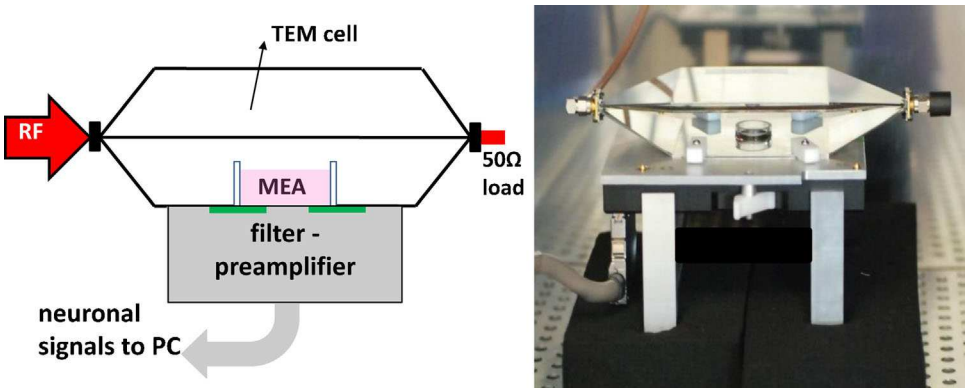

Fig. 2. Experimental setup. **Left**: schematic representation; **Right**: location inside the incubator.

cell where the GSM-1800 signal was propagating (Fig. 2). Dosimetric modeling of the exposure system has been published [Merla et al., 2011]. For an input power of 1 W, a SAR level of 3.2 W/kg was calculated, measured, and used in this work. This level is above the SAR level calculated in the human cortex during mobile phone use (around 0.15 W/kg for the GSM-1800 signal) and corresponds to a 0.06 °C temperature elevation in the culture medium.

Preparation of Cortical Neurons

Extracellular recordings of the electrical activity of cortical cell cultures were performed on the 60-channel planar MEAs described above. The MEAs were successively coated with polyethyleneimine and laminin (Sigma–Aldrich, St. Quentin-Fallavier, France). Primary neuronal cell cultures were obtained from the cortex of embryonic (E18) Sprague–Dawley rats (Charles River Laboratories, L'Arbresle, France). All chemicals quoted below were acquired from Fisher Scientific (Illkirch, France). Cortices were dissected in Dulbecco's Modified Eagle Medium (DMEM)–GlutaMAX and treated with trypsin for 25 min. The fragments were subjected to mechanical dissociation using Pasteur pipettes and briefly centrifuged. The supernatant was transferred into a new tube and centrifuged at 140*g* for 5 min. The pellet was then successively treated with trypsin, soybean trypsin inhibitor, DNase, and finally centrifuged at 140*g* for 5 min. Pellet-dissociated cortical cells were suspended in the culture medium (neurobasal medium supplemented with 2% B-27, 1% GlutaMAX, and 1% penicillin/streptomycin). Each MEA was plated with a suspension of 10^5 cells and kept in a 5% CO_2 incubator at 37 °C in a humidified atmosphere until recording. The culture medium was half-exchanged twice a week [Berdondini et al., 2006].

Acquisition of Electrical Activity

To maintain the proper cell culture conditions during the recordings, the experiments were carried out in a dry incubator (37 °C, 5% CO_2), which contained the pre-amplifier, the MEA, and the exposure system. A removable membrane of fluorinated ethylene-propylene (ALA Scientific Instruments, New York, NY) was used to seal the MEA culture chamber, preventing evaporation but allowing for gas exchange.

The pre-amplification gain was 1200 and a shielded cable allowed data transfer from the preamplifier inside the incubator to a personal computer equipped with an MCS-dedicated data acquisition board. Raw data were sampled at 25 kHz/channel. Signals were recorded and monitored using MC Rack software (MCS) for on-line visualization and raw data storage.

The neuronal networks were exposed between 15 days in vitro (DIV) and 21 DIV, when neuronal activity is optimal in terms of a balance between random spikes and bursts [Chiappalone et al., 2005; Van Pelt et al., 2005]. All recordings were carried out in three subsequent 3 min periods, that is, before, during, and after exposure. Sham exposures were also carried out on the day before, using the same exposure protocol but with the generator off (Fig. 3).

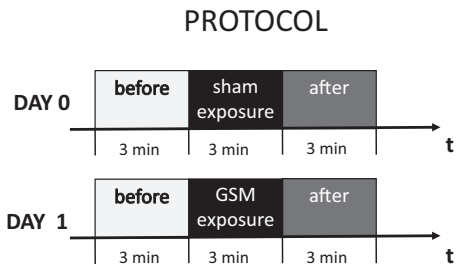

Fig. 3. Time profile of the test protocol.

DATA ANALYSIS

Signal Processing

Offline signal processing was performed using SPYCODE software [Bologna et al., 2010] developed in MATLAB (Mathworks, Natick, MA). SPYCODE is designed to work with multi-site extracellular recordings and can process MCS data files (.mcd) and convert them into MATLAB-format files. A second-order Butterworth high-pass filter with a cut-off frequency at 50 Hz was first applied to the raw data to eliminate slow variations in the signal baseline. During GSM exposure, we observed the presence of an artifact created by interference with the GSM RF signal, as shown in Figure 4 (right). The artifact amplitude never exceeded 1 mV, which guarantees that the pre-amplifier operated in its linear range (0–4 mV). We were thus able to apply a second-order linear filter in order to remove this artifact; the "GSM filter" consisted of a set of 30 band-stop Butterworth filters, each one centered on one of the GSM harmonic frequencies (217, 434, up to 6510 Hz), with a bandwidth of 4 Hz.

To ensure the reliability of our method, we tested the impact of this GSM filter on the number of detected spikes under two conditions: (i) recording of spontaneous activity in the absence of exposure for an electrode in one of the 16 cultures (reference signal); and (ii) a composite signal including exposure, obtained as the sum of the reference signal and a pure GSM artifact recording (Fig. 5, top). Using the GSM filter on this composite signal allowed us to remove the GSM interference (Fig. 5, bottom). This signal processing had a very small effect on spike detection in terms of the total number of spikes (Table 1). The same test was carried out using, as a reference signal, the spontaneous activity recorded of the six most active electrodes, and analogous results were obtained (see the Online Supplementary Material).

Spike and Burst Detection

Spikes were detected using an algorithm implemented in SPYCODE, which relies on a differential threshold (precision timing spike detection, PTSD) [Maccione et al., 2009] and detects a spike when the peak-to-peak amplitude of the signal exceeds eight times the standard deviation (SD) of the biological noise in a 2 ms sliding window (peak lifetime period = 2 ms, refractory period = 1 ms). The SD of the biological noise was evaluated for each recording channel in the pre-exposure phase.

Bursts were detected using the method described by Pasquale et al. [2010]. The algorithm is based on the computation of the logarithmic inter-spike interval (ISI) histogram and automatically detects the best threshold for distinguishing between inter- and intra-burst ISIs for each recording channel of the array.

Choice of Metrics

Electrodes were considered as active in terms of neuronal electrical activity if they had a spike rate of at least 0.1 Hz [Boehler et al., 2012]. For describing

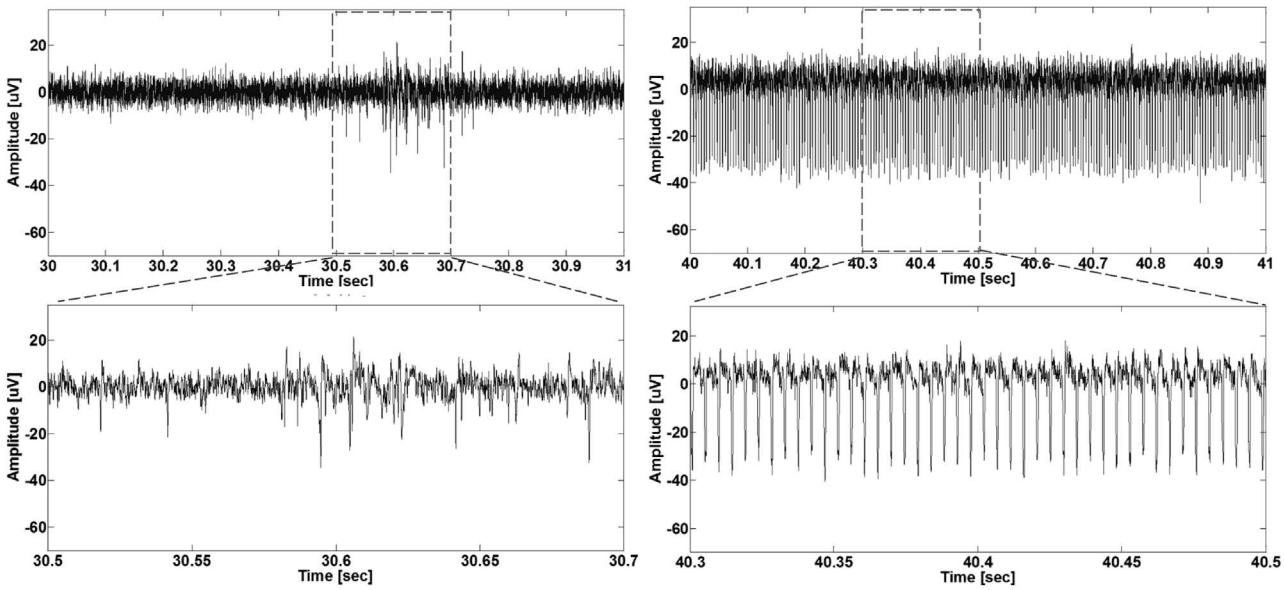

Fig. 4. Examples of recorded activity. **Left**: activity without GSM exposure; **Right**: activity during GSM exposure.

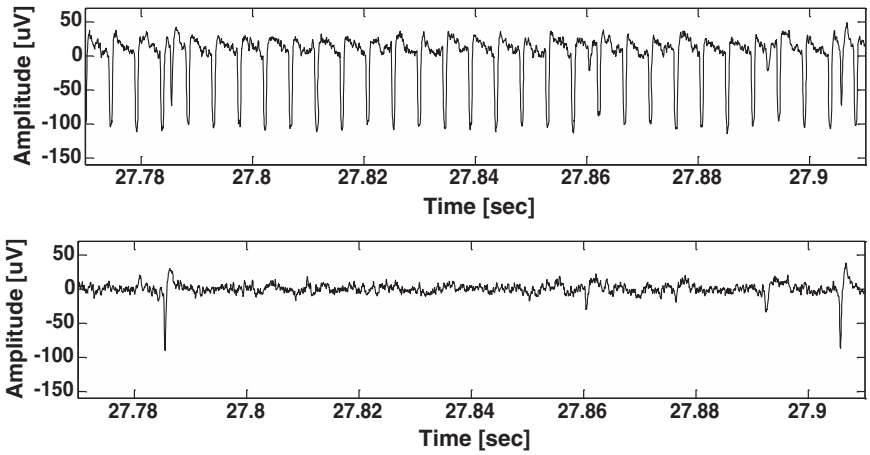

Fig. 5. Composite signal of electrical activity (μV) during exposure before (**top**) and after (**bottom**) the GSM filter.

electrical activity we used two parameters: the firing rate (FR), and the bursting rate (BR). The FR of a given culture is defined as the total number of spikes collected during 3 min for the six most active electrodes identified in the pre-exposure period. The BR is defined in terms of bursts/minute and is the total number of bursts for all burst-active electrodes over 3 min.

Statistical Analysis

As the sample size was small ($n = 16$ independent cultures), statistical analysis required the use of non-parametric tests. In the analysis of sham and exposure data, the Shapiro–Wilk test (Anastat software, Rilly sur Vienne, France) was used to process the ratios of FR and BR to detect a possible effect of GSM exposure on spontaneous activity. This test is used for analyzing the normality of a population but it can also assess the comparison with a fixed value, in a similar way as the Student's *t*-test but with a fewer number of independent samples.

RESULTS

During 2 consecutive days the cells were sham exposed and RF exposed according to the protocol described in Figure 3. Both sets of data were analyzed by testing two parameters related to spikes and bursts (FR and BR).

Pre- Versus Post-Exposure Data

In order to analyze the variations of each parameter during the different runs, before and after exposure, we evaluated the ratio $R_X = X_{\text{before}}/X_{\text{after}}$, where R_X is the ratio for parameter X (FR or BR) and X_{before} and X_{after} are the counts for parameter X before and after exposure, respectively. R_{FR} and R_{BR} were evaluated for both sets of exposures (sham and GSM). Table 2 shows that in all cases, R_{FR} and R_{BR} were not significantly different from unity ($P > 0.25$, Shapiro test), which indicates that the baseline of the FR and BR was stable over 9 min for both sham and real exposures.

TABLE 1. Impact of the GSM Filter on the Reference and Composite Signals in Terms of Number of Detected Spikes

Signal	Filter	# of detected spikes	% relative error
Reference signal	None	1536	—
	GSM filter	1514	−1%[a]
Composite signal = reference signal + GSM artifact	GSM filter	1611	+6%[b]

[a]Reference signal with no filter.
[b]Reference signal with GSM filter.

TABLE 2. Values of the Ratios for the Firing Rate (FR) and Bursting Rate (BR) Parameters and Corresponding *P* Values Based on the Shapiro–Wilk Test

	GSM	Sham
R_{FR}		
Mean	1.00	1.01
P-value	0.92	0.90
R_{BR}		
Mean	1.11	1.13
P-value	0.27	0.35

TABLE 3. Values of the Ratios for the FR and BR for Exposure and Sham Experiments, and Corresponding *P* Values Based on the Shapiro–Wilk Test

	GSM	Sham
R'_{FR}		
Mean	0.75	1.00
P-value	0.0002	0.95
R'_{BR}		
Mean	0.70	1.03
P-value	0.0001	0.72

Effects of Exposure

For each of these parameters, the ratio R'_X was calculated to express the changes observed during sham or GSM exposure with respect to the averaged counts before and after exposure, to account for any small slope in the signal baseline: $R'_X = X_{\text{exposure}}/((X_{\text{before}} + X_{\text{after}})/2)$, where X_{exposure} is the count for parameter X during exposure. Table 3 and Figure 6 show that FR and BR were not altered during sham exposure but were reduced by around 30% during GSM exposure. Moreover, these preliminary data suggest that the amplitude of the effect decreased with age when going from 15 to 21 DIV.

DISCUSSION AND CONCLUSION

The main aim of this work was to assess the feasibility of studying the electrical activity of neuronal networks under exposure to mobile-phone RF signals at 1800 MHz. The use of MEAs has already been successfully applied to pharmacological [Piet et al., 2011], toxicological [Scelfo et al., 2012], and patho-physiological investigations [Volmer et al., 2007; Dribben et al., 2010]. For our purpose, a RF system was built to expose the biological samples inside the MEAs and was well characterized in terms of dosimetry [Merla et al., 2011]. As described above, the GSM artifact was eliminated using a spectral filter but we also needed to exclude the possibility that this interference was the direct cause of the effect. The "GSM artifact", which was observed as an "apparent"

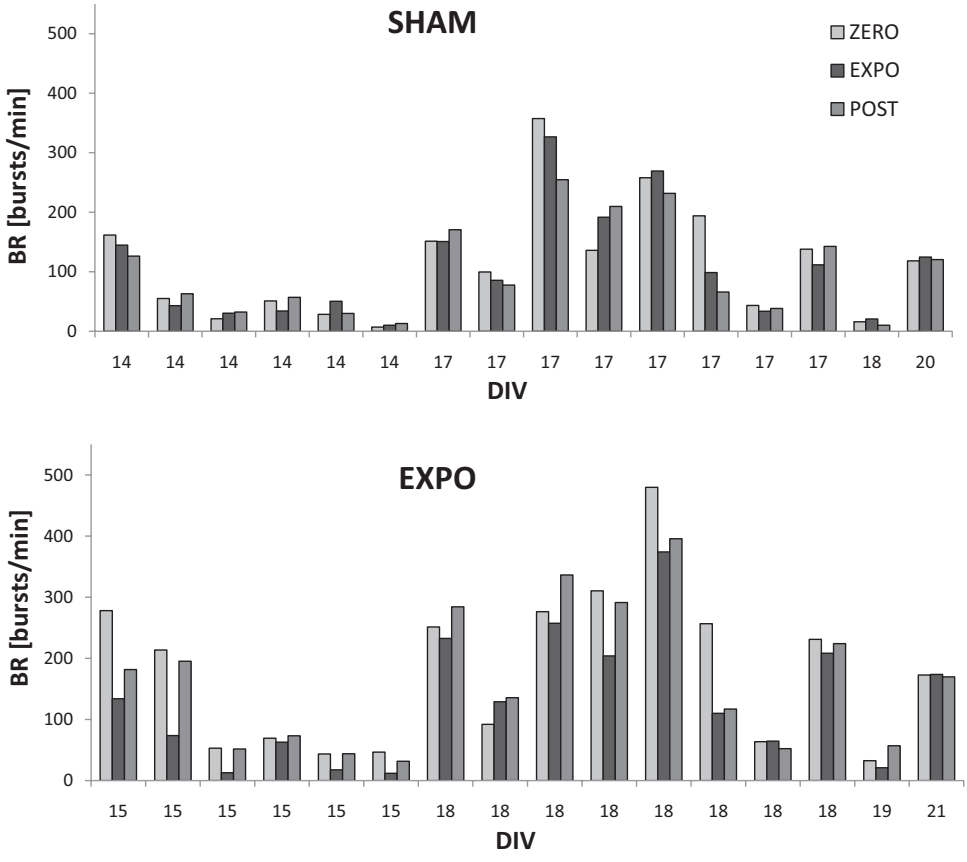

Fig. 6. Bursting Rate before, during, and after exposure for the 16 independent cultures. Age of the cultures is given in abscissa in days in vitro (DIV). Data for a given culture are shown for sham exposure (**top**) and GSM exposure (**bottom**).

induced voltage on the electrodes, was always much less than 1 mV in amplitude, and thus no electrical neuronal stimulation was expected as the threshold for such processes is known to be typically 1000-fold higher. Moreover, some preliminary tests showed that shielding the amplifier circuits using RF-absorbing material decreased the recorded amplitude of the artifact by 10-fold. Further evidence for a lack of contribution of the artifact in the elicitation of the effect came from the observation of a decrease in the amplitude of the observed effect with the age of the culture. In conclusion, there is evidence that the artifact corresponds to electromagnetic interference with the amplifier and not to an induced voltage at the electrodes in contact with the neurons.

The results of 16 independent experiments showed no alteration in electrical activity following cessation of 3 min RF exposures. However, a significant decrease in both the spontaneous spiking activity (FR) and bursting rate (BR) was observed during RF exposure. This effect was phasic and reversible as it lasted through the whole exposure period but ended with the exposure.

There are several stimuli that are known to elicit inhibitory effects on neuronal networks, such as pharmacological agents [McCabe et al., 2007; Piet et al., 2011], toxic agents such as the nickel ion [Gavazzo et al., 2011], or a decrease in temperature [Rubinsky et al., 2010]. However, none of those operate in a reversible manner as rapidly as observed in our work. Therefore, the inhibitory effect of GSM exposure seems to be specific at least for short exposure durations. The rapid onset of the effect and its reversibility are both in favor of a mechanism occurring at the neuronal membrane, where fast bioelectric phenomena can be generated with relatively little inertia.

The role of temperature elevation in the elicitation of the observed effect of GSM exposure must be discussed in terms of "thermal effects", that is, biological effects caused by temperature elevation in the tissues. To date, these are the only effects that have been well documented. In the investigations of the Gimsa group, performed using continuous wave (CW) and Universal Mobile Telecommunications System (UMTS) signals at up to 2.6 W/kg, there was a rise in temperature of up to 0.24 °C [Sakowski and Gimsa, 2008]. Around 33% of the evaluable neurons showed an increase in activity, which correlated with the power of the UMTS signal. No influence of the power control of the UMTS signal was found at 10 or 740 Hz. The conclusion of the authors was that the mechanism behind the increase in activity was of a thermal nature.

In our experimental system, the temperature elevation of the neurons had a time constant of 13 min and reached 0.3 °C at steady state for a SAR of 3.2 W/kg [Merla et al., 2011]. Under our exposure conditions, the temperature elevation at the end of the 3 min exposure was thus around 0.06 °C. This elevation is very small compared to the 0.24 °C temperature elevation measured in the experimental work of the Gimsa group described above, and is very unlikely to be sufficient to cause a reversible effect in a cellular system. However, when using the GSM signal, the energy is not deposited in a continuous manner since during the "on" timeslot, the power is eight times the average power. The only way to ascertain the role of this time domain multiple access (TDMA) amplitude modulation is to perform exposures using CW RF. The elicitation of the effect will be further studied systematically as a function of SAR, modulation, duration of exposure, age of the culture, and pharmacological stimulation.

Assuming that this effect of GSM exposure is validated, the consequences in terms of interpretation of the human EEG data that were obtained using GSM signals and not CW [Croft et al., 2010] are obviously difficult to assess at this time.

Experimental demonstration of the feasibility was achieved in this work and this opens new perspectives regarding the study of the effects of exposure to RF signals on neuronal tissue functioning.

ACKNOWLEDGMENTS

The authors want to thank C. Merla in Limoges for her help in designing, building, and characterizing the exposure system.

REFERENCES

Anastats Company, Les Vigneaux, France, www.anastats.fr/stats/Download.htm#shapiro_wilk (Last accessed February 2013).

Advisory Group on Non-Ionising Radiation (AGNIR). 2012. Health effects from radiofrequency electromagnetic fields. RCE 20 document of the British Health Protection Agency; Radiation, chemical and environmental hazards. Didcot, UK. www.hpa.org.uk./Publications/Radiation/HPAResponseStatementsOnRadiationTopics/radresp_AGNIR2012/ (Last accessed May 2013).

Berdondini L, Chiappalone M, Van Der Wal PD, Imfeld K, De Rooij NF, Koudelka-Hep M, Tedesco M, Martinoia S, Van Pelt J, Le Masson G, Garenne A. 2006. A microelectrode array (MEA) integrated with clustering structures for investigating in vitro neurodynamics in confined interconnected sub-populations of neurons. Sens Actuators B Chem 114:530–541.

Boehler MD, Leondopulos SS, Wheeler BC, Brewer GJ. 2012. Hippocampal networks on reliable patterned substrates. J Neurosci Methods 203:344–353.

Bologna LL, Pasquale V, Garofalo M, Gandolfo M, Baljon PL, Maccione A, Martinoia S, Chiappalone M. 2010. Investigating neuronal activity by SPYCODE multi-channel data analyzer. Neuronal Netw 23:685–697.

Chiappalone M, Novellino A, Vajda I, Vato A, Martinoia S, Van Pelt J. 2005. Burst detection algorithms for the analysis of spatio-temporal patterns in cortical networks of neurons. Neurocomputing 65:653–662.

Croft RJ, Leung S, McKenzie RJ, Loughran SP, Iskra S, Hamblin DL, Cooper NR. 2010. Effects of 2G and 3G mobile phones on human alpha rhythms: Resting EEG in adolescents, young adults, and the elderly. Bioelectromagnetics 31:434–444.

Dribben WH, Eisenman LN, Mennerick S. 2010. Magnesium induces neuronal apoptosis by suppressing excitability. Cell Death Dis 1(e63):1–9.

Gavazzo P, Tedesco M, Chiappalone M, Zanardi I, Marchetti C. 2011. Nickel modulates the electrical activity of cultured cortical neurons through a specific effect on *N*-methyl-D-aspartate receptor channels. Neuroscience 177: 43–55.

Gimsa J. 2007. Demodulation and mobile communications. Report to the German Federal Office for Radiation Protection. BfS, Neuherberg, Germany. www.emf-forschungsprogramm.de/forschung/biologie/biologie_abges/bio_010.html (Last accessed May 2013).

Koester P, Sakowski J, Baumann W, Glock HW, Gimsa J. 2007. A new exposure system for the in vitro detection of GHz field effects on neuronal networks. Bioelectrochemistry 70:104–114.

Maccione A, Gandolfo M, Massobrio P, Novellino A, Martinoia S, Chiappalone M. 2009. A novel algorithm for precise identification of spikes in extracellularly recorded neuronal signals. J Neurosci Methods 177:241–249.

McCabe AK, Easton CR, Lischalk JW, Moody WJ. 2007. Roles of glutamate and GABA receptors in setting the developmental timing of spontaneous synchronized activity in the developing mouse cortex. Dev Neurobiol 67:1574–1588.

Merla C, Ticaud N, Arnaud-Cormos D, Veyret B, Lévêque P. 2011. Real-time RF exposure setup based on a multiple electrode array (MEA) for electrophysiological recording of neuronal networks. IEEE Trans Microw Theory Tech 59:755–762.

Pasquale V, Martinoia S, Chiappalone M. 2010. A self-adapting approach for the detection of bursts and network bursts in neuronal cultures. J Comput Neurosci 29:213–229.

Piet R, Garenne A, Farrugia F, Le Masson G, Marsicano G, Chavis P, Manzoni OJ. 2011. State-dependent, bidirectional modulation of neuronal network activity by endocannabinoids. J Neurosci 31:16591–16596.

Rubinsky L, Raichman N, Baruchi I, Shein M, Lavee J, Frenk H, Ben-Jacob E. 2010. Study of hypothermia on cultured neuronal networks using multi-electrode arrays. J Neurosci Methods 160:288–293.

Sakowski J, Gimsa J. 2008. Exposure of neuronal networks on MEA using UMTS generic signals. Deutsches Mobilfunk-Forschungsprogramm (DMF) programme report (German Research Program on Mobile Telephony). www.emf-forschungsprogramm.de/forschung/biologie/biologie_abges/bio_010_AB_Anhang_2.pdf (Last accessed February 2012).

Scelfo B, Politi M, Reniero F, Palosaari T, Whelan M, Zaldivar JM. 2012. Application of multielectrode array (MEA) chips for the evaluation of mixtures neurotoxicity. Toxicology 299:172–183.

Schmid MR, Loughran SP, Regel SJ, Murbach M, Bratic Grunauer A, Rusterholz T, Bersagliere A, Kuster N, Achermann P. 2012. Sleep EEG alterations: Effects of different pulse-modulated radio frequency electromagnetic fields. J Sleep Res 21:50–58.

Van Pelt J, Vajda I, Wolters PS, Corner MA, Ramakers GJ. 2005. Dynamics and plasticity in developing neuronal networks in vitro. Prog Brain Res 147:173–188.

Van Rongen E, Croft R, Juutilainen J, Lagroye I, Miyakoshi J, Saunders R, de Seze R, Tenforde T, Verschaeve L, Veyret B, Xu Z. 2009. Effects of radiofrequency electromagnetic fields on the human nervous system. J Toxicol Environ Health B Crit Rev 12:572–597.

Volmer R, Prat CM, Le Masson G, Garenne A, Gonzalez-Dunia D. 2007. Borna disease virus infection impairs synaptic plasticity. J Virol 81:8833–8837.

Supporting Information

Additional supporting information may be found in the online version of this article at the publisher's web-site.

Abstract

The central nervous system is the most likely target of mobile telephony radiofrequency field (RF) exposure in terms of biological effects. Several EEG (electroencephalography) studies have reported variations in the alpha-band power spectrum during and/or after RF exposure, in resting EEG and during sleep. In this context, the observation of the spontaneous electrical activity of neuronal networks under RF exposure can be an efficient tool to detect the occurrence of low-level RF effects on the nervous system. In this thesis research work we developed a dedicated experimental setup in the GHz range for the simultaneous exposure of neuronal networks and monitoring of electrical activity. A transverse electromagnetic (TEM) cell was used to expose the neuronal networks to GSM-1800 signals at a SAR level of 3.2 W/kg. Recording of the neuronal electrical activity and detection of the extracellular spikes and bursts under exposure were performed using Micro Electrode Arrays (MEAs). This work provides the proof of feasibility and preliminary results of the integrated investigation regarding exposure setup, culture of the neuronal network, recording of the electrical activity and analysis of the signals obtained under RF exposure. In the main experiment (16 cultures), there was a 30% reversible decrease in mean firing rate (MFR) and bursting rate (BR) during the 3 min exposures to RF. Additional experiments are needed to further characterize this effect, especially in terms of temperature elevation at the microscopic level.

Key words: feasibility study, GSM-1800 signal, neuronal networks, electrical activity, Micro Electrode Arrays, in vitro.

Résumé

Le système nerveux central est la cible la plus probable d'effets biologiques dûs à l'exposition aux radiofréquences (RF) de la téléphonie mobile. Plusieurs études sur l'EEG (électroencéphalogramme) ont montré des variations dans le spectre de la bande alpha pendant et / ou après l'exposition aux radiofréquences, avec les yeux fermés ou pendant le sommeil. Dans ce contexte, l'observation de l'activité électrique spontanée des réseaux neuronaux sous exposition aux radiofréquences représente un outil efficace pour détecter de possibles effets des RF de faible niveau sur le système nerveux. Dans ce travail de thèse, nous avons développé un dispositif expérimental dédié à l'exposition dans la gamme des GHz de réseaux neuronaux et permettant simultanément l'enregistrement de l'activité électrique des neurones. Une cellule électromagnétique transversale (TEM) a été utilisée afin d'exposer les réseaux neuronaux aux signaux GSM-1800 à un niveau de DAS de 3,2 W / kg. L'enregistrement de l'activité électrique neuronale et la détection en termes de spikes et bursts sous exposition ont été réalisées à l'aide de réseaux de micro-électrodes (MEAs). Ce travail démontre la faisabilité de l'étude (culture de réseaux de neurones primaires, enregistrement de l'activité électrique et analyse des signaux obtenus sous exposition aux radiofréquences) et expose des résultats préliminaires. Dans l'expérience principale (16 cultures), il y avait une diminution réversible de 30% du taux moyen de spikes (MFR) et de bursts (BR) pendant les 3 min d'exposition aux RF. Des expériences supplémentaires sont nécessaires pour mieux caractériser cet effet, notamment en termes d'élévation de la température au niveau microscopique.

Mots clés: étude de faisabilité, signal GSM-1800, réseaux de neurones, activité électrique, Micro Electrode Arrays, in vitro.